



EUROPEAN COMMISSION
EIGHTH FRAMEWORK PROGRAMME
HORIZON 2020
GA No. 634149

Deliverable No.	D2.3		
Deliverable Title	Assessment of the PROSPECT safety systems including socio-economic evaluation		
Dissemination level		Dd/mm/yyyy	
Written by	Kovaceva, Jordanka Bálint, András Schindler, Ron	Chalmers University of Technology	
	Schneider, Anja Stoll, Johann	Audi AG	
	Breunig, Sandra Bräutigam, Julia	Bundesanstalt für Straßenwesen (BASt)	
	Jaussein, Marie Bruyas, Marie-Pierre	IFSTTAR	
	Puente Guillen, Pablo	TME	
	Large, David	UoN	
	Perlet, Klaus	BMW	
	Petersson, Mats	VCC	
	Esquer, Alvaro	IDIADA	
Checked by	Arbitmann, Maxim	Continental	27/09/2018
	Krebs, Sebastian	Daimler	03/10/2018
Approved by	Last Name, Name	Organisation	Dd/mm/yyyy
Issue date	31 October 2018		



The research leading to the results of this work has received funding from the European Community's Eighth Framework Program (Horizon2020) under grant agreement n° 634149.

EXECUTIVE SUMMARY

This report provides a new methodology for safety benefit assessment of real-world benefit of the Advanced Driver Assistance Systems (ADAS) in terms of saved lives and prevented injuries as well as the resulting monetary benefit for society. This methodology is demonstrated and applied to PROSPECT systems that address potential crashes of passenger cars with vulnerable road users (VRUs) such as pedestrians and cyclists.

Pre-crash kinematics data from crashes between passenger cars and VRUs from the Pre-Crash Matrices (PCM) based on the German In-Depth Accident Study (GIDAS) have been analysed with respect to twelve use cases derived in task 2.1 and 3.1 (described in Deliverable 2.1 “Accident Analysis, Naturalistic Driving Studies and Project Implications” and Deliverable 3.1 “The addressed VRU scenarios within PROSPECT and associated test catalogue”).

Counterfactual simulations using relevant models for PROSPECT sensors and algorithms have been performed on car-to-cyclist and car-to-pedestrian crashes corresponding to the use cases. The counterfactual simulation is a method that has been used to analyse crashes amenable to the technology and assess what the crash outcome would have been had the vehicle been equipped with the investigated technology. Four algorithms of the PROSPECT systems have been modelled and implemented in the counterfactual simulation tool.

The simulation results were updated with the results from vehicle-based testing on closed test tracks for each use case. A key aspect in this task was the combination of results from different sources concerning the effectiveness of the PROSPECT systems in different use cases, e.g. simulation results and test results. For this purpose, Bayesian statistical methods were proposed as an appropriate mathematical framework.

Injury Risk Functions (IRF) for all cyclist use cases as well as for all pedestrian use cases per severity were developed based on the police coded injury severity and the collision speed. The computation of the local safety benefit of the PROSPECT systems was based on a combination of models for crash avoidance probability and collision speed in case of a crash (resulting from the Bayesian analysis combining simulation results and test results) with the developed IRFs, using a variant of the dose-response model.

The local benefit regarding fatalities, serious and slight injuries showed 55%-98% benefit of the algorithms, depending on the use case. The system gives a somewhat greater overall fatality reduction (82-86%) for all cyclist use cases combined than for pedestrian use cases combined (69-76%, depending on the algorithm). These use cases are addressing 86% of car-to-cyclist fatalities and 39% of car-to-pedestrian fatalities in GIDAS PCM data, hence the reductions within the use cases correspond to an overall estimated local reduction of 70-74% within car-to-cyclist fatalities and 27-30% within car-to-pedestrian fatalities.

The reduction for serious injuries is somewhat lower than for fatalities, especially for pedestrians. The results are in the range of 53-93% for cyclists and 23%-58% for pedestrians depending on the use case and yielding an overall reduction of 71-76% for cyclists and 36-44% for pedestrians within the use cases for the different algorithms.

This corresponds to an overall reduction of 53-56% for seriously injured within car-to-cyclist and a 19-23% decrease of seriously injured within car-to-pedestrian crashes. The reduction of slight injuries is generally smaller than the reduction for serious or fatal injuries, especially for pedestrians.

This local benefit was extrapolated to EU-28 by using a decision tree method. It was assumed that market penetration and user acceptance of the PROSPECT systems gradually increase, from 5.8% and 84.5% in 2025 to 20% and 87% in 2030. Due to the assumed increasing market penetration and user acceptance, the annual number of lives saved in EU-28 increases from an estimate of 79-95 in 2025 to 280-336 in 2030, while the corresponding estimates for the reduction of seriously injured are 439-697 in 2025 and 1558-2474 in 2030. Accordingly, the socio-economic benefit of PROSPECT systems increases from 203-296 million euros in 2025 to monetary values exceeding 878-1280 million euros from 2030 on.

The results have potential implications for policies and regulations in understanding the real-world benefit of new ADAS.

CONTENTS

Executive summary	1
1 Introduction	12
1.1 The EU project PROSPECT	12
1.2 Objectives of the deliverable.....	12
1.3 Literature review on the benefit estimation of passive safety	13
2 Method.....	16
2.1 GIDAS data	18
2.1.1 Database description	18
2.1.2 Identification of data in PCM.....	19
2.1.3 Match between PCM and demonstrator use cases.....	20
2.1.4 Analysis of the demonstrator use cases	20
2.2 What-if simulation	52
2.2.1 System algorithms	52
2.2.2 Simulation with rateEFFECT	57
2.2.3 Simulation with openPASS	58
2.3 Incorporating test results	59
2.3.1 Bayesian framework	59
2.3.2 Test results chosen.....	62
2.3.3 Injury risk functions: cyclists	64
2.3.4 Injury risk functions: pedestrians	66
2.3.5 Computing local benefit	67
2.4 Extrapolation	68
2.4.1 Recursive decision trees.....	68
2.4.2 Fleet penetration rate.....	70
2.5 Societal benefit	71
2.5.1 User acceptance.....	71
2.5.2 VTI simulator study and VCC test track study	75
2.5.3 Societal costs.....	76
3 Results	78
3.1 Simulation results from openPASS	78
3.2 Local benefit.....	79
3.2.1 Analysis of simulation results from rateEFFECT tool	79
3.2.2 Update with test results	82
3.3 Extrapolation	87
3.4 Societal benefit	92
4 Discussion	95
5 Conclusion.....	97
6 Summary and highlights.....	98

7	References	101
8	Appendix A	106
8.1	Box plot description	106
8.2	Initial speed	107
8.3	Trajectories	108
8.3.1	UC_DEM_1	108
8.3.2	UC_DEM_2	110
8.3.3	UC_DEM_3	111
8.3.4	UC_DEM_4	112
8.3.5	UC_DEM_5	113
8.3.6	UC_DEM_6	114
8.3.7	UC_DEM_9	115
8.3.8	UC_DEM_10	116
8.3.9	UC_DEM_11	117
8.3.10	UC_DEM_12	118
8.4	Local safety benefits including confidence intervals	118
8.5	IRF for cyclists using MAIS levels	122
8.6	IRF for pedestrians using MAIS levels	125
	Acknowledgments	129

List of Abbreviations

ABS	Anti-lock Braking System
ACC	Adaptive Cruise Control
ADAS	Advanced Driver Assistance Systems
AEB	Autonomous Emergency Braking
ASC	Automatic Stability Control
CARE	Community Database on Accidents on the Roads in Europe
CC	Cruise Control
DEM	Demonstrator
ESC	Electronic Stability Control
Euro NCAP	Euro New Car Assessment Program
FCW	Forward Collision Warning
GIDAS	German In-Depth Accident Study
GSR	General Safety Regulation
JARI	Japan Automobile Research Institute
NCAP	New Car Assessment Program
NHTSA	National Highway Traffic Safety Administration
openPASS	Open-Source Simulation Platform for Development and Functional Validation of ADAS and Automated Driving
PCM	Pre-Crash Matrix
P.E.A.R.S.	Prospective Effectiveness Assessment of Road Safety
PSR	Pedestrian Safety Regulations
UC	Use Case
UMTRI	University of Michigan Transportation Research Institute
VRU	Vulnerable Road Users
VTI	Virginia Tech Transportation Institute

LIST OF FIGURES

Figure 1: Assessment framework. Color coding: green=input, blue=processed data, orange=output.	17
Figure 2: Example of an accident between a passenger car (red box) intending to turn right and a cyclist (blue box) crossing from the right in PCM.	19
Figure 3: Overview of demonstrator use cases	20
Figure 4: The green box is the vehicle and the blue dots are the contact points between VRU and vehicle.	21
Figure 5: Use cases and number of crashes per use case.	22
Figure 6: Matched accident types for UC_DEM_1.	22
Figure 7: Distribution of view obstructions in UC_DEM_1.	23
Figure 8: Box plot of detection times for UC_DEM_1 without view obstruction.	23
Figure 9: Box plot of detection times for UC_DEM_1 with view obstruction.	23
Figure 10: Box plots of the collision speed of the vehicle in UC_DEM_1.	24
Figure 11: contact points from GIDAS and simulation in UC_DEM_1.	25
Figure 12: Matched accident types for UC_DEM_2.	25
Figure 13: Distribution of view obstructions in UC_DEM_2.	26
Figure 14: Box plot of detection times for UC_DEM_2 without view obstruction.	26
Figure 15: Box plot of detection times for UC_DEM_2 with view obstruction.	26
Figure 16: Boxplots of the collision speed of the vehicle in UC_DEM_2.	27
Figure 17: contact points from GIDAS and simulation in UC_DEM_2.	28
Figure 18: Matched accident types for UC_DEM_3.	28
Figure 19: Distribution of view obstructions in UC_DEM_3.	29
Figure 20: Box plot of detection times for UC_DEM_3 without view obstruction.	29
Figure 21: Box plot of detection times for UC_DEM_3 with view obstruction.	30
Figure 22: Box plots of the collision speed of the vehicle in UC_DEM_3.	30
Figure 23: contact points from GIDAS and simulation in UC_DEM_3.	31
Figure 24: Matched accident types for UC_DEM_4. View obstruction:	32
Figure 25: Distribution of view obstructions in UC_DEM_4.	32
Figure 26: Box plot of detection times for UC_DEM_4 without view obstruction.	32
Figure 27: Box plot of detection times for UC_DEM_4 with view obstruction.	33
Figure 28: Box plots of the collision speed of the vehicle in UC_DEM_4.	33
Figure 29: contact points from GIDAS and simulation in UC_DEM_4.	34
Figure 30: Matched accident types for UC_DEM_5. View obstruction:	35
Figure 31: Distribution of view obstructions in UC_DEM_5.	35
Figure 32: Box plot of detection times for UC_DEM_5 without view obstruction.	35
Figure 33: Box plot of detection times for UC_DEM_5 with view obstruction.	36
Figure 34: Box plots of the collision speed of the vehicle in UC_DEM_5.	36
Figure 35: contact points from GIDAS and simulation in UC_DEM_5.	37
Figure 36: Matched accident types for UC_DEM_6. View obstruction:	38
Figure 37: Distribution of view obstructions in UC_DEM_6.	38
Figure 38: Box plot of detection times for UC_DEM_6 without view obstruction.	38
Figure 39: Box plot of detection times for UC_DEM_6 with view obstruction.	39
Figure 40: Box plots of the collision speed of the vehicle in UC_DEM_6.	39
Figure 41: contact points from GIDAS and simulation in UC_DEM_6.	40
Figure 42: Matched accident types for UC_DEM_9.	41
Figure 43: Distribution of view obstructions in UC_DEM_9.	41

Figure 44: Box plot of detection times for UC_DEM_9 without view obstruction.	41
Figure 45: Box plot of detection times for UC_DEM_9 with view obstruction.	42
Figure 46: Boxplots of the collision speed of the vehicle in UC_DEM_9.	42
Figure 47: contact points from GIDAS and simulation in UC_DEM_9.	43
Figure 48: Matched accident types for UC_DEM_10.	43
Figure 49: Distribution of view obstructions in UC_DEM_10.	44
Figure 50: Box plot of detection times for UC_DEM_10 without view obstruction. ...	44
Figure 51: Box plot of detection times for UC_DEM_10 with view obstruction.	44
Figure 52: Box plots of the collision speed of the vehicle in UC_DEM_10.	45
Figure 53: contact points from GIDAS and simulation in UC_DEM_10.	46
Figure 54: Matched accident types for UC_DEM_11.	47
Figure 55: Distribution of view obstructions in UC_DEM_11.	47
Figure 56: Box plot of detection times for UC_DEM_11 without view obstruction. ...	47
Figure 57: Boxplot of detection times for UC_DEM_11 with view obstruction.	48
Figure 58: Box plots of the collision speed of the vehicle in UC_DEM_11.	48
Figure 59: contact points from GIDAS and simulation in UC_DEM_11.	49
Figure 60: Matched accident types for UC_DEM_12.	49
Figure 61: Distribution of view obstructions in UC_DEM_12.	50
Figure 62: Box plot of detection times for UC_DEM_12 without view obstruction. ...	50
Figure 63: Boxplot of detection times for UC_DEM_12 with view obstruction.	50
Figure 64: Box plots of the collision speed of the vehicle in UC_DEM_12.	51
Figure 65: contact points from GIDAS and simulation in UC_DEM_12.	52
Figure 66: Time to Collision (TTC).	53
Figure 67: Work flow of Algorithm 2.	54
Figure 68: Trajectory model based on the Kammscher Kreis (Dirndorfer, 2015).	54
Figure 69: Trajectory model.	55
Figure 70: Work flow of Algorithm 3.	56
Figure 71: Schematic of systems in rateEFFECT (Wille, Jungbluth, Kohsiek, & Zatloukal, 2012).	58
Figure 72: Test cases.	63
Figure 73: Probability of being slightly (blue), seriously (orange), and fatally (red) injured for cyclists in an accident with a car based on n=1,356 GIDAS cases identified as PROSPECT use-cases.	66
Figure 74: Probability of being slightly (blue), seriously (orange), and fatally (red) injured for pedestrians in an accident with a car based on n=576 GIDAS cases identified as PROSPECT use-cases.	67
Figure 75: Fleet penetration curve for frontal airbag in Germany.	71
Figure 76: German penetration rates 2011 of the newest systems: new cars vs vehicle population.	71
Figure 77: Drivers' intention to use the PROSPECT functions.	73
Figure 78: Layout of the simulated scenario.	78
Figure 79: Absolute frequency of simulated accidents per TTC value.	79
Figure 80: Prior distribution for the probability of crash avoidance in UC 6 for initial speed 15 km/h.	81
Figure 81: Posterior distribution for the probability of crash avoidance in UC 6 for initial speed 15 km/h. The solid curve is the posterior distribution and the dotted curve is the prior.	84

Figure 82: Local benefit for algorithm 1 per use case: percent of injury (fatal, serious, slight) reduction for cyclists.....	85
Figure 83: Local benefit for algorithm 1 per use case: percent of injury (fatal, serious, slight) reduction for pedestrians.....	85
Figure 84: Relative frequencies of injuries from GIDAS and CARE.....	87
Figure 85: Classification tree for cyclist injuries from GIDAS. In each box the first row shows the node number and the predicted injury class for that node; the second row shows the number of cases that are classified as fatal/serious/slight.....	89
Figure 86: Classification tree for cyclist injuries from CARE. In each box the first row shows the node number and the predicted injury class for that node; the second row shows the number of cases that are classified as fatal/serious/slight.....	89
Figure 87: Classification tree for pedestrian injuries from GIDAS. In each box the first row shows the node number and the predicted injury class for that node; the second row shows the number of cases that are classified as fatal/serious/slight.	90
Figure 88: Reduction of casualties annually in EU-28, with lower and upper boundaries, assuming 100% market penetration and 100% user acceptance.	92
Figure 89: Yearly increasing market penetration.	92
Figure 90: Yearly increasing user acceptance.....	92
Figure 91: Yearly societal benefit of algorithm 1	93
Figure 92: Yearly societal benefit of algorithm 2	94
Figure 93: Yearly societal benefit of algorithm 3.....	94
Figure 94: Yearly societal benefit of steering and braking algorithm	95
Figure 95: Illustration of the steps in the safety assesment methodology.....	100
Figure 96: Exemplary boxplot.....	106
Figure 97: VRU initial speed per use case.	107
Figure 98: Car initial speed per use case.	108
Figure 99: Probability for injury severity of MAIS1 (blue), MAIS2+ (orange), and fatality (red) for cyclists in an accident with a car based on n= 1.308 GIDAS cases identified as PROSPECT use-cases.	123
Figure 100: Probability of being slightly (blue), seriously (orange), and fatally (red) injured for cyclists in an accident with a car based on n=1,308 GIDAS cases identified as PROSPECT use-cases.	124
Figure 101: IRF for cyclists based both on police coding and MAIS.....	124
Figure 102: Probability for injury severity of MAIS1 (blue), MAIS2+ (orange), and fatality (red) for pedestrians in an accident with a car based on n=519 GIDAS cases identified as PROSPECT use-cases.	125
Figure 103: All IRF for pedestrians plotted together.	126
Figure 104: Probability of being slightly (blue), seriously (orange), and fatally (red) injured for pedestrians in an accident with a car based on n=537 GIDAS cases identified as PROSPECT use-cases.	127

LIST OF TABLES

Table 1: PCM filters for identifying relevant simulation files.....	19
Table 2: The proportion of casualties in car-to-VRU crases in GIDAS PCM matched to the use cases	20
Table 3: Descriptive statistics of collision speed in UC_DEM_1.	24
Table 4: Descriptive statistics of collision speed in UC_DEM_2.....	27

Table 5: Descriptive statistics of collision speed in UC_DEM_3.	30
Table 6: Descriptive statistics of collision speed in UC_DEM_4.	33
Table 7: Descriptive statistics of collision speed in UC_DEM_5.	36
Table 8: Descriptive statistics of collision speed in UC_DEM_6.	39
Table 9: Descriptive statistics of collision speed in UC_DEM_9.	42
Table 10: Descriptive statistics of collision speed in UC_DEM_10.	45
Table 11: Descriptive statistics of collision speed in UC_DEM_11.	48
Table 12: Descriptive statistics of collision speed in UC_DEM_12.	51
Table 13 Initial vehicle speeds considered for modelling crash avoidance (km/h)....	60
Table 14: Matching of test scenarios and use cases.	64
Table 15: Parameter estimates of the probit model for pedestrians based on police coded injury severity.	65
Table 16: Parameter estimates of the probit model for pedestrians based on police coded injury severity.	66
Table 17: Transformation of categorical variables into binary variables.	69
Table 18: Variables name and their categories.	70
Table 19: Willingness to buy according to the drivers' mileage	73
Table 20: Willingness to buy according to the system functioning	73
Table 21: Injury unit costs [ASSESS D2.2, updated].	77
Table 22: Frequency of total, avoided and mitigated crashes for algorithm 1 and 2 and use case.	79
Table 23: Frequency of total, avoided and mitigated crashes for algorithm 3 and use case.	79
Table 24: Frequency of avoided, mitigated and total number of crashes for steering and braking algorithm.	80
Table 25: Pearson correlation for collision speed and the metrics (initial speed, longitudinal distance, lateral distance, TTC at first detection) for algorithm 1 per use case for the mitigated crashes.	80
Table 26: Pearson correlation for collision speed and the metrics (initial speed, longitudinal distance, lateral distance, TTC at first detection) for algorithm 1 per use case for all crashes.	81
Table 27: Variables used in the linear regression models for the collision speed in case of a crash	82
Table 28: Test results used for updating simulation results.	82
Table 29: Posterior models for the probability of crash avoidance	84
Table 30: Fatality reduction estimates for the PROSPECT systems	85
Table 31: Estimates of the reduction of non-fatal serious injuries for the PROSPECT systems	86
Table 32: Estimates of the reduction of slight injuries for the PROSPECT systems.	86
Table 33: Factors for extrapolation of cyclist injuries from GIDAS to CARE.	89
Table 34: Factors for extrapolation of pedestrian injuries from GIDAS to CARE.	90
Table 35: Number of reduced cyclist injuries for one year by different algorithms for use cases 1-9.	91
Table 36: Number of reduced cyclist injuries for one year by steering and braking algorithm for use case 9.	91
Table 37: Number of reduced pedestrian injuries for one year by different algorithms for use cases 10-12.	91

Table 38: Number of reduced pedestrian injuries for one year by steering and braking algorithm for use case 12.	91
Table 39: Estimated benefits of the systems in 2030	93
Table 40: Estimated benefits of the systems by 2030 (sum of 10 years).....	93
Table 41: Reduction of casualties of different severities by use case with confidence intervals	119
Table 42: Local benefits for cyclists to be used for extrapolation to EU-28	121
Table 43: Local benefits for pedestrians to be used for extrapolation to EU-28.....	121
Table 44: Parameter estimates of the probit model for cyclists.	122
Table 45: Parameter estimates of the probit model for pedestrians based on police coded injury severity.	123
Table 46: Parameter estimates of the probit model for pedestrians based on MAIS levels.	125
Table 47: Parameter estimates of the probit model for pedestrians based on police coded injury severity.	126

1 INTRODUCTION

1.1 THE EU PROJECT PROSPECT

The past decade has seen significant progress on active Vulnerable Road User (VRU) safety systems, as a result of advances in video and radar technology. In the intelligent vehicle domain, this has recently culminated in the market introduction of first-generation active pedestrian safety systems, which can perform autonomous emergency braking (AEB-PED) in case of critical traffic situations. PROSPECT is significantly improving the effectiveness of active VRU safety systems compared to those currently on the market. This is achieved in two complementary ways: (a) by expanded scope of VRU scenarios addressed and (b) by improved overall system performance.

The primary goal of the work package 2 (WP2) in the project is to generate the user requirements for next generation proactive safety systems for deployment in vehicles (passenger cars, VANS, trucks and buses), with a focus on the specific needs of VRUs. The project is focusing on the complex, yet significant needs of cyclists, pedestrians, as well as mopeds and motorized scooter users.

In achieving this goal, WP2 analysed and derived in-depth understanding of the prevalence and underlying characteristics of vehicle-to-VRU accidents within the European Union. Moreover, the project incorporated also the information from drivers' performance and behaviour when using active vehicle safety systems to ensure maximum utility for the technology and no unintended side effects of system use. The partners primarily draw upon their expertise and analysis of issues/data from the EU perspective, but also utilised their international links (e.g. with VTTI, UMTRI, NHTSA, JARI) in order to gain a worldwide view.

The outcome from WP2 was provided to the project through four tasks:

1. Detailed analyses of accident databases (T2.1),
2. Naturalistic observations within selected European cities to establish how vehicles and VRUs interact in real traffic situations (T2.2),
3. Focused qualitative and quantitative research studies and literature reviews to establish user needs and functional requirements (T2.3) and
4. Estimations of the benefits of the PROSPECT safety system for VRUs (T2.4).

1.2 OBJECTIVES OF THE DELIVERABLE

The objective of this report is to estimate the real-world benefit of the developed PROSPECT systems, i.e. the improvement for traffic safety in terms of saved lives or serious injuries and the resulting overall benefit - not only the system performance measured in detection rate or speed reduction.

According to description of work, socio-economic assessment is performed without cost-benefit assessment (system costs are not included). Task 2.4 used the results from task 2.1 to define and apply a methodology to estimate the socio-economic impact of PROSPECT safety systems. This methodology includes an assessment of the combined effect of active and passive safety measures (i.e. integrated safety).

The task was primarily focused on the development of methodology for assessment of active measures, and the resulting methodology is described and discussed in sections 2 to 4. Benefit estimation of passive safety measures was conducted on the basis of a literature review, which is described in the next section (section 1.3).

1.3 LITERATURE REVIEW ON THE BENEFIT ESTIMATION OF PASSIVE SAFETY

The benefit estimation for passive safety is based on literature review. The aim was to take into account the benefits due to Euro NCAP and legislation and deployable systems such as pedestrian and cyclist airbags or pop-up bonnets.

1.3.1.1 Passive safety measures addressed by legislation and Euro NCAP

In Europe passive pedestrian protection for type M1 vehicles is mainly driven by legislation and Euro NCAP. However, while legislation is compulsory to all M1 vehicles (up to 2.5t), Euro NCAP only considers the majority of the most popular cars in Europe. The protection of pedestrians and other vulnerable road users (VRU) was addressed by legislation by the directive 2003/102/EG (EUDirective, 2003) which came into force in 2005. This was displaced by regulation (EC) 78/2009 (EU, 2009) ("Pedestrian Safety Regulation") dealing with the type approval for motor vehicles and including passive safety requirements to mitigate the risk of serious injury for VRUs in an accident.

Euro NCAP (EURONCAP, 2018) as a tool of consumer protection also addresses pedestrian protection in the test protocols since 1997 which were updated in 2002 and 2014/2015. These tests assess the front structure of the vehicle regarding a head impact as well as upper and lower leg impact. Since 2018, AEB pedestrian protection is included in the test protocol.

In (Seeck, Seiniger, & Zander, 2012), a benefit estimation was given regarding Euro NCAP test procedures for bicyclists and pedestrians involved in a collision with a vehicle based on a GIDAS analysis. For cyclists (80% of them without a helmet), it is shown that approx. 25% of all injuries were suffered in Euro NCAP test zones of which head injuries make about 20%. For pedestrians the share of injuries suffered in Euro NCAP test zones is much higher at 50%. Hereof, 25% are head injuries.

Pastor gives an overview between correlations between Euro NCAP test results and real-world crash data to estimate the benefit of passive safety measures for pedestrian protection (Pastor, 2013). This study was based on the German National Accident Records from 2009-2011, analysed single pedestrian (aged 6-64) to single passenger car crashes in urban crossing accidents, with Euro NCAP rated vehicles (post 2002) part of which complying pedestrian protection legislation (EUDirective, 2003). Correlation analysis between pedestrians' casualty severity and explanatory variables was performed via an ordinal probit model and significant correlation was found between Euro NCAP pedestrian score and injury outcome in real-crash.

In particular, it was found in (Pastor, 2013) that a high pedestrian score (22 points) brings 35% reduction compared to low pedestrian score (5 points) for pedestrians' conditional probability of getting fatally injured and 16% reduction for pedestrians' conditional probability of getting seriously injured. As a rule of thumb, each NCAP point brings reduction in probability of 2.5% for fatalities and 1% for serious injuries. At the same time, no significant injury reduction effect was found associated with the introduction of pedestrian protection legislation (phase 1; (EUDirective, 2003)). An estimation of the injury reduction potential by assuming a fleet completely meeting a pedestrian NCAP score of 22 points was a 6 % reduction in fatal cases and 9% in serious cases.

1.3.1.2 Pop-up-bonnets

Pop-up bonnet is a pedestrian protection system that aims to increase the head deceleration space beneath the bonnet and the underlying hard structures. This is realised by quickly lifting the bonnet in case of the vehicle having contact with a pedestrian. The variety of existing systems is large regarding the mechanical solution as well as software solutions, including limit values for the activation of the system.

In testing (type approval and Euro NCAP), pop-up bonnets are tested statically in the course of the head impact testing while the bonnets are fully popped up. The assurance of the functionality of the system is shown by virtual testing. So far there is no real-world test procedure for the complete system, i.e. pedestrian sensing, timing, deployment threshold (Ames & Martin, 2015).

Based on the scales of the so-called Vehicle Related Pedestrian Safety Index (VERPS-Index), a significant improvement in the protection of children is shown in (Kuehn, Froeming, & Schindler, Assessment of vehicle related pedestrian safety, 2005) if a vehicle is equipped with a pop-up bonnet compared to the same vehicle without an active bonnet. The performance is even more enhanced for the combination of a pop-up bonnet and an airbag that covers the A-pillar and the lower windscreen frame.

In (Ames & Martin, 2015), an extensive study is provided regarding the safety benefits of pop-up bonnets for pedestrians based on the analysis of Euro NCAP pedestrian test results. It was found that since 2010, vehicles equipped with pop-up bonnets performed better on average than vehicles with non-deploying bonnets in pedestrian safety. Vehicles with pop-up bonnets comprise only about 8% of all new light vehicles in Europe and those vehicles tend to be in higher price class. Pop-up bonnets can compensate for poorer testing results (if not equipped with deploying hood) due to the desired vehicle style. However, the development of standardized test criteria is difficult due to very different realizations of pop-up deployment designs.

In (Hamacher, Kuehn, Hummel, & Eckstein, 2017), the safety benefit of deployable hoods for cyclists was investigated by means of extensive simulation studies. In this study, it was found that head impact positions are characteristically located further rearward compared to pedestrian frontal collisions. Cyclists have much higher head impact velocities and angles. Cyclists are often not addressed by an active bonnet, or even negative effects are determined. Pop-up bonnets in combination with a windscreen airbag can reduce the injury risk significantly; the whole A-pillar must be covered for shorter front geometries.

However, it seems that not much information about real-life effectiveness is available. An analysis of the German In-Depth Accident Study (GIDAS) regarding pop-up bonnets reveals only a small number of pedestrian accidents (n=10) with a vehicle equipped with a deployable pedestrian protection system (Pastor, 2013). Regarding the use case of such a system, one ends up with 6 cases and a 50% effectiveness of the system as in 3 cases the system did not deploy. Reasons for the systems not being activated are yet unknown, however, it might be simply due to e.g. the system being out of the deployment threshold.

1.3.1.3 Pedestrian and cyclist airbags

VRU airbags are external airbags located in the area of the windscreen and/or the A-pillars that are deployed when an impact of a VRU is detected. In current Volvo vehicles such an airbag is combined with a deployable hood.

In (Edwards, et al., 2015) a benefit-based methodology was developed for the assessment of integrated pedestrian protection systems with AEB and passive safety components based on the pedestrian AEB tests and the standard impactor tests within Euro NCAP in the course of the AsPeCSS project (IDIADA, <http://www.aspecss-project.eu/>, 2013). The key measure is the harm suffered by the VRU estimated from AIS and the performance of good, average and poor performing cars was calculated into casualty costs. In the passive safety testing Euro NCAP impactor test data and input data provided by the manufacturers were used for the impactor injury criteria for the most of the car's frontal area that is likely to be hit by a pedestrian (at 40 km/h). These data were extrapolated to other speeds using literature and empirical simulations within the project.

In this study, the in-depth data from the road crash databases On The Spot (OTS) and GIDAS were weighted to the respective national databases (i.e. STATS19 from Great Britain and the German National Statistics). AEB input data was classified as "No AEB" vs. "Current AEB" and testing of method was performed on real and composite vehicles with overall good, average and poor performance in Euro NCAP tests. It was found that while the order of the AsPeCSS rating (good, average, poor) aligns with Euro NCAP results, the scaling was different: there was a large gap between poor-average and a small gap between average-good while in NCAP there was a large gap in both cases. The benefits of a (hypothetical) A-pillar airbag is estimated to be about 40-50% in terms of casualty cost reduction.

Fredriksson and Rosén use another approach and end up in a benefit of 20-30% in terms of the reduction of serious AIS3+ head injuries for A-pillar and windscreen base airbags (Fredriksson & Rosén, 2014).

In (Barrow, et al., 2018) a study is presented that is dealing with the data-driven benefit estimation of pedestrian and cyclists protection systems. Since in the course of the second stage of the General Safety Regulations (GSR) review a research gap for the portion of VRUs in contact with the windscreen was identified, this study aims to close that gap for the third stage of the GSR review. Besides active protection systems the study estimates the benefit of a Pedestrian Protection Airbag (PPA). The analysis is based on British accident data, namely Road Accident In-Depth Studies (RAIDS, years 2000-2009, 2012-2015) and STATS19 (years 2011, 2015), including an upscaling from in-depth to national data. VRU-to-front of M1 vehicle accidents are analysed (excluding multiple vehicle accidents, child casualties < 13 years). The sample included 54 pedestrians and 20 cyclists in total of which 4 pedestrians and no cyclists were in the target population. The relevant impact zones are divided into A-pillar and scuttle, header rail and central windscreen.

Keeping in mind the restricted representativeness of the target population for a PPA the combined effectiveness for all severities and VRU types scaled to STATS19 was found to be 1.07% in frontal collisions with M1 vehicles. A PPA is predicted to save 72 fatally injured and 27 seriously injured pedestrians in a five-year period. No prediction for cyclists prevented by the PPA was possible as the target population in the sample did not include any cyclists. The prevalence of head contacts to the areas of the

vehicle (unregulated by the Pedestrian Safety Regulations (PSR)) was 41.9% (n=31 of 74) of killed or seriously injured (KSI) pedestrians. The unregulated windscreen areas pose a serious head injury risk as 21.6% (n=16 of 74) for KSI casualties with AIS2+ head injuries caused in respective areas. Although the PPA is the best measure currently available to protect the head, this study found that it is able to influence a target population of 5.4% of the overall casualty population before its effectiveness is considered. It is crucial for all VRU collisions to reduce the collision speed as the injury risk directly correlates with the collision speed.

1.3.1.4 Summary

In-depth accident data show that the currently regulated testing zones in Euro NCAP cover a large share of head injuries suffered by pedestrians and cyclists. The comparison of Euro NCAP test results with real-world accident data reveal a significant correlation between the performance in NCAP testing and the ability to prevent harm for pedestrians. As a rule of thumb, each NCAP point brings a reduction in probability of 2.5% for fatalities and 1% for serious injuries.

Regarding pop-up bonnets, only restricted information on real-world effectiveness is published which is probably due to the small penetration rate of such a system. Even if a deployable hood in general increases the performance in NCAP testing, there is no test protocol that takes system specifications in the moment of actual deployment into account. The small amount of real-world accident data indicates that there are issues to be solved regarding the knowledge of the system specifications and their limits. For cyclists, a simulation study shows that the kinematics are different from that of pedestrians regarding head impact velocities, angles, and also the further rearward point of impact. Here, the combination of an active bonnet with an external airbag seems to be most beneficial.

External airbags are estimated to bring a beneficial effect for only specific types of accidents, i.e. to a limited target group of about 5% of all pedestrian casualties amongst other reasons due to the specifications of the systems boundary conditions. The benefit of pedestrian and cyclist airbags strongly depends on the methodology of assessment. In terms of cost reduction, the benefit is estimated much higher (50%) than in terms of injury reduction (20-30%), e.g. because the approach also assigns higher casualty costs for more severe injuries (with an Abbreviated Injury Score (AIS) of 4 or 5).

There are several indications that the passive safety measures are most effective when combined with AEB systems (i.e. integrated safety) since the reduction of impact velocities is one of the most crucial parameters to enhance the performance of any passive safety measure. However, there is also a potential drawback of a speed reduction that kicks a speed-sensitive passive safety system out of its threshold.

2 METHOD

As indicated in the Introduction, task 2.4 was primarily focused on methodology development for the safety benefit assessment of active measures. The developed method is described in this section, the results of the implementation of the method are provided in Section 3, followed by a discussion in Section 4.

Based on an extensive literature review on existing benefit estimation methods, two main assessment strategies have been identified that could be applied in the present context. One is based on the dose-response model (Bálint, Fagerlind, & Kullgren, 2013), estimating the safety benefit based on the crash frequency and the injury risk functions; a summary of this model will be given in Section 2.3.5. The other approach is based on counterfactual (“what-if”) simulation, with two tools: rateEffect (Wille, Jungbluth, Kohsiek, & Zatloukal, 2012) and openPASS (Wang, et al., 2015) . These tools will be described in detail in Section 2.2. An assessment framework combining these strategies and introducing novel elements has been proposed, see Figure 1.

The assessment framework expects input data such as accident scenarios about car-to-cyclist crashes generated in previous tasks in PROSPECT (T2.1, T3.1) and car-to-pedestrian crashes identified from previous projects like AsPeCSS (IDIADA, <http://www.aspecss-project.eu/>, 2013) and specification of the sensors’ parameters and state-of-the-art algorithms. This input is used in “what-if” simulation (with the rateEffect tool), which is performed to assess the outcome of crashes without and with the safety system in the vehicle. The output of the simulation is whether the crash was avoided and the reduction of the collision speed of the car in crashes that are not avoided with the safety system.

Besides simulation results, test results from WP7 are also considered for the benefit assessment. A novel element of the benefit assessment method is a Bayesian framework for combining simulation results and test results. The Bayesian framework gives an appropriate mathematical method for updating prior information, from the simulation results, with new observations from the test results. This framework also gives the possibility of updating the results with more observations even after the project, for example if the prototype systems have been improved in production phase. The output of the Bayesian framework is the local benefit, which is an estimate of the safety benefit of the PROSPECT systems in the database used for generating the accident scenarios (i.e. GIDAS). Therefore, in order to quantify the effect of systems in Europe, the results need to be extrapolated to EU-level.

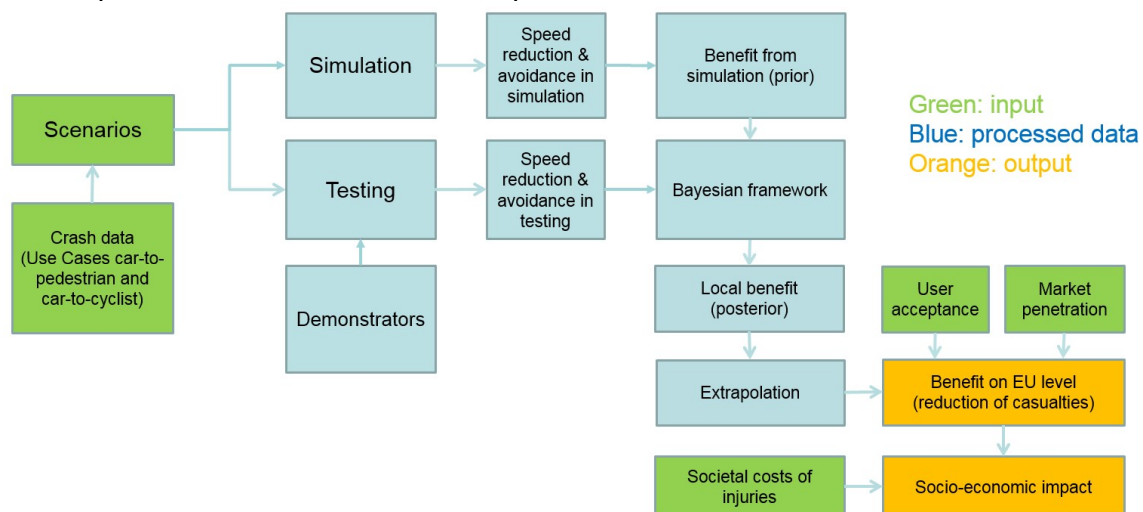


Figure 1: Assessment framework. Color coding: green=input, blue=processed data, orange=output.

Extrapolation of the results to EU-28 level was performed by the decision tree method which is the best method up-to-date according to the literature review. A decision tree

was built based on GIDAS data for the classification of the cyclist injuries in the car-to-cyclist crashes, using a set of relevant variables (e.g. weather, surface, light, site, gender and age). The same classification criteria are then applied to the Community Database CARE containing crash data from all EU countries. A comparison of the classification tree results from both databases yield weighting factors that are then used for the extrapolation of the benefit to EU level.

In the assessment process, user acceptance results (from WP7) and fleet penetration rates for the safety systems and their trend for the period 2020-2030 based on input from the OEMs have been also taken into account. Societal costs of injuries from the research literature were added as an input to the framework. Finally, the output of the framework is the benefit of the developed systems on EU level in terms of reduction in casualties (i.e. fatalities, serious and slight injuries) and saved costs as calculated from the societal costs of the casualties.

The details about the method are further explained in the following sections.

2.1 GIDAS DATA

2.1.1 Database description

The German In-Depth Accident Study (GIDAS) is the largest and most comprehensive in-depth road accident study in Germany. Since mid-1999, the GIDAS project has been investigating about 2,000 crashes per year in the areas of Hannover and Dresden and records up to 3,000 variables per crash. The project is supported by the Federal Highway Research Institute (BAST) and the German Association for Research in Automobile Technology (FAT). In GIDAS, road traffic crashes involving personal injury are investigated according to a statistical sampling process using the “on-scene” approach. This means that teams are called promptly after the occurrence of any kind of road traffic accident with at least one injured person that is reported to the police during determined time shifts. In addition, the investigation areas were chosen in accordance with the national road network characteristics and the share between built-up areas and non-built-up areas. Thus, the data collected by this sampling plan in both cities is close to being representative for the accident situation in Germany.

The detailed documentation of the crashes is performed by survey teams consisting of specially trained students, technical and medical staff. The data scope includes technical vehicle data, crash information, road design, active and passive safety systems, on-scene details and causes of the crashes. After the accident analysis a computer-based accident reconstruction is conducted to determine information on the crash kinematics and on crash avoidance.

As a simulation database, the so-called Pre-Crash Matrices (PCM) based on the GIDAS data modelled in PC-Crash (DSD Dr. Steffan Datentechnik, Linz - Austria) were used (Erbsmehl, 2008).

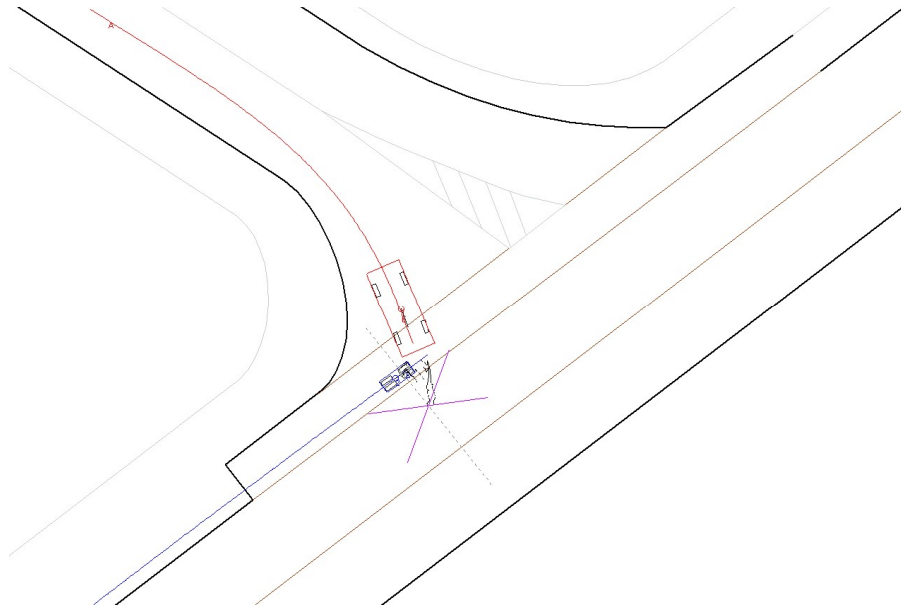


Figure 2: Example of an accident between a passenger car (red box) intending to turn right and a cyclist (blue box) crossing from the right in PCM.

The PCM data contains information about the trajectories of both accident participants as well as information about lane markings and sight obstructions, see Figure 2.

2.1.2 Identification of data in PCM

In total, 17506 participants are available in PCM (status: 2016-2). The PCM data was filtered to identify the relevant simulation files, according to the filter steps shown in Table 1.

Table 1: PCM filters for identifying relevant simulation files.

Filter	Number of accidents
Only accidents between cyclists/pedestrians and passenger cars	3922
Only accidents with slight simulation tolerances (difference between PCM and PC-Crash file in position $\leq 0.25\text{m}$ and in velocity $\leq 0.25\text{m/s}$)	3045

In total, 3045 accidents between passenger cars and VRUs were simulated in PC-Crash, including 1111 pedestrian accidents as well as 1934 cyclist accidents.

In GIDAS there are 4.406 accidents between passenger car and cyclists and 4.231 accidents with only 2 participants (one car and one cyclist) from which 77% (3.239 from 4231) are covered by the accident types that are described in the deliverable. From the PCM data in total 70% (1356 from 1934) of car-cyclist accidents were matched to the cyclist use cases.

The total number of accidents between passenger cars and pedestrians in GIDAS is 1.768 and 1.574 accidents are between 2 participants from which 44% (687 from 1574) are covered by the accident types that are described in the deliverable. From the PCM data in total 51% (578 of 1111) of car-pedestrian accidents were matched to the pedestrian use cases.

Table 2 below specifies the percentage of all car-to-VRU casualties of different injury severity in GIDAS PCM data that are addressed by the use cases.

Table 2: The proportion of casualties in car-to-VRU crashes in GIDAS PCM matched to the use cases

	Fatally injured VRU	Seriously injured VRU	Slightly injured VRU
Cyclists	86%	74%	69%
Pedestrians	39%	54%	52%

The next sections contain a detailed description of the demonstrator use cases.

2.1.3 Match between PCM and demonstrator use cases

The demonstrator use cases are defined in Deliverable 3.2. “Specification of the PROSPECT demonstrators (Kunert, Stoltz, Flohr, Hartmann, & Koch, 2016).

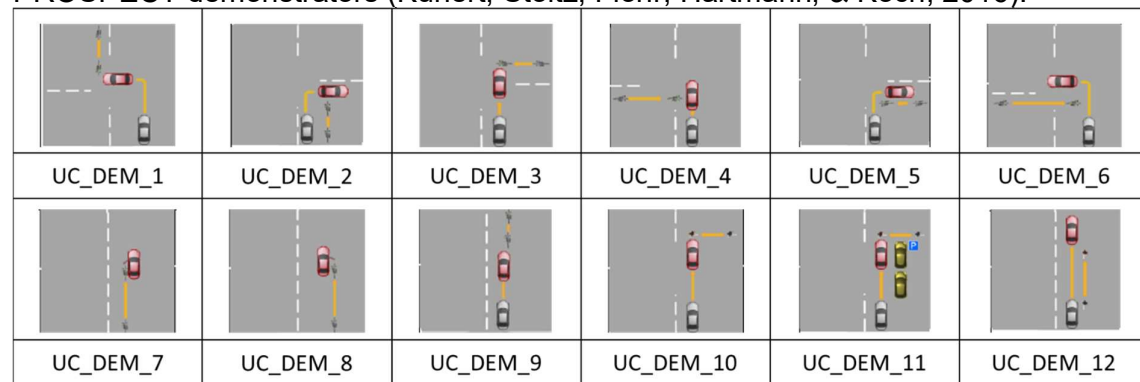


Figure 3: Overview of demonstrator use cases

Those use cases were derived based on the accident analysis published in D3.1 “The addressed VRU scenarios within PROSPECT and associated test catalogue” (Audi, 2016). Herein, for accidents between passenger cars and cyclists, every accident was analysed based on the infrastructure, manoeuvre intention of the passenger car, cyclist direction as well as traffic regulation. For accidents between passenger cars and pedestrians, only accident type coding was used to identify accidents that match the use cases. Based on the planned systems within PROSPECT, it was decided, that some of the very detailed differentiations from D3.1 (Audi, 2016) do not have to be considered from a system standpoint. Therefore, in order to have a comparable selection for both accidents between passenger cars and cyclists as well as pedestrians, the link between accident scenarios and use cases was repeated.

2.1.4 Analysis of the demonstrator use cases

In order to evaluate the match between PCM and the demonstrator use cases, a detailed analysis was conducted including the following information:

- Short description of the scenario
- Relevant accident types
- Total case number

- Trajectories over ground – collision north, showing the absolute trajectories of both participants adjusted, so that the vehicle is heading in northern direction at the point of impact
- Trajectories over ground – starting north and average trajectories (median and mean), showing the absolute trajectories of both participants adjusted, so that the vehicle is starting in northern direction at the point of impact. In addition, the median and mean of all trajectories is depicted.
- Trajectories relative to ego, showing the relative trajectory of the VRU in a coordinate system that is fixed for the vehicle.
- All trajectory plots are depicted in two different ways (and included in Appendix 8.3):
 - o Only trajectories: green trajectories depict the vehicle's trajectories, while blue trajectories belong to the VRU. Starting points are depicted with blue diamonds.
 - o Trajectories with TTCs, where the depicted diamonds show the position of both participants at different TTCs:
 - Blue: Original starting points
 - Turquoise: TTC 4 s
 - Green: TTC 3 s
 - Yellow: TTC 2 s
 - Red: TTC 1 s
- Pictures (example for all UC, see Figure 4) showing the contact points resulting from simulation and based on GIDAS coding. Contact points can differ between simulation and GIDAS coding due to rectangular vehicle and VRU dimensions. The contact points are coded as the distance from the front along the longitudinal axis of the vehicle in x-direction in centimetres and the lateral distance in y-direction to the middle line of the vehicle in centimetres, coded as positive towards the right side.

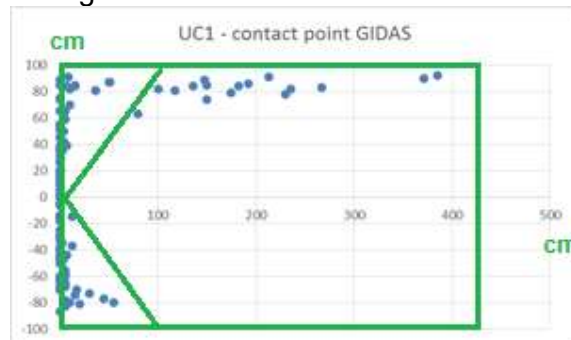


Figure 4: The green box is the vehicle and the blue dots are the contact points between VRU and vehicle.

- Overall distribution of view obstructions from GIDAS coding
- Boxplots of the resulting TTCs for cases, in which the the VRU was detected before the collision, separately for cases w/ and w/o view obstructions (detection based on the sensor assumptions described in Section 2.2.1). The structure of the boxplots follows the MATLAB ® (Mathworks) standard convention; for a detailed description, see Appendix 8.1).

- Summary of the initial speeds of the car and VRU per UC (for the details, see Appendix 8.2).

After the above analysis, the total number of crashes per use case is shown in Figure 5, the details of the analysis per use case is described in the Sections 2.1.4.1 to 2.1.4.12.

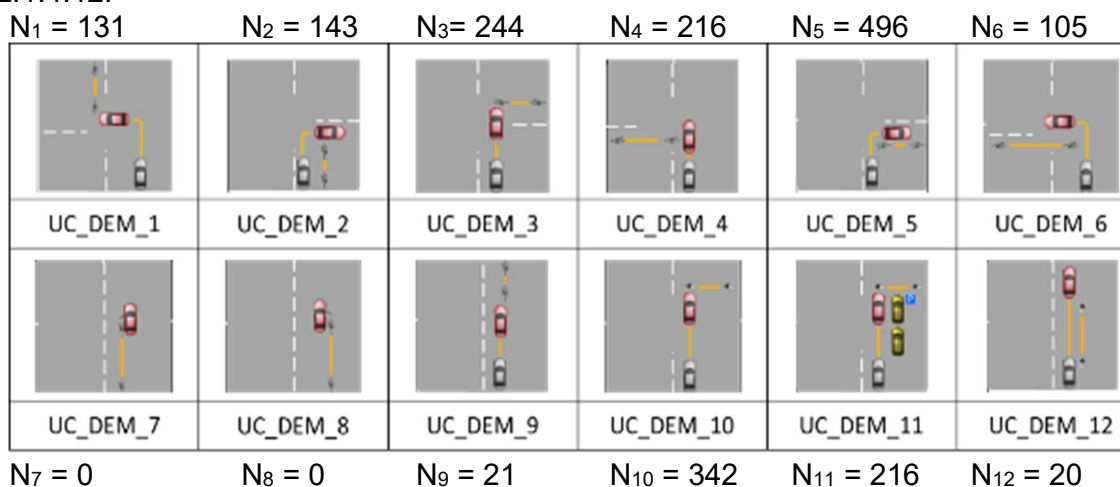


Figure 5: Use cases and number of crashes per use case.

2.1.4.1 UC_DEM_1

UC_DEM_1 describes a situation in which a car driver intends to turn left while a cyclist is coming from the opposite direction on the street or on the sidewalk. The accident types 211B and 224B were identified to match this description. In total, 131 accidents were available in PCM.

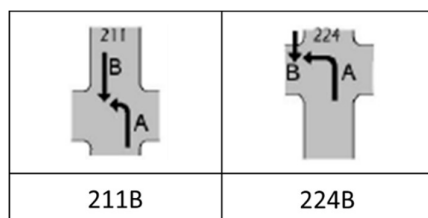


Figure 6: Matched accident types for UC_DEM_1.

View obstruction:

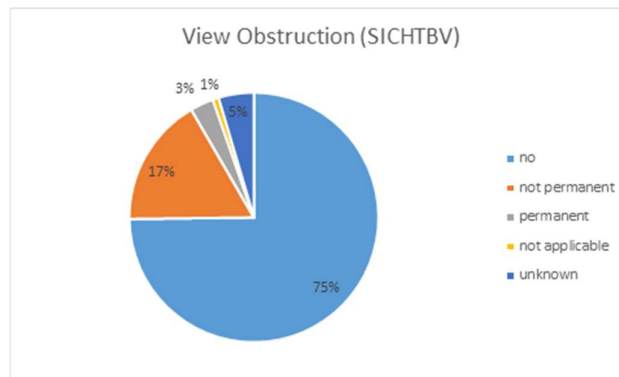


Figure 7: Distribution of view obstructions in UC_DEM_1.

Based on GIDAS coding, 75% of the UC_DEM_1 accidents happened without relevant view obstructions. All such cases were detected before the collision, and mean TTC at detection (i.e. TTC at first detection) of the VRU was 4.42s. A box plot of the detection times for cases in UC1 without view obstruction is given in Figure 8.

PROSPECT UC1 w/o view obstruction

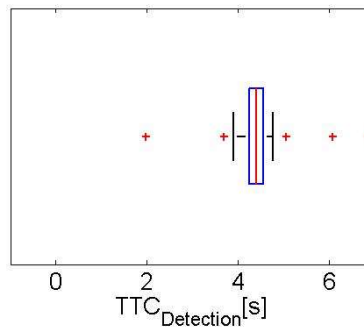


Figure 8: Box plot of detection times for UC_DEM_1 without view obstruction.

In 20% of the cases, a view obstruction was present. All such cases were detected before the collision and mean TTC at detection of the VRU was 3.68s. Figure 9 shows a box plot of the detection times for UC1 cases with a view obstruction.

PROSPECT UC1 w/ view obstruction

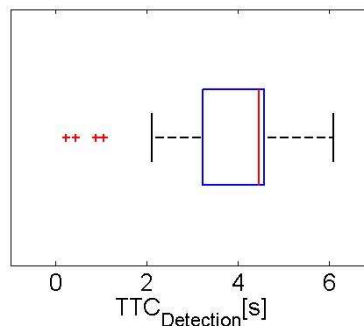


Figure 9: Box plot of detection times for UC_DEM_1 with view obstruction.

Collision speed:

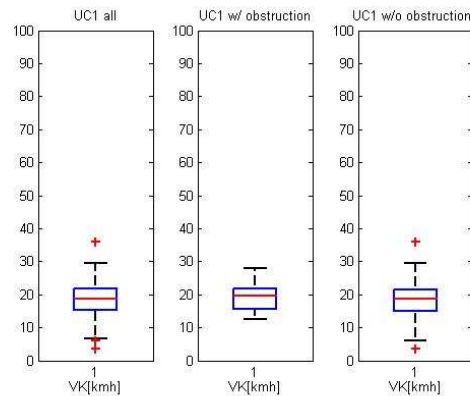


Figure 10: Box plots of the collision speed of the vehicle in UC_DEM_1.

Figure 10 shows the box plots of the passenger car collision speed for all UC_DEM_1 accidents, differentiated between cases with and without view obstructions. The box plots indicate no significant differences in the distribution of collision speeds based on view obstructions.

Table 3: Descriptive statistics of collision speed in UC_DEM_1.

	Collision speed [km/h]
Mean	18.6
5 th quantile	10.0
25 th quantile	15.4
75 th quantile	21.7
95 th quantile	27.3

Priority regulation:

In UC_DEM_1, 47% of the passenger cars were driving on a priority road with no additional regulation, while 29% of the accidents happened at signalized intersections.

Contact points:

A comparison of the contact points in the GIDAS data and the UC_DEM_1 cases is provided in Figure 11.

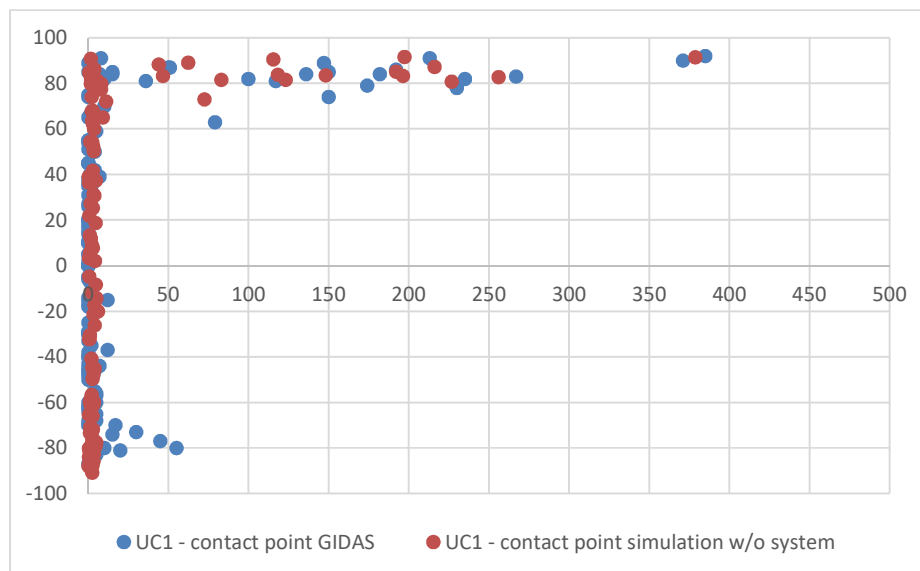


Figure 11: contact points from GIDAS and simulation in UC_DEM_1.

Based on the simulation, 87% of the according accidents have a contact point at the front of the vehicle (within 15cm). In GIDAS, 81% of the according accidents have a contact point at the front of the vehicle (within 15cm).

2.1.4.2 UC_DEM_2

UC_DEM_2 describes a situation, in which a car driver intends to turn right, while a cyclist is coming from the same direction on the street or on the sidewalk. The accident types 232B and 243B were identified to match this description. In total, 143 accidents were available in PCM.



Figure 12: Matched accident types for UC_DEM_2.

View obstruction:

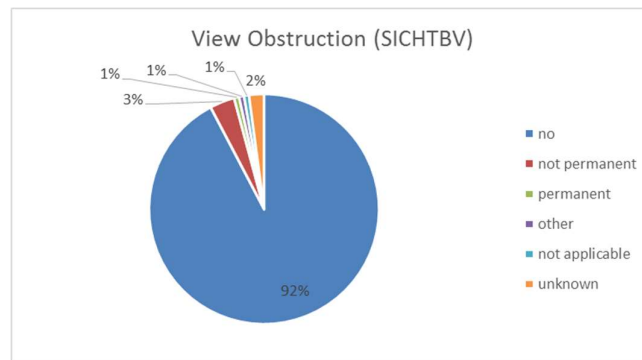


Figure 13: Distribution of view obstructions in UC_DEM_2.

Based on GIDAS coding, 92% of the UC_DEM_2 accidents happened without any relevant view obstruction. 46% of these cases were not detected before the collision, and mean TTC at detection of the VRU for the remaining accidents was 3.46s.

PROSPECT UC2 w/o view obstruction

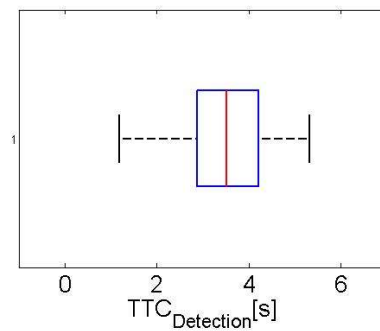


Figure 14: Box plot of detection times for UC_DEM_2 without view obstruction.

In 5% of the cases a view obstruction was present. 71% of these cases were not detected before the collision, and mean TTC at detection of the VRU for the remaining accidents was 2.83s.

PROSPECT UC2 w/ view obstruction

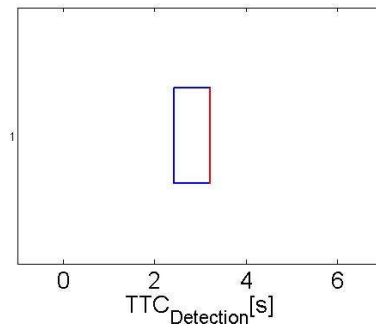


Figure 15: Box plot of detection times for UC_DEM_2 with view obstruction.

Collision speed:

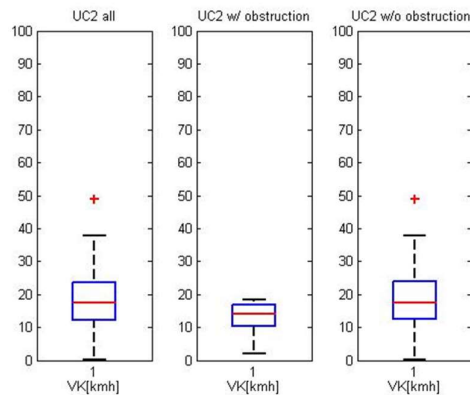


Figure 16: Boxplots of the collision speed of the vehicle in UC_DEM_2.

Figure 16 shows the box plots of the passenger car collision speed for all UC_DEM_2 accidents, differentiated between cases with and without view obstructions. There is no significant difference in the distribution of collision speeds based on view obstructions.

Table 4: Descriptive statistics of collision speed in UC_DEM_2.

	Collision speed [km/h]
Mean	18.0
5 th quantile	6.4
25 th quantile	12.3
75 th quantile	23.5
95 th quantile	30.3

Priority regulation:

In UC_DEM_2, 42% of the accidents happened at signalized intersections, while 34% of the passenger cars had to yield for crossing traffic.

Contact points:

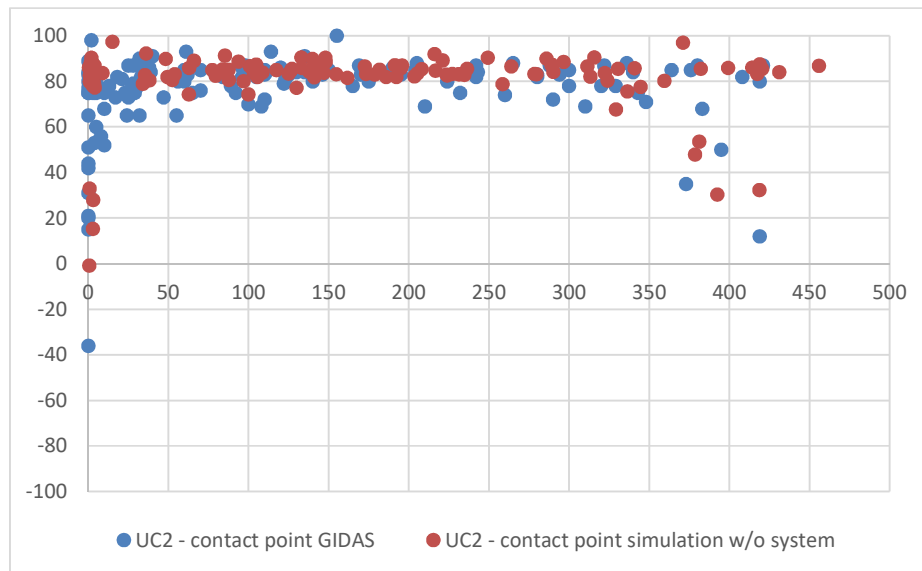


Figure 17: contact points from GIDAS and simulation in UC_DEM_2.

Based on the simulation, 37% of the accidents for UC_DEM_2 have a contact point at the front of the vehicle (within 15cm), mainly at the front right corner, while the remaining 63% of the accidents show a contact at the right side of the vehicle. In GIDAS, 21% of the according accidents have a contact point at the front of the vehicle (within 15cm).

2.1.4.3 UC_DEM_3

UC_DEM_3 describes a situation in which a car driver intends to go straight and a cyclist is crossing from the right side. The accident types 271B, 301A, 302A, 303A, 311A, 321B, 322B, 342B, 344B and 371B were identified to match this description. In total, 244 accidents were available in PCM.

271B	301A	302A	303A	311A
321B	322B	342B	344B	371B

Figure 18: Matched accident types for UC_DEM_3.

View obstruction:

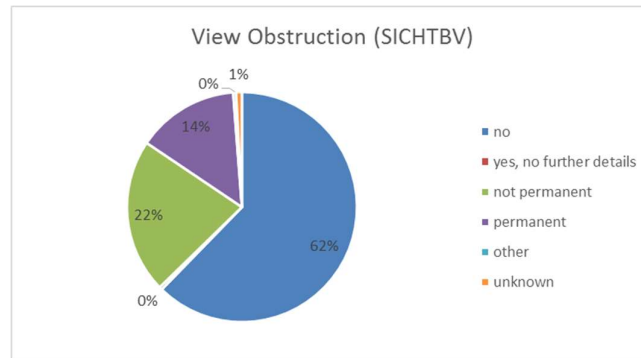


Figure 19: Distribution of view obstructions in UC_DEM_3.

Based on GIDAS coding, 62% of the UC_DEM_3 accidents happened without any relevant view obstruction, while 22% had non-permanent and 14% permanent view obstructions coded. 1% of cases w/o view obstruction were not detected before the collision, and the mean TTC at detection of the VRU for the remaining cases was 4.38s.

PROSPECT UC3 w/o view obstruction

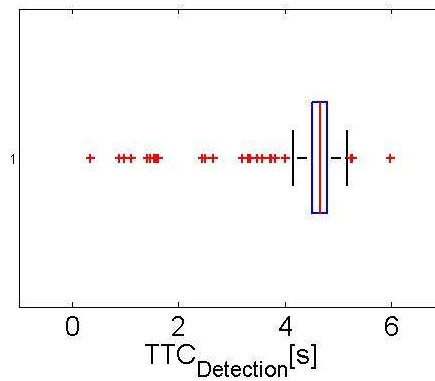


Figure 20: Box plot of detection times for UC_DEM_3 without view obstruction.

37% of the UC_DEM_3 accidents included a view obstruction. 1% of cases with a view obstruction were not detected before the collision, and the mean TTC at detection of the VRU for the remaining cases was 3.63s.

PROSPECT UC3 w/ view obstruction

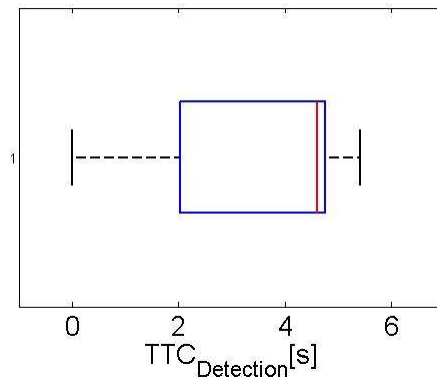


Figure 21: Box plot of detection times for UC_DEM_3 with view obstruction.

In conclusion, 62% of UC_DEM_3 cases have no view obstruction at all. For the remaining 37% of the cases with view obstructions, 75% of the VRUs can be detected at TTCs >2s. Collision speed:

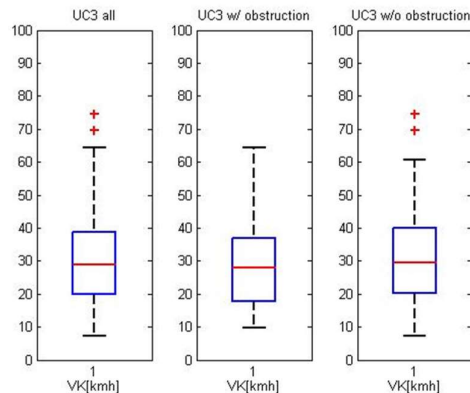


Figure 22: Box plots of the collision speed of the vehicle in UC_DEM_3

Figure 22 shows the box plots of the passenger car collision speed for all UC_DEM_3 accidents, differentiated between cases with and without view obstructions. There is no significant difference in the distribution of collision speeds based on view obstructions.

Table 5: Descriptive statistics of collision speed in UC_DEM_3.

	Collision speed [km/h]
Mean	30.3
5 th quantile	12.2
25 th quantile	20.0
75 th quantile	38.9

95 th quantile	50.7
---------------------------	------

Priority regulation:

In UC_DEM_3, 53% of the passenger cars had priority, while 22% had to give way to the right.
Contact points:

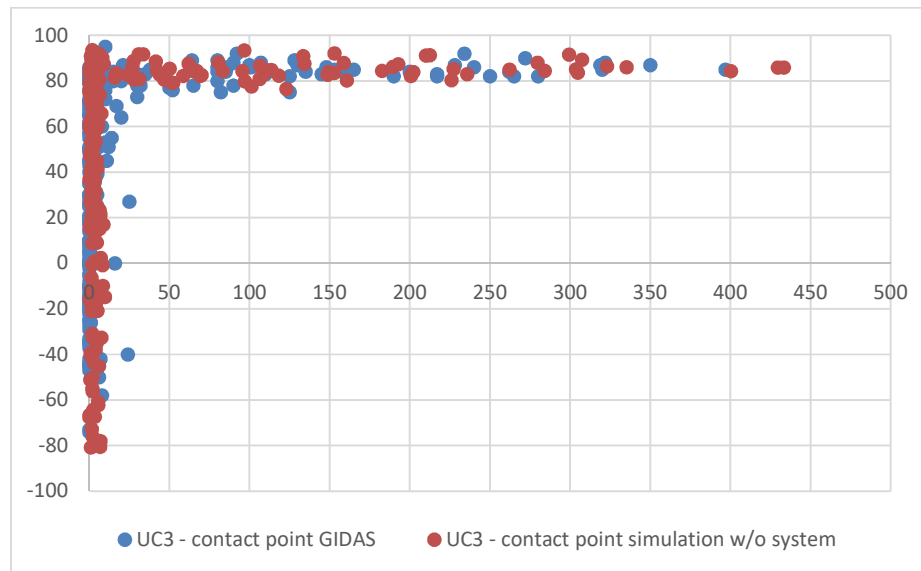


Figure 23: contact points from GIDAS and simulation in UC_DEM_3.

Based on the simulation, 73% of the according accidents have a contact point at the front of the vehicle (within 15cm). In GIDAS, 73% of the according accidents have a contact point at the front of the vehicle (within 15cm).

2.1.4.4 UC_DEM_4

UC_DEM_4 describes a situation in which a car intends to go straight, while a cyclist is crossing from the left side. The accident types 301B, 303B, 304B, 321A, 322A, 341B, 343B, 352B and 372B were identified to match this description. In total, 216 accidents were available in PCM.

301B	303B	304B	321A	322A
341B	343B	352B	372B	

Figure 24: Matched accident types for UC_DEM_4.

View obstruction:

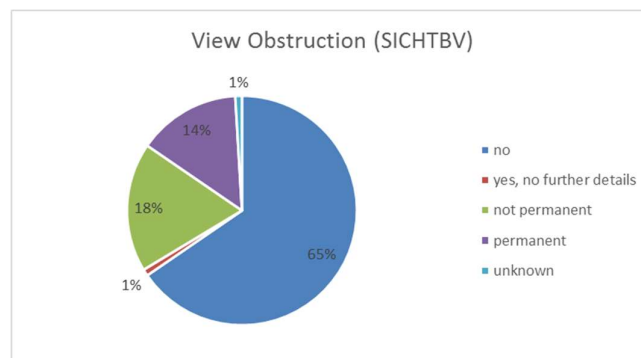


Figure 25: Distribution of view obstructions in UC_DEM_4.

Based on GIDAS coding, 65% of the UC_DEM_4 accidents happened without any relevant view obstruction, while 18% had non-permanent and 14% permanent view obstructions coded.

Of the cases without view obstruction (65%), 1% were not detected before the collision; mean TTC at detection of the VRU for the remaining accidents was 4.27s.

PROSPECT UC4 w/o view obstruction

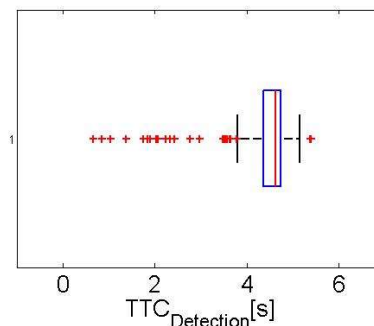


Figure 26: Box plot of detection times for UC_DEM_4 without view obstruction.

Of the cases with view obstruction (34%), 1% were not detected before the collision and mean TTC at detection of the VRU for the remaining accidents was 3.37s.

PROSPECT UC4 w/ view obstruction

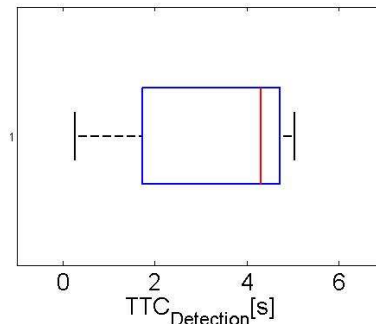


Figure 27: Box plot of detection times for UC_DEM_4 with view obstruction.

In conclusion, 65% UC_DEM_4 cases have no view obstruction at all. For the remaining 34% of the cases with view obstructions, 75% of the VRUs can be detected at a TTC >2s.

Collision speed:

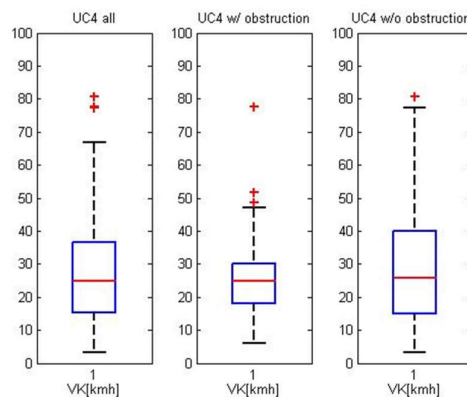


Figure 28: Box plots of the collision speed of the vehicle in UC_DEM_4.

Figure 28 shows the box plots of the passenger car collision speed for all UC_DEM_4 accidents, differentiated between cases with and without view obstructions. There is no significant difference in the distribution of collision speeds based on view obstructions.

Table 6: Descriptive statistics of collision speed in UC_DEM_4.

	Collision speed [km/h]
Mean	27.4
5 th quantile	7.6

25 th quantile	15.2
75 th quantile	36.6
95 th quantile	49.9

Priority regulation:

In UC_DEM_4, 33% of the passenger cars had priority, 32% had to give way to the right and further 21% had to yield for crossing traffic.

Contact points:

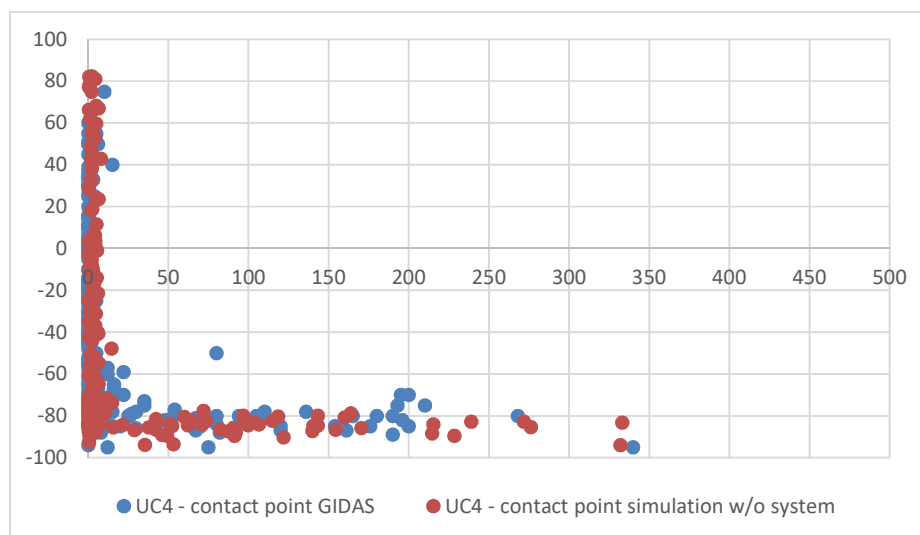


Figure 29: contact points from GIDAS and simulation in UC_DEM_4.

Based on the simulation, 77% of the according accidents have a contact point at the front of the vehicle (within 15cm). In GIDAS, 77% of the according accidents have a contact point at the front of the vehicle (within 15cm).

2.1.4.5 UC_DEM_5

UC_DEM_5 describes a situation in which a car intends to turn right and a cyclist is crossing from the right sided sidewalk (against travel direction). The accident type 342B was identified to match this description. In total, 496 accidents were available in PCM.

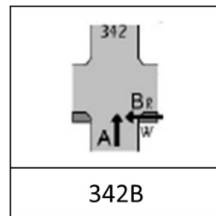


Figure 30: Matched accident types for UC_DEM_5.

View obstruction:

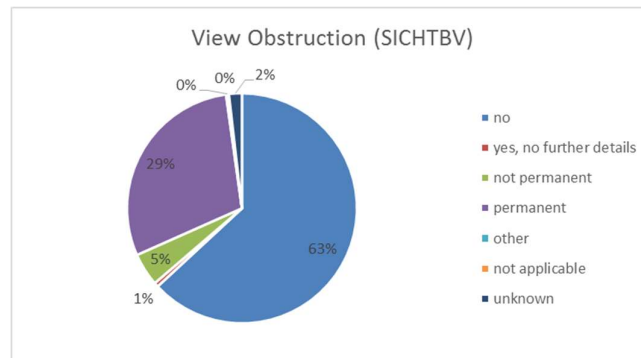


Figure 31: Distribution of view obstructions in UC_DEM_5

Based on GIDAS coding, 63% of the UC_DEM_5 accidents happened without any relevant view obstruction, while 5% had non-permanent and 29% permanent view obstructions coded.

Of the cases without view obstruction (63%), all cases were detected before the collision and mean TTC at detection of the VRU was 3.94s.

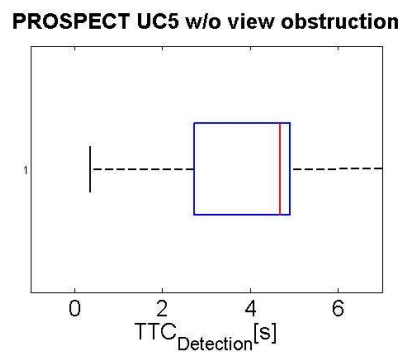


Figure 32: Box plot of detection times for UC_DEM_5 without view obstruction.

Also, all cases with a view obstruction (35%) were detected before the collision and mean TTC at detection of the VRU was 3.02s.

PROSPECT UC5 w/ view obstruction

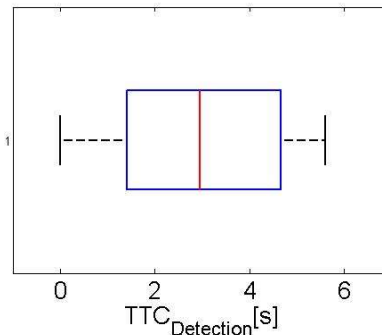


Figure 33: Box plot of detection times for UC_DEM_5 with view obstruction.

Collision speed:

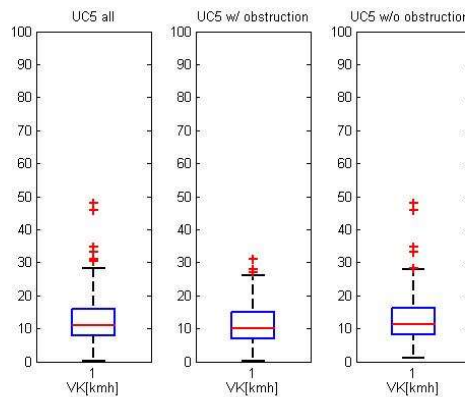


Figure 34: Box plots of the collision speed of the vehicle in UC_DEM_5.

Figure 34 shows the box plots for the passenger cars collision speed for all UC_DEM_5 accidents and differentiated between cases with and without view obstructions. There is no significant difference in the distribution of collision speeds based on view obstructions.

Table 7: Descriptive statistics of collision speed in UC_DEM_5.

	Collision speed [km/h]
Mean	12.3
5 th quantile	3.3
25 th quantile	7.8
75 th quantile	16.0
95 th quantile	24.0

Priority regulation:

In UC_DEM_5, 61% of the passenger cars had to yield for crossing traffic, while 24% underlay the German traffic law §10 StVO ("Straßenverkehrsordnung" - the vehicle has to yield for crossing traffic coming from parking lots over a sidewalk).

Contact points:

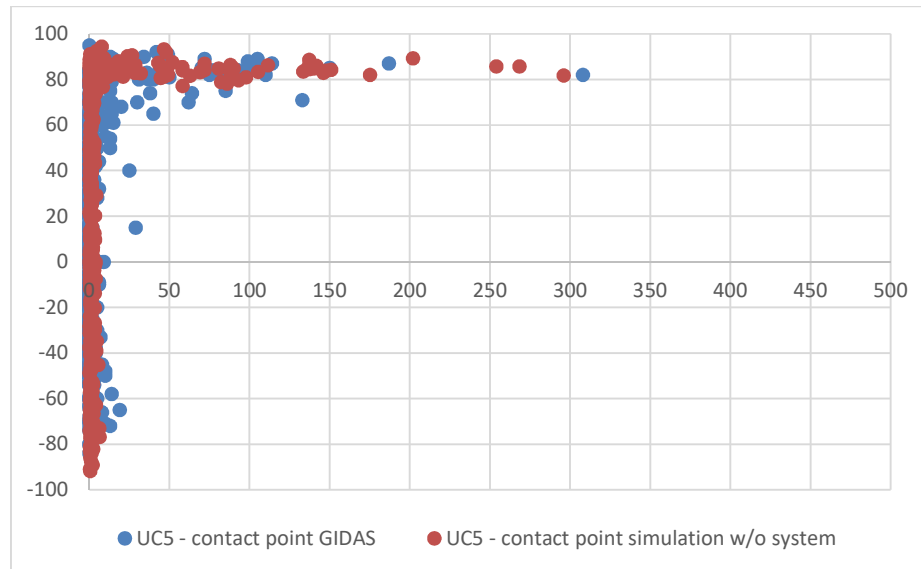


Figure 35: contact points from GIDAS and simulation in UC_DEM_5.

Based on the simulation, 87% of the according accidents have a contact point at the front of the vehicle (within 15cm). In GIDAS, 90% of the according accidents have a contact point at the front of the vehicle (within 15cm).

2.1.4.6 UC_DEM_6

UC_DEM_6 describes a situation, in which a car intends to turn left and a cyclist is crossing from the left side. The accident types 261A, 301B, 302B, 321A and 341B were identified to match this description. In total, 105 accidents were available in PCM.

261A	301B	302B
321A	341B	

Figure 36: Matched accident types for UC_DEM_6. [View obstruction:](#)

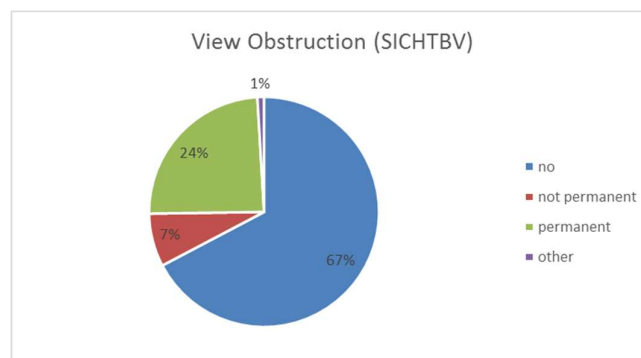


Figure 37: Distribution of view obstructions in UC_DEM_6.

Based on GIDAS coding, 67% of the UC_DEM_6 accidents happened without any relevant view obstruction, while 7% had non-permanent and 24% permanent view obstructions coded.

All UC_DEM_6 cases without view obstruction (67%) were detected before the collision and mean TTC at detection of the VRU was 4.24s.

PROSPECT UC6 w/o view obstruction

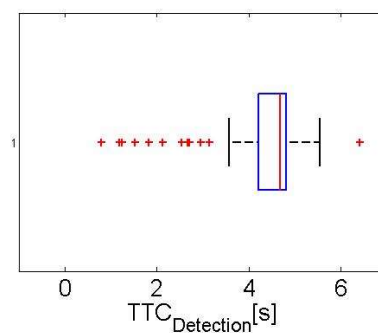


Figure 38: Box plot of detection times for UC_DEM_6 without view obstruction.

Also, all UC_DEM_6 cases with view obstruction (33%) were detected before the collision and mean TTC at detection of the VRU was 3.30s.

PROSPECT UC6 w/ view obstruction

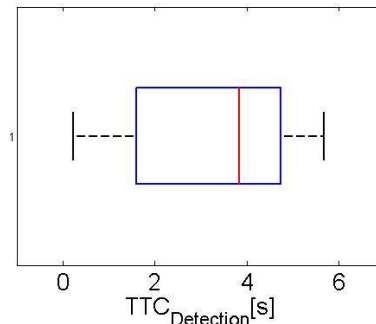


Figure 39: Box plot of detection times for UC_DEM_6 with view obstruction.

Collision speed:

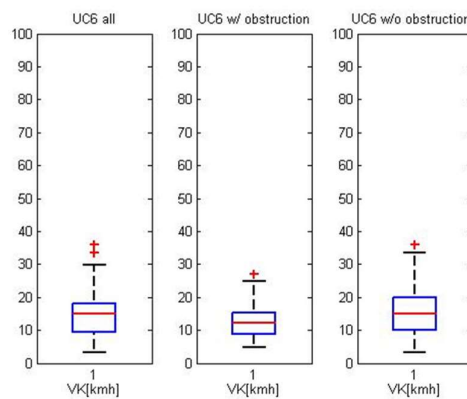


Figure 40: Box plots of the collision speed of the vehicle in UC_DEM_6.

Figure 40 shows the box plots of the passenger car collision speed for all UC_DEM_6 accidents, differentiated between cases with and without view obstructions. There is no significant difference in the distribution of collision speeds based on view obstructions.

Table 8: Descriptive statistics of collision speed in UC_DEM_6.

	Collision speed [km/h]
Mean	14.5
5 th quantile	4.9
25 th quantile	9.5
75 th quantile	18.2
95 th quantile	26.9

Priority regulation:

In UC_DEM_6, 66% of the passenger cars had to yield for crossing traffic, while 14% underlay the German traffic law §10 StVO (the vehicle has to yield for crossing traffic coming from parking lots over a sidewalk).

Contact points:

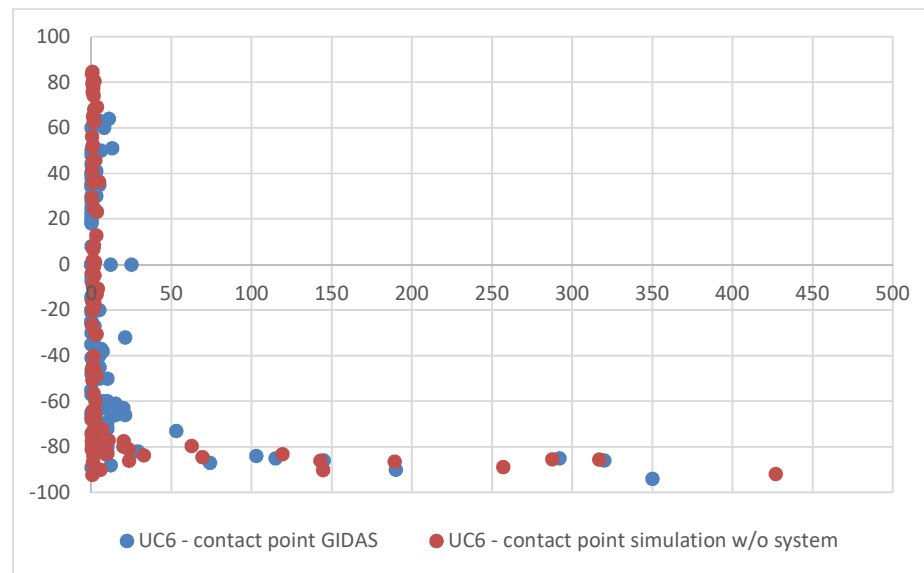


Figure 41: contact points from GIDAS and simulation in UC_DEM_6.

Based on the simulation, 85% of the according accidents have a contact point at the front of the vehicle (within 15cm). In GIDAS, 85% of the according accidents have a contact point at the front of the vehicle (within 15cm).

2.1.4.7 UC_DEM_7

UC_DEM_7 describes a situation in which a cyclist is approaching from behind on the driver side of the vehicle and collides with the opened door. These situations are not included in the PCM.

2.1.4.8 UC_DEM_8

UC_DEM_8 describes a situation in which a cyclist is approaching from behind on the passenger side of the vehicle and collides with the opened door. These situations are not included in the PCM.

2.1.4.9 UC_DEM_9

UC_DEM_9 describes a situation in which a car approaches a cyclist from behind and rear-ends the cyclist. The accident types 201B, 321B and 601B were identified to match this description. In total, 21 accidents were available in PCM.

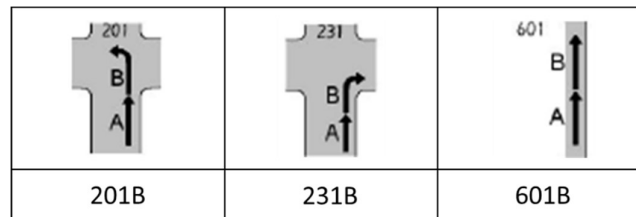


Figure 42: Matched accident types for UC_DEM_9.

View obstruction:

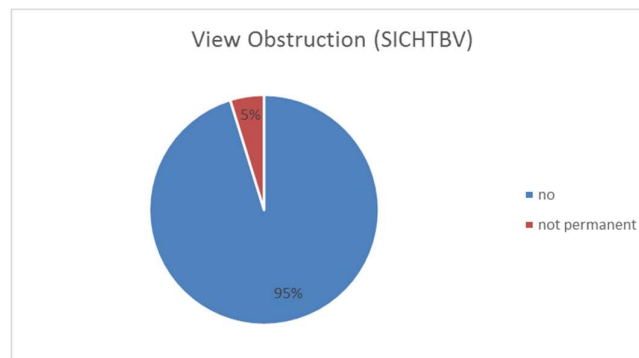


Figure 43: Distribution of view obstructions in UC_DEM_9.

Based on GIDAS coding, 95% of the UC_DEM_9 accidents happened without any relevant view obstruction.

All cases in UC_DEM_9 without a view obstruction (95%) were detected before the collision, and mean TTC at detection of the VRU was 4.71s.

PROSPECT UC9 w/o view obstruction

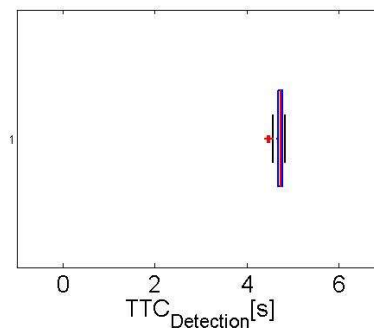


Figure 44: Box plot of detection times for UC_DEM_9 without view obstruction.

Similarly, all cases in UC_DEM_9 with view obstruction (5%) were detected before the collision and mean TTC at detection of the VRU was 4.78s.

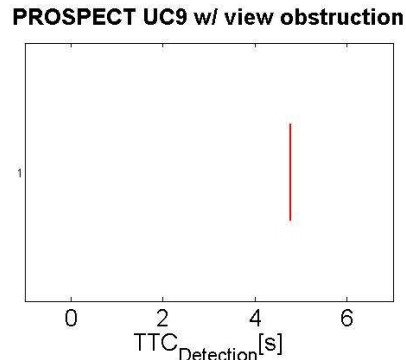


Figure 45: Box plot of detection times for UC_DEM_9 with view obstruction.

Collision speed:

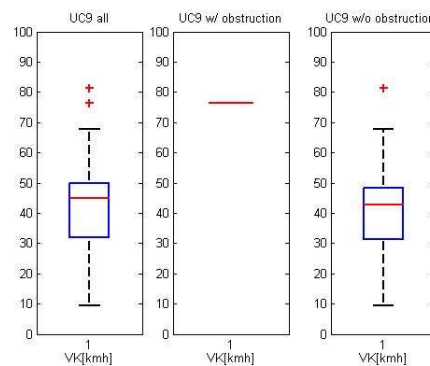


Figure 46: Boxplots of the collision speed of the vehicle in UC_DEM_9.

Figure 46 shows the box plots of the passenger car collision speed for all UC_DEM_9 accidents, differentiated between cases with and without view obstructions. As there are only 5% of the cases with view obstructions, no statistical analysis is possible for that case.

Table 9: Descriptive statistics of collision speed in UC_DEM_9.

	Collision speed [km/h]
Mean	42.6
5 th quantile	18.0
25 th quantile	32.0
75 th quantile	49.7
95 th quantile	78.6

Contact points:

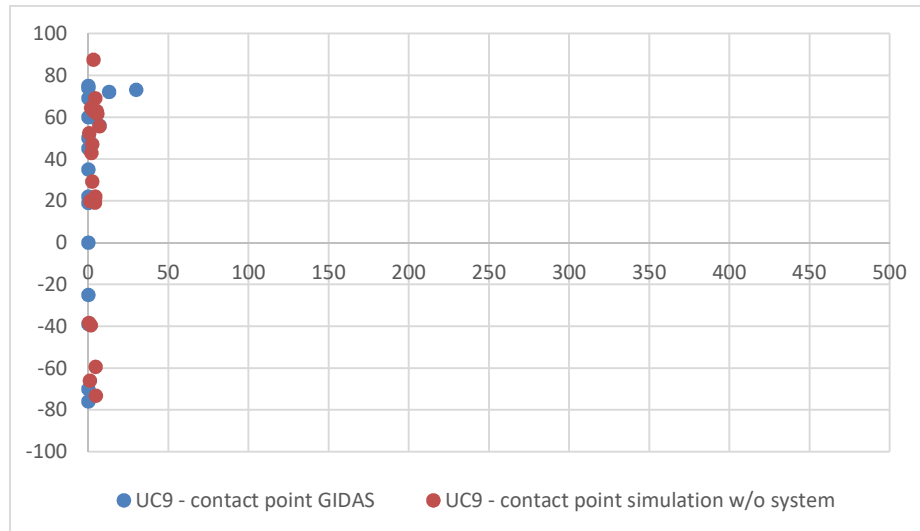


Figure 47: contact points from GIDAS and simulation in UC_DEM_9.

Based on the simulation, 100% of the according accidents have a contact point at the front of the vehicle (within 15cm). In GIDAS, 95% of the according accidents have a contact point at the front of the vehicle (within 15cm).

2.1.4.10 UC_DEM_10

UC_DEM_10 describes a situation in which a pedestrian is crossing from the right side independently from the car's manoeuvre intention. The accident types 421B, 451B, 452B, 471B, 492B and 493B were identified to match this description. In total, 342 accidents were available in PCM.

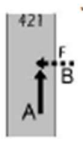




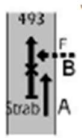
		
421B	451B	452B
		
471B	492B	493B

Figure 48: Matched accident types for UC_DEM_10.

View obstruction:

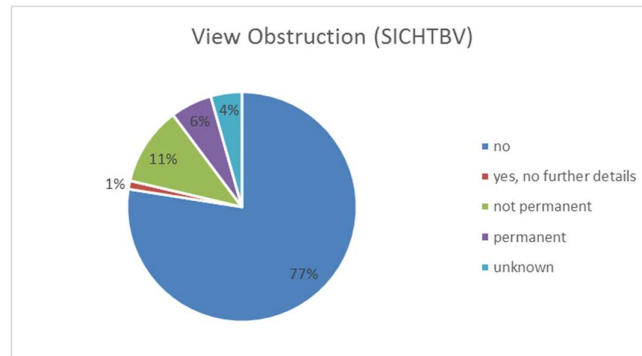


Figure 49: Distribution of view obstructions in UC_DEM_10.

Based on GIDAS coding, 77% of the UC_DEM_10 accidents happened without any relevant view obstruction, while 11% had non-permanent and 6% permanent view obstructions coded.

All UC_DEM_10 cases without view obstruction (77%) were detected before the collision, and mean TTC at detection of the VRU was 4.40s.

PROSPECT UC10 w/o view obstruction

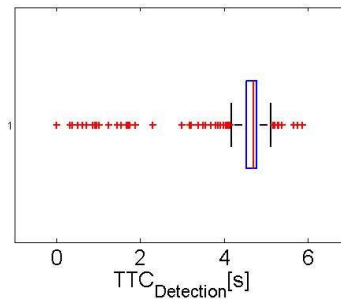


Figure 50: Box plot of detection times for UC_DEM_10 without view obstruction.

Of the UC_DEM_10 cases without view obstruction (18%), 2% were not detected before the collision; the mean TTC at detection of the VRU for the remaining accidents was 4.05s.

PROSPECT UC10 w/ view obstruction

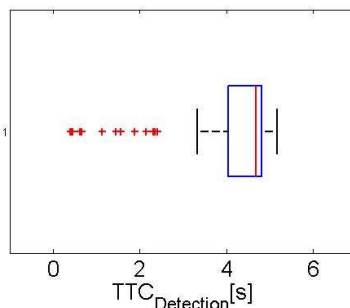


Figure 51: Box plot of detection times for UC_DEM_10 with view obstruction.

Collision speed:

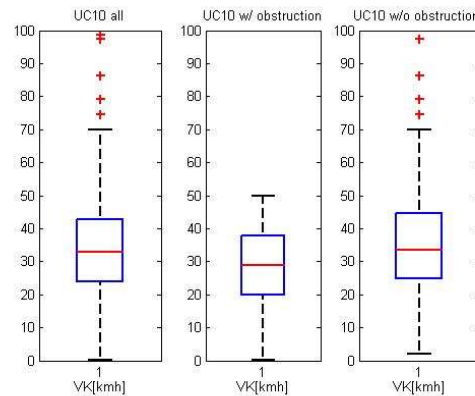


Figure 52: Box plots of the collision speed of the vehicle in UC_DEM_10.

Figure 52 shows the box plots of the passenger car collision speed for all UC_DEM_10 accidents, differentiated between cases with and without view obstructions. There is no significant difference in the distribution of collision speeds based on view obstructions.

Table 10: Descriptive statistics of collision speed in UC_DEM_10.

	Collision speed [km/h]
Mean	33.4
5 th quantile	6.0
25 th quantile	24.0
75 th quantile	42.9
95 th quantile	58.7

Contact points:

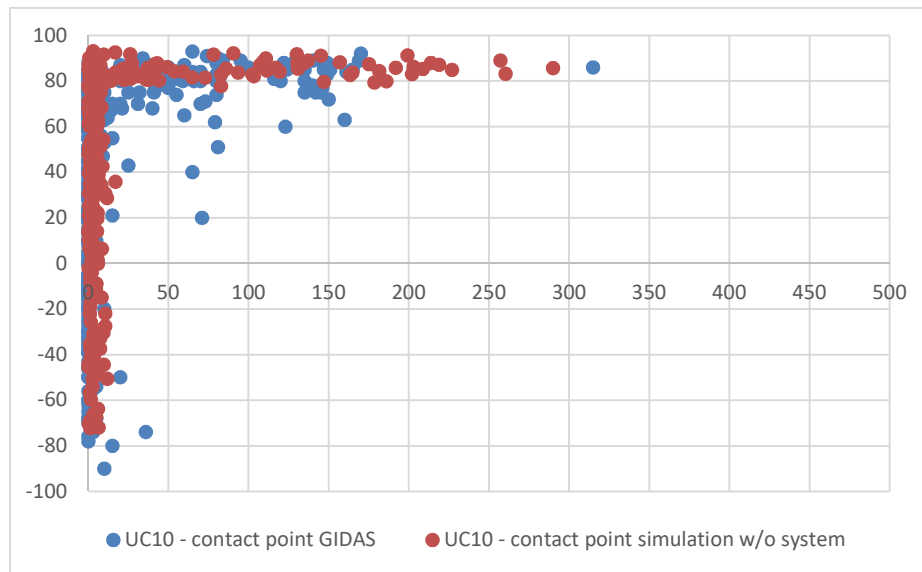


Figure 53: contact points from GIDAS and simulation in UC_DEM_10.

Based on the simulation, 80% of the according accidents have a contact point at the front of the vehicle (within 15cm). In GIDAS, 73% of the according accidents have a contact point at the front of the vehicle (within 15cm).

2.1.4.11 UC_DEM_11

UC_DEM_11 describes a situation in which a pedestrian is crossing from the right side from an obstructed view independently from the car's manoeuvre intention. The accident types 422B, 423B, 424B, 453B, 454B, 472B and 473B were identified to match this description. In total, 216 accidents were available in PCM. It has to be noted, that even though the accident type indicates view obstructions, not all of those accidents involved a view obstruction. The percentage of accidents without view obstruction can be found in Figure 55.








			
422B	423B	424B	453B
			
454B	472B	473B	

Figure 54: Matched accident types for UC_DEM_11.

View obstruction:

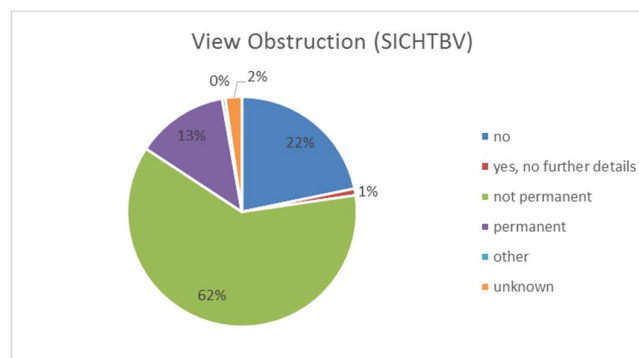


Figure 55: Distribution of view obstructions in UC_DEM_11.

Based on GIDAS coding, 22% of the UC_DEM_11 accidents happened without any relevant view obstruction, while 62% had non-permanent and 13% permanent view obstructions coded.

All UC_DEM_11 cases without view obstruction (22%) were detected before the collision. The mean TTC at detection of the VRU was 3.84s.

PROSPECT UC11 w/o view obstruction

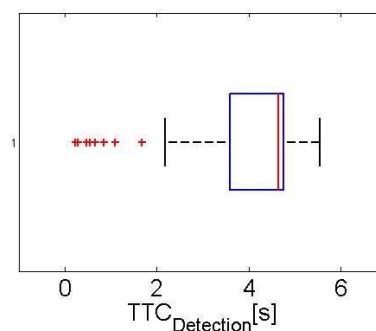


Figure 56: Box plot of detection times for UC_DEM_11 without view obstruction.

Of the UC_DEM_11 cases with view obstruction (76%), 1% were not detected before the collision. The mean TTC at detection of the VRU for the remaining accidents was 3.57s.

PROSPECT UC11 w/ view obstruction

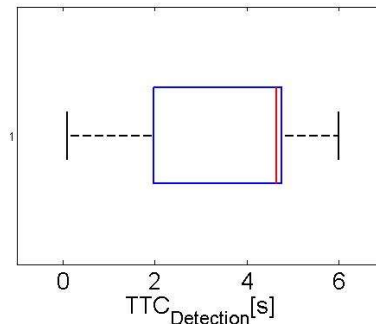


Figure 57: Boxplot of detection times for UC_DEM_11 with view obstruction.

Collision speed:

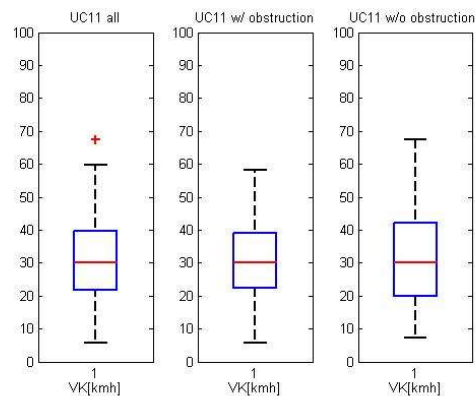


Figure 58: Box plots of the collision speed of the vehicle in UC_DEM_11.

Figure 58 shows the box plots of the passenger car collision speed for all UC_DEM_11 accidents, differentiated between cases with and without view obstructions. There is no significant difference in the distribution of collision speeds based on view obstructions.

Table 11: Descriptive statistics of collision speed in UC_DEM_11.

	Collision speed [km/h]
Mean	30.6
5 th quantile	9.4
25 th quantile	21.8
75 th quantile	39.8
95 th quantile	50.5

Contact points:

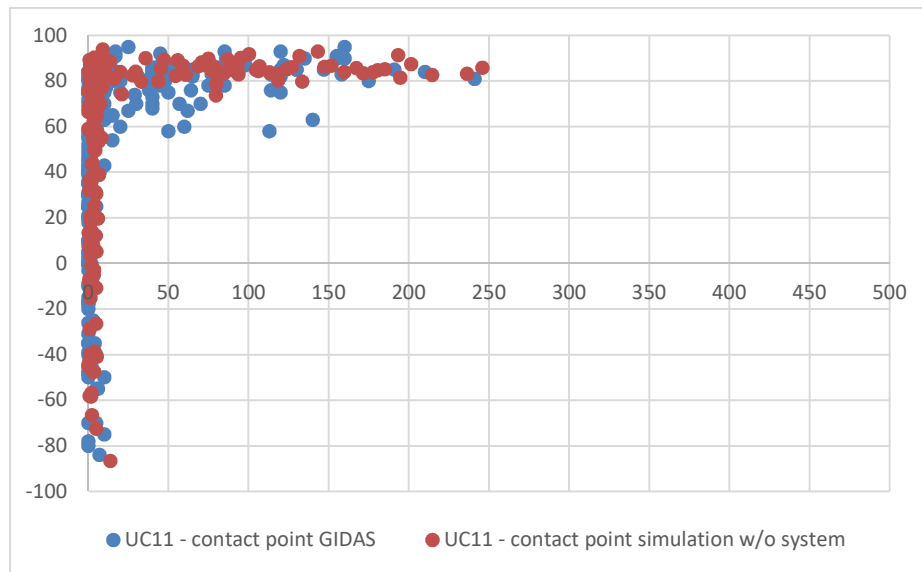


Figure 59: contact points from GIDAS and simulation in UC_DEM_11.

Based on the simulation, 72% of the according accidents have a contact point at the front of the vehicle (within 15cm). In GIDAS, 63% of the according accidents have a contact point at the front of the vehicle (within 15cm).

2.1.4.12 UC_DEM_12

UC_DEM_12 describes a situation in which a car is approaching a pedestrian from behind. The accident types 101, 141, 583B, 671B, 674B and 679B were identified to match this description. In total, 20 accidents were available in PCM.

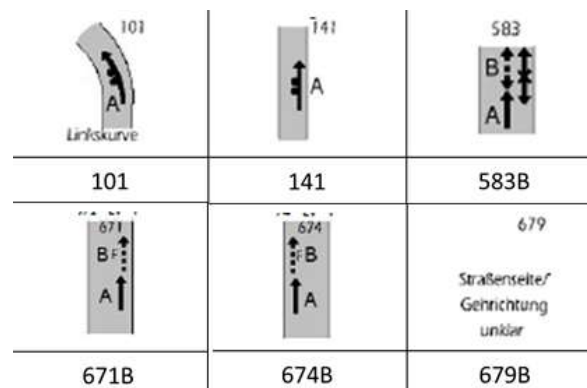


Figure 60: Matched accident types for UC_DEM_12.

View obstruction:

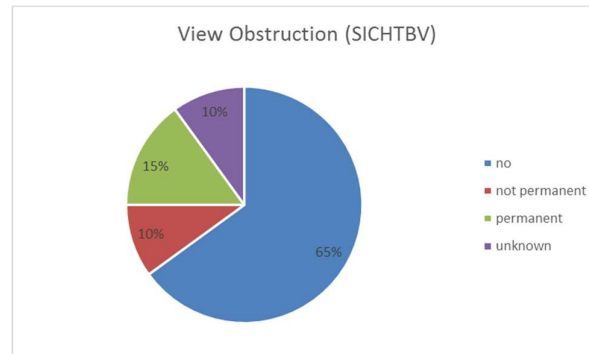


Figure 61: Distribution of view obstructions in UC_DEM_12.

Based on GIDAS coding, 65% of the UC_DEM_12 accidents happened without any relevant view obstruction, while 10% had non-permanent and 15% permanent view obstructions coded.

All UC_DEM_12 cases without view obstruction (65%) were detected before the collision. The mean TTC at detection of the VRU was 4.78s.

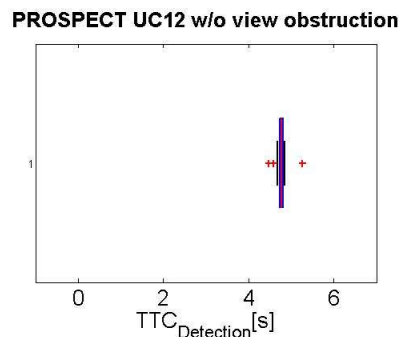


Figure 62: Box plot of detection times for UC_DEM_12 without view obstruction.

Also, all UC_DEM_12 cases with view obstruction (25%) were detected before the collision, and the mean TTC at detection of the VRU was 3.60s.

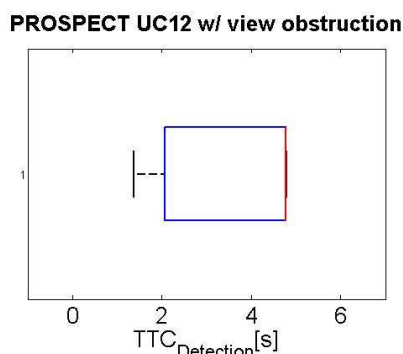


Figure 63: Boxplot of detection times for UC_DEM_12 with view obstruction.

Collision speed:

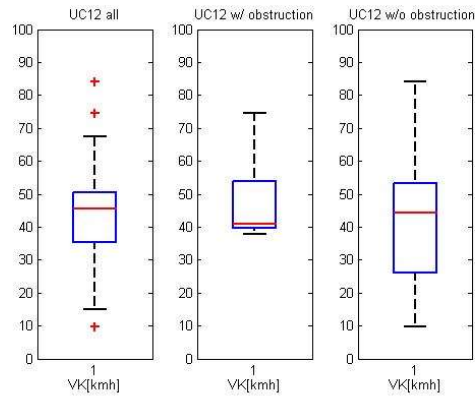


Figure 64: Box plots of the collision speed of the vehicle in UC_DEM_12.

Figure 64 shows the boxplots of the passenger car collision speed for all UC_DEM_12 accidents, differentiated between cases with and without view obstructions. There is no significant difference in the distribution of collision speeds based on view obstructions.

Table 12: Descriptive statistics of collision speed in UC_DEM_12.

	Collision speed [km/h]
Mean	44.2
5 th quantile	12.3
25 th quantile	35.4
75 th quantile	50.4
95 th quantile	79.3

Contact points:

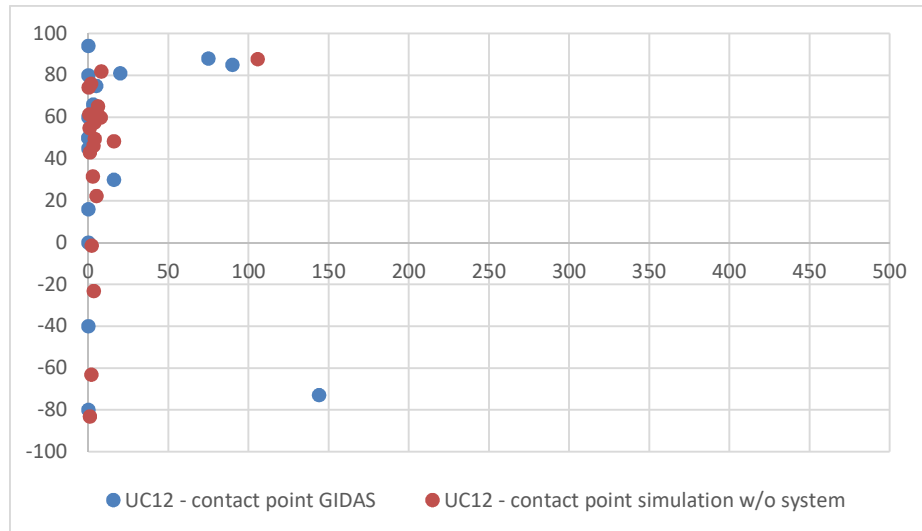


Figure 65: contact points from GIDAS and simulation in UC_DEM_12.

Based on the simulation, 89% of the according accidents have a contact point at the front of the vehicle (within 15cm). In GIDAS, 74% of the according accidents have a contact point at the front of the vehicle (within 15cm).

2.2 WHAT-IF SIMULATION

This section describes the implemented systems' algorithms and the simulation tools used for counterfactual simulations.

2.2.1 System algorithms

There are 4 systems algorithms implemented, described in the following sections.

2.2.1.1 Sensor

The complete sensor set from the demonstrator cars is simplified for simulation purposes. It is modelled as a single sensor cone covering the opening angles of all considered sensors with the following parameters:

- Opening angle 200°
- Mounted at mid front bumper
- Range 120m
- Angle step size: 0.25°
- Acquisition time: 200ms
- Tracking time: 200ms
- Cycle time: 50ms
- Detection mode: Complete mode, no bicycle mode (i.e. all 4 corners of the bounding boxes have to be within the field of view for detection).

2.2.1.2 Brake

The emergency brake is simulated with the following parameters:

- Comfort brake:

- Gradient 20m/s³
- Max. deceleration 4m/s²
- Emergency brake:
 - Gradient 20m/s³
 - Max. deceleration 9m/s²
- Lag time: 300ms (only applicable, if the brake is not yet applied by the driver in the original collision)

2.2.1.3 Algorithm 1: Time to Collision (TTC)

The first algorithm takes into account the time to collision based on relative distance and relative velocity of both participants (passenger car and VRU).

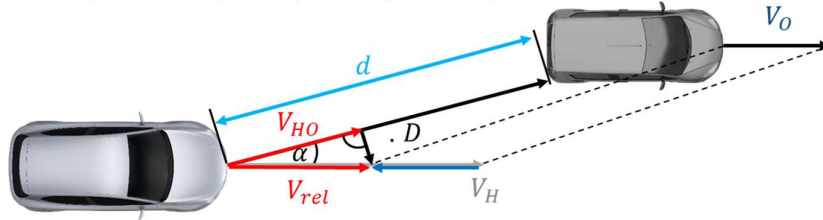


Figure 66: Time to Collision (TTC).

The calculated TTC is used as a trigger for different brake manoeuvres, if the VRU is detected from the sensor. The maximum requested deceleration of the car ($a_{passenger\ car}$) depends on the calculated TTC:

$$a_{passenger\ car} = \begin{cases} 0, & TTC > 1.5s \\ -4 \frac{m}{s^2}, & 0.5 < TTC \leq 1.5s \\ -9 \frac{m}{s^2}, & 0 < TTC \leq 0.5s \end{cases}$$

If the TTC is higher than 1.5s, no braking is activated. As soon as the TTC goes below 1.5s, a comfort brake of 4m/s² is activated and the deceleration is further increased to 9m/s², if the TTC goes below 0.5s.

2.2.1.4 Algorithm 2: Unavoidability with maximum evasive manoeuvres of both participants

The second algorithm uses an unavoidability criterion combined with the TTC from algorithm 1.

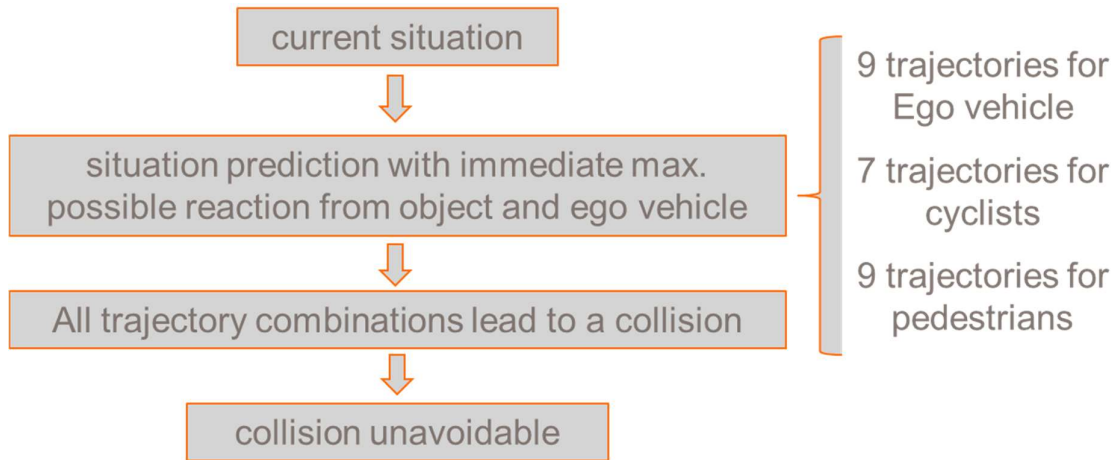


Figure 67: Work flow of Algorithm 2.

In every time step, the algorithm predicts trajectories for the vehicle, as well as for the VRU for the duration of 3 seconds. The trajectories are based on the concept of the “Kammscher Kreis” (circle of forces), see Figure 68.

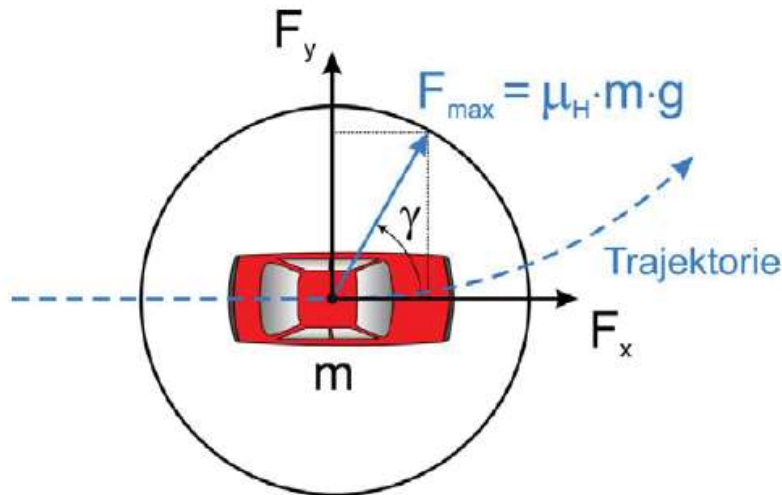


Figure 68: Trajectory model based on the Kammscher Kreis (Dirndorfer, 2015).

For passenger cars as well as for pedestrians, nine different states are modelled for γ values between 0° and 360° in 45° steps, where for example $\gamma = 0^\circ$ represents a full acceleration manoeuvre, $\gamma = 90^\circ$ a maximum steering manoeuvre to the left, $\gamma = 180^\circ$ a full brake manoeuvre and $\gamma = 270^\circ$ a maximum manoeuvre to the right (Dirndorfer, 2015). In addition to these eight manoeuvre combinations, it is also considered, that the passenger car/pedestrian does not change their current manoeuvre leading to a “no change” trajectory.

For cyclists it is assumed, that due to physical interaction between the cyclist’s knees and the handlebar, the combined trajectory of full acceleration and full steering is not possible (see Figure 69).

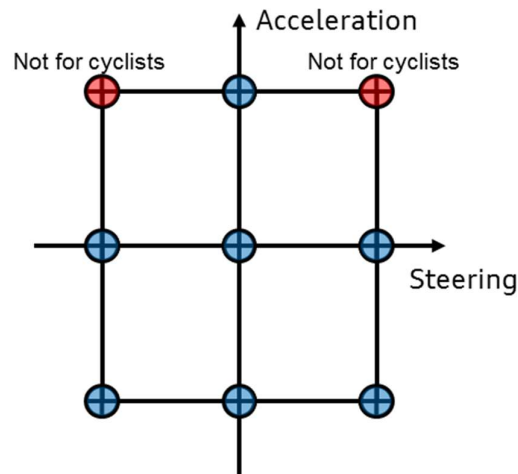


Figure 69: Trajectory model.

The possible trajectories are furthermore restricted by a defined turning radius, as follows.

- Passenger car trajectories:
 - 9 states (combination of deceleration, steering, acceleration and no change)
 - Turning radius: 10 m
 - Max. deceleration: $9.81 \text{ m/s}^2 * \mu$
- Pedestrian trajectories:
 - 9 states (combination of deceleration, steering, acceleration and no change)
 - Turning radius: 0.5 m
 - Max. velocity: 5 m/s
 - Max. deceleration: 8 m/s^2
- Cyclist trajectories:
 - 7 states (combination of deceleration, steering, acceleration and no change without steering & acceleration)
 - Turning radius: 3.9 m
 - Max. deceleration: $9.81 \text{ m/s}^2 * \mu$

If all combinations of the predicted trajectories lead to a collision within the next 3 seconds, the collision is defined as unavoidable.

The calculated TTC combined with unavoidability is used as a trigger for different brake manoeuvres, if the VRU is detected from the sensor. The maximum requested deceleration of the car ($a_{\text{passenger car}}$) depends on the calculated TTC:

$$a_{passenger\ car} = \begin{cases} 0, & TTC > 1.5s \\ -4 \frac{m}{s^2}, & 0.5 < TTC \leq 1.5s \\ -9 \frac{m}{s^2}, & 0 < TTC \leq 0.5s \text{ and unavoidable} \end{cases}$$

If the TTC is higher than 1.5s, no braking is activated. As soon as the TTC goes below 1.5s, a comfort brake of 4m/s² is activated and the deceleration is further increased to 9m/s², if the TTC goes below 0.5s and the collision is predicted as unavoidable.

2.2.1.5 Algorithm 3: Unavoidability with maximum evasive manoeuvres of the passenger car

The third algorithm uses an unavoidability criterion combined with the TTC from algorithm 1.

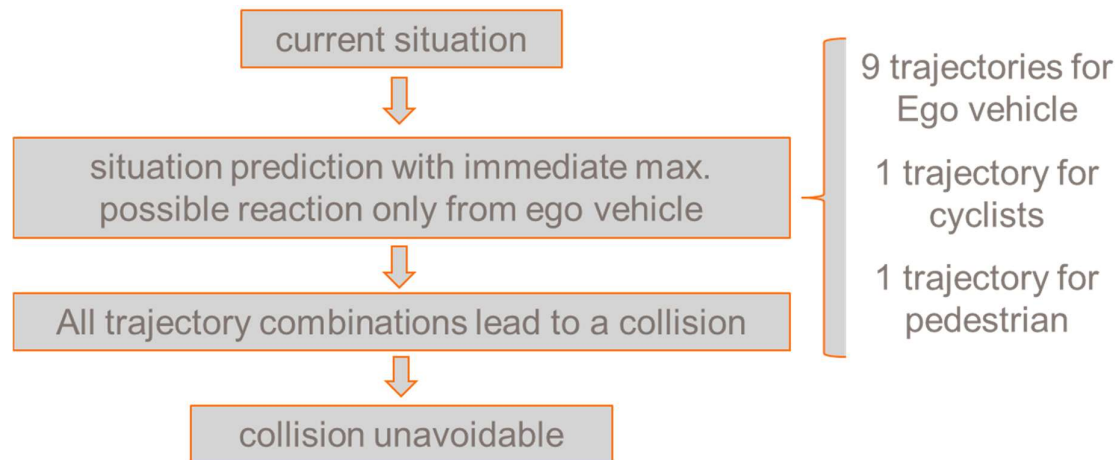


Figure 70. Work flow of Algorithm 3.

In every time step, the algorithm predicts trajectories for the vehicle for the next 3 seconds. The algorithm uses the following parameters to define the maximum evasive manoeuvres depending on the type of road users (see Figure 70):

- Passenger car trajectories:
 - 9 states (combination of deceleration, steering, acceleration and no change)
 - Turning radius: 10 m
 - Max. deceleration: 9.81 m/s² * μ

- Pedestrian trajectories:
 - 1 state (no change)
- Cyclist trajectories:
 - 1 state (no change)

If all combinations of the predicted trajectories lead to a collision within the next 3 seconds, the collision is defined as unavoidable.

The calculated TTC combined with unavoidability is used as a trigger for different brake manoeuvres, if the VRU is detected from the sensor. The maximum requested deceleration of the car ($a_{passenger\ car}$) depends on the calculated TTC:

$$a_{passenger\ car} = \begin{cases} 0, & TTC > 1.5s \\ -4 \frac{m}{s^2}, & 0.5 < TTC \leq 1.5s \\ -9 \frac{m}{s^2}, & 0 < TTC \leq 0.5s \text{ and } unavoidable \end{cases}$$

If the TTC is higher than 1.5s, no braking is activated. As soon as the TTC goes below 1.5s, a comfort brake of 4m/s² is activated and the deceleration is further increased to 9m/s², if the TTC goes below 0.5s and the collision is predicted as unavoidable.

2.2.1.6 Algorithm 4: Steering and braking

The algorithm calculates in every time step the risk of a collision and evaluates the criticality in lateral and longitudinal direction in terms of required accelerations for avoidance (Boliang, 2016). If those criticality values are above a certain threshold, the algorithm evaluates if the collision can be avoided by braking only. In this case, the brake manoeuvre is initiated. If the collision can no longer be avoided by braking only, the algorithm evaluates if a steering manoeuvre is possible. In this case, the steering manoeuvre is initiated. If the collision can't be avoided by braking or steering, a crash mitigating brake manoeuvre is initiated to reduce collision speed as much as possible. The what-if simulation with this algorithm are made without a detailed driver model. The driver model can influence by braking or steering the outcome of the interventions in the simulated scenario. The influence of the driver reaction is mainly in the longitudinal scenarios when the driver has time to react, for example, to FCW warning.

2.2.2 Simulation with rateEFFECT

In order to simulate the changes of the accident scenarios caused by the defined systems, the rateEFFECT tool is used (Wille, Jungbluth, Kohsiek, & Zatloukal, 2012). The tool utilizes PC-Crash as simulation core (see Figure 71).

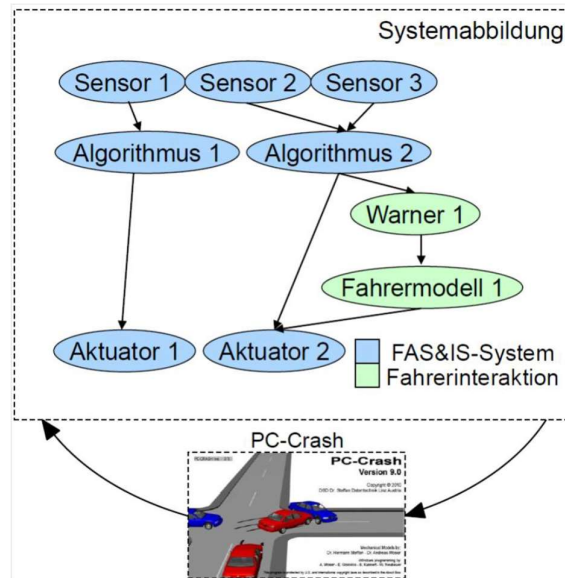


Figure 71: Schematic of systems in rateEFFECT (Wille, Jungbluth, Kohsiek, & Zatloukal, 2012).

Every accident is simulated in the loop. That means that information from PC-Crash about both accident participants as well as the environment is extracted in every time step and forwarded to the sensor module. The sensor module converts the information and sends it to the algorithm module. Based on the algorithm, different actuators are triggered. The resulting changes are then simulated for the next time step in PC-Crash until the collision is avoided or a collision appears (Schneider, 2015).

2.2.3 Simulation with openPASS

Virtual re-simulation based on reconstructed accident trajectories may show if a system had affected particular accidents on a case-by-case basis. However, reconstruction relies on limited traces and does not cover the complete traffic situation. Next to the accident re-simulation approach, the ISO Technical Report /NP 21934-1 (ISO/NP 21934-1 ISO/TC 22 SC36 WG7, 2018) defines also a stochastic approach to investigate a technology's impact on traffic safety. The stochastic traffic simulation bases on distributions of accident data and can model how conflicts emerge and how to avoid or mitigate them. However, their exposure in real world traffic systems is not known.

A novel open-source platform, openPASS (**Open** Platform for **A**ssessment of **S**afety **S**ystems (openPASS, 2018)), based on an initiative of BMW, Daimler and Volkswagen and in accordance with the P.E.A.R.S. (Prospective Effectiveness Assessment for Road Safety (Yves, et al., 2015)) approach, is being developed. This open-source initiative runs under the infrastructure of an Eclipse foundation. openPASS has the objective to provide a platform to configure and run multi-agent, microscopic traffic simulation with stochastic scenarios. It is designed to apply this holistic methodology of ADAS safety assessment in a comprehensive way. A functional framework is implemented for a reliable, state-of-the-art and standardized method of completing effectiveness analysis.

In PROSPECT, the scenario that has been analysed by openPASS is the use case UC_DEM_2 (vehicle turning right and a bicycle approaching straight forward). For this

use case a virtual Monte-Carlo experiment has been performed in order to determine the effect of the system with different lateral distance between vehicle and bicycle. For the simulation the use case has been implemented according to the definition provided in section 2.1.4, although slight modifications were conducted to ensure fast and reliable simulation. The fast simulation is an important aspect for the stochastic approach, since an accident scenario is not simulated a couple of times but hundred respectively thousand times. The conducted modification includes also that the two side sensors of the actual demonstrator vehicle (see section 2.2.1.1) have been merged in one sensor that is covers the same area as the original sensors. Furthermore, it must be noted that the simulation cycle time is limited to 100 ms. Hence, also the sensor can operate at the same cycle time at maximum. The simulated cyclist as well as the driver of the vehicle under test do not react to the given situation. Hence, this situation is comparable to inattentive road users that might collide. The analyses of PROSPECT systems have been implemented according to the available information. The system is activated once the pre-defined threshold is met. The activation threshold of the system is varied among the conducted analysis.

2.3 INCORPORATING TEST RESULTS

2.3.1 Bayesian framework

A key aspect in this project is to combine results from different sources concerning the effectiveness of the PROSPECT systems in different scenarios, e.g. simulation results and test results. Bayesian statistical methods have been identified as an appropriate mathematical framework for this purpose as they provide a mathematically optimal way of updating prior information with new observations, as long as the mathematical representations of the prior information and the sampling model represent a rational person's beliefs (Hoff, 2009). In the next paragraph, the Bayesian statistical approach is described briefly on a conceptual level, based on equation (1) below. This equation is included primarily in order to introduce the terminology used in Bayesian inference and it is not essential to understand the mathematical details of equation (1) in order to follow the assessment method.

Bayesian models are based on the following equation called Bayes' rule:

$$p(\theta|y) = \frac{p(y|\theta)p(\theta)}{\int_{\theta} p(y|\tilde{\theta})p(\tilde{\theta}) d\tilde{\theta}} \quad (1)$$

In this setting, θ is a numerical parameter that needs to be estimated. In the right hand side of the equation, $p(\theta)$, called the *prior distribution*, is a probability distribution representing prior information regarding the probability of different values of θ (which could potentially originate from expert opinion, previous experiments, or from other information sources), $p(y|\theta)$ represents the sampling model describing the probability of a new outcome y given a fixed value of θ being the true parameter, and the integral in the denominator is constant in θ . These quantities determine the *posterior distribution* $p(\theta|y)$ which represents our updated beliefs about the probability of different values of θ after having observed the new outcome y . Further details about Bayesian methods can be found e.g. in (Kruschke, 2015) or in (Hoff, 2009) whose terminology is used throughout this report.

To summarize, equation (1) is the mathematical formulation of how prior beliefs about an unknown parameter θ , represented by the prior distribution $p(\theta)$, are updated based on new information y , yielding the posterior distribution $p(\theta|y)$. In the benefit assessment method in PROSPECT, simulation results, described in Section 3.2.1, will be considered as prior information about the PROSPECT systems and this will be updated with test results as new observations (see Section 3.2.2). As the characteristics of the use cases can be generally different, modelling occurs on use case level.

For each use case, two models are considered: one estimates the probability of the collision avoidance by the safety system and the other model estimates the collision speed, given that the collision is not avoided. Simulation results provide sufficient information to construct priors for these models, and the general idea was to update these priors based on the test results. However, in the tests performed with the demonstrator vehicles, all collisions were avoided, see Section 3.2.2; therefore, the update process will only be specified for the model estimating the probability of crash avoidance. As there are no observations in the tests for concerning the collision speed in case of no avoidance, the posterior distribution equals the prior for the corresponding model. Sections 2.3.1.1 and 2.3.1.2 contain detailed descriptions of the aforementioned models.

2.3.1.1 Modelling the probability of crash avoidance

For each use case and each algorithm, a model was developed based on the simulation results to estimate the probability of crash avoidance and this probability was updated based on the test results corresponding to the use case. The current section gives a description of building the model and the update process and the mapping between use cases and tests is specified in Section 2.3.1.2 below.

For a fixed use case and algorithm, in the terminology of the previous section, θ is a numerical parameter, representing the probability of crash avoidance. This parameter may depend on several factors, e.g. those listed in Section 2.3.1.2 below. However, in order to have a matching between simulation and test cases, only the dependence on the initial speed of the car was taken into account for this model.

In order to perform the update of information according to equation (1), various initial speeds were considered that correspond to the initial speeds used in the demonstrator tests and in such a way that for each considered initial speed, there is a sufficient number of cases; see Table 13.

Table 13 Initial vehicle speeds considered for modelling crash avoidance (km/h)

UC1	UC2	UC3	UC4	UC5	UC6	UC9	UC10	UC11	UC12
10	10	10	10	10	5	45	10	10	20
15	15	20	20	15	10	55	20	20	50
20	20	30	30	20	15	65	30	30	70
25	25	40	40	25	20		40	40	
30	30	50	50	30	25		50	50	
	35						60		
	40								

For each initial speed specified in Table 13, the prior probability of crash avoidance was assumed to follow a Beta(a, b) distribution whose parameters were determined by

the number of crashes avoided (a) and the number of crashes not avoided (b), respectively. Formally, this means that, for each fixed use case, algorithm and initial speed value, the prior distribution is defined as follows: for all $0 \leq \theta \leq 1$,

$$p(\theta) = \text{dbeta}(\theta, a, b) = \frac{\Gamma(a+b)}{\Gamma(a)\Gamma(b)} \theta^{a-1} (1-\theta)^{b-1} \quad (2)$$

where Γ denotes the gamma function which is an extension of the factorial function. As described in Section 3.1.1 of (Hoff, 2009), the Beta distribution is a conjugate prior for binomial sampling which means that the posterior distribution is again in the family of Beta distributions. In the benefit assessment method, test results were assigned double weight compared to the simulation results; this means that the posterior distribution is determined by the following equation:

$$p(\theta|y) = \text{dbeta}(\theta, c, d) \quad (3)$$

for $c = a + w \sum y_i$ and $d = b + wn - w \sum y_i$, where n is the number of new observations, $w = 2$ is the weight of test results compared to simulation results, and for $i \in \{1, 2, \dots, n\}$, y_i takes value 1 if the crash was avoided in test i and 0 otherwise. While the weight of $w = 2$ relating test values to simulation values is fixed throughout this report, it would be possible to apply the method without changes using other values of w .

The posterior distribution prescribed by equation (3) can then be specified for each fixed use case, algorithm and initial speed value which allows the identification of estimates and confidence intervals for the parameter θ . In each case, the estimate was taken as the median of the distribution and a 90% posterior confidence interval was obtained by taking the 0.05 and 0.95 quantiles of the corresponding posterior Beta distribution. Finally, the estimates and confidence intervals were extended to all initial speeds by fitting a logistic curve to the values obtained as above, with the exception of the steering and braking algorithm for which the logistic curve did not give an appropriate fit and a polynomial curve was used instead.

2.3.1.2 Modelling collision speed in case of a crash

For each use case and each algorithm, a linear regression model was built to model the collision speed when the crash is not avoided. The motivation for constructing such a model as opposed to using the observed collision speeds in simulations was threefold: 1) the regression model yields confidence intervals and can be used to consider best case and worst case scenarios; 2) the model can be applied to those crashes as well which were avoided in the simulations but based on the probabilistic model developed in Section 2.3.1.1 had a nonzero probability of ending up in a crash; 3) the linear regression model is well suited to a Bayesian update with new information. This third point proved to be only a theoretical advantage, though: as mentioned right before Section 2.3.1.1, the tests performed with the demonstrator vehicles did not result in any collisions. Therefore, the model of collision speed when the crash is not avoided was not updated with new, test-based observations and the posterior distribution equals the prior in this case.

Since the simulation results were not updated with test results in this model, the parameters between simulations and test results did not need to be matched. Therefore, a larger set of variables were considered as covariates when constructing the model, as follows:

- Initial speed of the car;
- Initial speed of the VRU;
- Longitudinal distance;
- Lateral distance;
- Sight obstruction (No/Not permanent/Permanent/Other);
- Location (Urban/Rural).

All subsets of these variables were considered as covariates and the linear regression model with the lowest Akaike Information Criterion (AIC) value (Akaike, 1974) was selected as the final model, with two exceptions: in use case 9 and use case 12, the models with the lowest AIC value showed multi-collinearity of the covariates and hence the models with the second lowest AIC value were selected.

2.3.2 Test results chosen

The goal of the vehicle-based testing activities on closed test tracks is to evaluate the performance of the three developed prototypes in the newly addressed urban intersection scenarios.

The prototypes are equipped with sensor and actuator technologies and algorithms that go beyond what is available on the market today. The scope is reaching from improved vulnerable road user (VRU) detection that allows assumptions regarding the intention, over high-speed brake actuation and emergency steering algorithms to high sensor angle coverage, enlarging field of view. The prototype use cases are selected by taking the individual equipment of each prototype into account.

The developed test protocol is aligned with current consumer testing procedures. This requires all tests to be conducted with driving robots, including a steering robot as well as brake and acceleration actuation. This allows the vehicle dynamics to be controlled over the whole test run within tight accuracies and ensures high repeatability of each run and a valid comparability between different test vehicles, also when assessed in different test locations.

All scheduled test cases are displayed in Figure 72. All test cases are conducted with a dummy of a bicyclist. Only the longitudinal test case (bottom right in the figure) is additionally conducted with a pedestrian dummy. The velocity of the bicyclist is 15 km/h, for the pedestrian the velocity is set to 5 km/h. All geometric relations of the scenario setup between VUT and VRU-dummy are determined by the proposed intersection in Deliverable 7.1 (IDIADA, 2018).

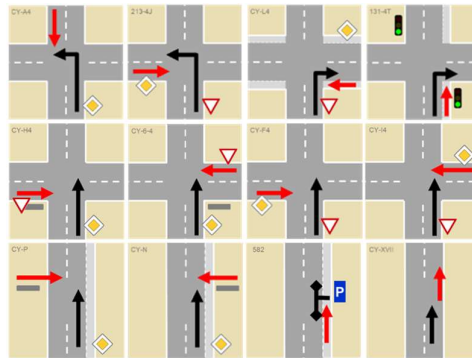


Figure 72: Test cases.

The top row of the figure contains all intersection scenarios where a turning trajectory is required. One exemplary trajectory for right and left turning was defined on the basis of several studies, workshops and testing activities throughout the project. The assigned prototypes are able to avoid an impact in all four scenarios.

In the middle row and the two left cases of the bottom row of the figure, crossing scenarios are shown. The far side scenarios could be conducted with impact avoiding performance of the assigned prototypes. For the nearside scenarios no performance could be recorded. The reasons are discussed in Deliverable 7.1 (IDIADA, 2018).

The second to last scenario describes a parking test case. The VUT is parked and the bicycle dummy is coming from the back. The test engineer opens the door when the dummy is close to the vehicle. Depending on the warning strategy and the HMI concept of the vehicle the assessment of this scenario is also described in Deliverable 7.1 (IDIADA, 2018).

The last scenario on the bottom right of the figure is the longitudinal test case. This scenario was conducted with more than one prototype and with different parameters regarding the placement of the VRU-dummy and the autonomous vehicle intervention. The basic setup of this scenario was conducted with 25% and 50% offset between VRU and VUT. For higher speeds ranging from 50 to 60 km/h, one prototype showed an ESP-induced emergency steering manoeuvre, while another prototype vehicle applied some torque on the steering wheel for the evasive manoeuvre. The dummy was placed to the very right side of the lane for this specific case. All impacts were avoided.

The longitudinal scenarios for pedestrians and cyclists have also been tested with distracted drivers in critical scenarios by VCC at a test track and by VTI in a simulator study. The tests included FCW warnings and steering interventions at different TTC. The vehicle speed in the tests was 70 km/h and the average offset was around 10-20%.

Apart from evaluating the developed prototypes four so-called baseline vehicles are being tested. These vehicles are current state-of-the-art high-class vehicles provided by different OEMs. Testing activities are conducted to be able to show a potential performance improvement towards the prototypes and to gain experience with the test protocol. As expected, the overall performance of the baseline cars was considerably poor over the assigned test cases. The reason for this is that the features implemented in the developed prototypes and described in Deliverable 4.2 (CONTI, 2018) and

Deliverable 6.2 (DAIMLER, 2018) build a requirement to address most of the new challenging PROSPECT test cases.

The general idea of updating simulation result with test results in a Bayesian framework requires a matching of test scenarios to the use cases. The matching used in the assessment method is specified in Table 14 below.

Table 14: Matching of test scenarios and use cases.

Test scenario	Represented use case	VRU type
CBSF/CBIP03/CBIN01	UC_DEM_4	Cyclist
CBIG	UC_DEM_2	Cyclist
Longitudinal	UC_DEM_12	Pedestrian
Longitudinal	UC_DEM_9	Cyclist
Crossing Static	UC_DEM_10	Pedestrian
Crossing Static	UC_DEM_3	Cyclist
CBIP 01	UC_DEM_1	Cyclist
CBIN 05	UC_DEM_5	Cyclist
CBIN 06	UC_DEM_6	Cyclist

The simulation results for a use case were updated with the test results for the matched test scenarios as described in Section 2.3.1. The updated results are used to estimate the crash frequency at different collision speeds for cars equipped with the PROSPECT systems. This is combined with the risk of injuries of various severity at given collision speed values, which are specified by injury risk functions, as described in Sections 2.3.3 and 2.3.4.

2.3.3 Injury risk functions: cyclists

Due to the relatively low number of GIDAS cases that are related to the individual 12 use case scenarios, Injury Risk Functions (IRF) for all cyclist use-cases combined, as well as for all pedestrian use cases combined, were designed. Splitting up the cases into each individual use case would only result in too low case numbers, which would make the resulting IRF unreliable. It was therefore decided to group the cases involving a cyclist together, as well as grouping the cases with a pedestrian together. This proceeding is somewhat problematic, as the different use cases will result in different crash and injury mechanisms, but overall this will still yield better results than conserving each use case individually. The pedestrian related use cases 10 to 12 are handled in section 2.3.4 in the same way.

Of the n=1,356 GIDAS car-to-cyclist cases, corresponding to the above stated PROSPECT Use Cases, 48 cases were excluded due to missing information on the injury severity. As data extrapolation to EU level is only possible based on the police-reported injury severity levels (slight, serious, fatal injury), IRFs using this classification, described in the Sections 2.3.3.1 and 2.3.4.1, will be used to compute the safety benefit of systems.

The police-coded injury severity is not always consistent with a classification based on the Maximum AIS (MAIS) value - even a MAIS3 injury might have a fatal outcome and a MAIS1 might be “serious”. In this data only MAIS4, 5 contain fatal cases, but 110 cases of MAIS1 were “serious”. IRFs based on the MAIS coding in GIDAS are

described in Appendix 8.5 and 8.6. An additional issue in this case is that the case numbers per category vary significantly (e.g. 1,247 cases for MAIS1&2, but only 55 cases for MAIS3+) and will result in different qualities and reliabilities of the resulting IRFs.

Furthermore, it is important to keep in mind that the dataset is biased towards injuries in general (there is no information available for uninjured cyclists) and that especially for higher collision speeds there are only few cases available. In the whole dataset, there are only five cases with cyclists available with a fatal outcome, which will result in a drastically reduced reliability of the resulting IRF.

2.3.3.1 IRF using police coding

An ordered probit regression (Aitchinson & Silvey, 1957) was applied to specify the probability of sustaining a certain injury, i.e. slightly injured, seriously injured and fatally injured. The estimator was the collision speed of the car. This model uses the inverse standard normal distribution of the probability as a linear combination of the predictors. The implementation of the model is done in R and the MASS package (function *polr*, Hess matrix = TRUE).

Based on this coding, there are 1,034 cases of slightly injured, 316 cases of seriously injured and 6 cases of fatally injured. Model corresponding coefficients, intercepts and the Akaike Information Criterion (AIC) value are provided Table 15. The resulting curves in Figure 73 show the three IRF for the 3 injury levels corresponding to police-coded injury severity. At each point of the x-axis the values of all 3 curves sum up to the total probability of 1. This means, as the probability of being seriously injured (and being fatally injured) increases with increased collision speed, the probability of being only slightly injured goes down.

Table 15: Parameter estimates of the probit model for pedestrians based on police coded injury severity.

	Estimate	Standard Error	t-value
Vehicle collision speed	0.03197	0.002981	10.73
Intercept MAIS1 → MAIS2+	1.3679	0.0732	18.6765
Intercept MAIS2+ → fatal	3.5633	0.1949	18.2813
Residual Deviance: 1,426.122			
AIC: 1,432.122			

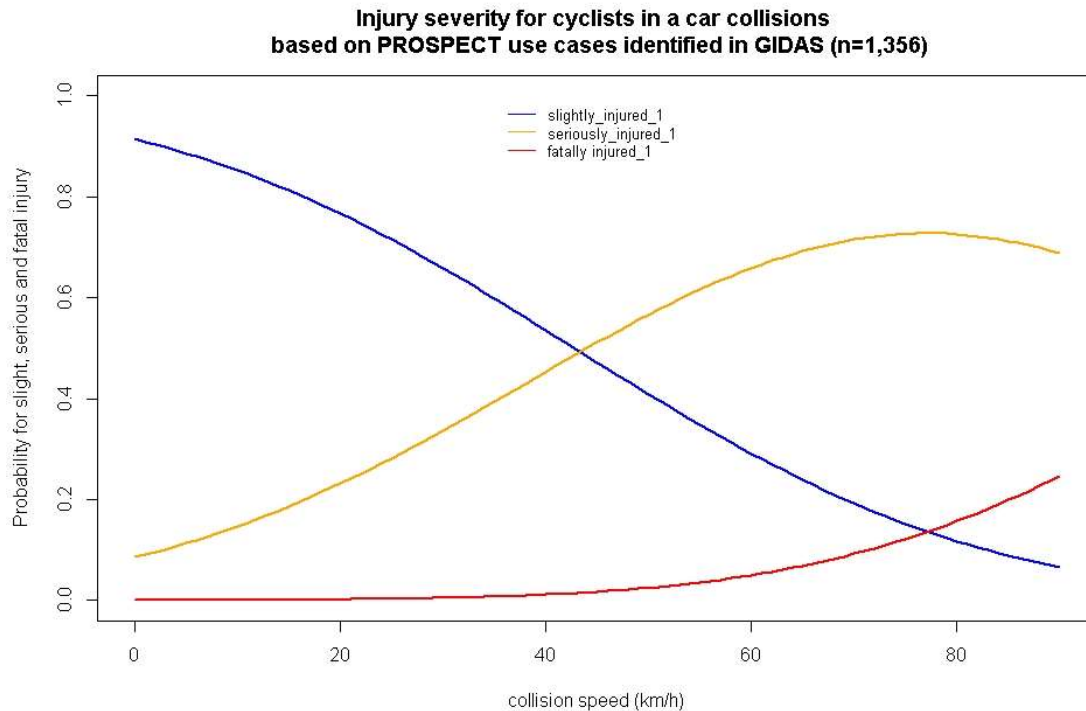


Figure 73: Probability of being slightly (blue), seriously (orange), and fatally (red) injured for cyclists in an accident with a car based on n=1,356 GIDAS cases identified as PROSPECT use-cases.

2.3.4 Injury risk functions: pedestrians

For pedestrians the use cases 10 – 12 are relevant. Here a data pool of n=578 cases is available. The same methodology as for the cyclist cases is used. Same as for cyclists, only a small number of cases is available for high collision speeds and only 16 cases with a fatal outcome.

2.3.4.1 IRF using police coding

For the computation of the IRFs using the police-coded injury severity levels for pedestrians, 2 cases were excluded of which one was coded unknown and one pedestrian was uninjured. This way, the resulting 576 cases were split into 262 cases of slightly injured, 298 cases of seriously injured and 16 cases of fatally injured. The results of the ordered probit model is described in Table 16 and the resulting injury risk functions are shown in Figure 74 below.

Table 16: Parameter estimates of the probit model for pedestrians based on police coded injury severity.

	Estimate	Standard Error	t-value
Vehicle collision speed	0.03303	0.003612	9.147
Intercept MAIS1 → MAIS2+	0.8926	0.1216	7.3398
Intercept MAIS2+ → fatal	3.2316	0.1973	16.3762
Residual Deviance: 829.4574			
AIC: 835.4574			

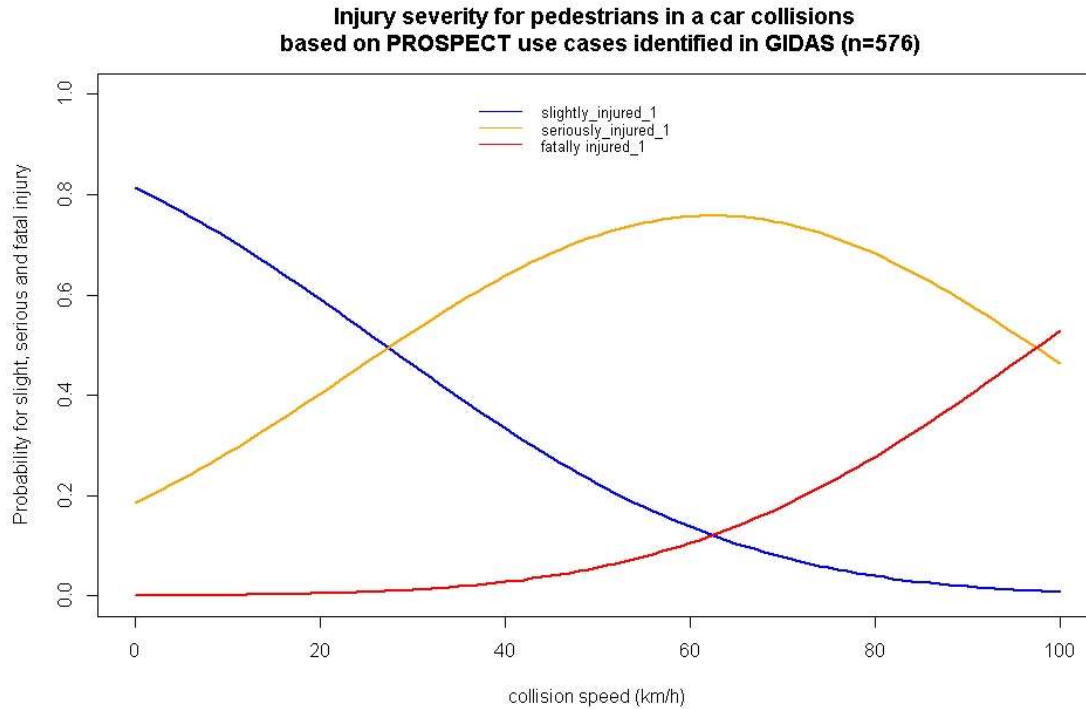


Figure 74: Probability of being slightly (blue), seriously (orange), and fatally (red) injured for pedestrians in an accident with a car based on n=576 GIDAS cases identified as PROSPECT use-cases.

2.3.5 Computing local benefit

The computation of the local safety benefit of the PROSPECT systems is based on the combination of the models for crash avoidance probability and collision speed in case of a crash with the injury risk curves specified in the previous section, using a variant of the dose-response model (see e.g. (Korner, 1989), (Kullgren, 2008) and (Bálint, Fagerlind, & Kullgren, 2013)). This model estimates the number of people with injuries of a given type or severity based on crash frequency and injury risk, with respect to a crash severity parameter which in this report is selected to be the collision speed.

In the assessment method described in this report, for any given use case and a specific speed value v , crash frequency at v is defined as $f(v)$ = the number of car-to-VRU crashes within the use case occurring at collision speed v and for a fixed injury severity (e.g. seriously injured), the injury risk $r(v)$ is the risk of sustaining an injury of the given severity. The dose-response model estimates the number of VRUs sustaining an injury of the given severity within the use case, denoted by $E(N)$, as follows:

$$E(N) = \int_0^{300} f(v)r(v) dv \quad (4)$$

In this formula, the dependence of these quantities on the use case is suppressed in the notation for simplicity and 300 as the upper limit of the integration could be replaced by the greatest value v such that $f(v) > 0$ (i.e. a speed value which is the upper limit of collision speeds within the use case). As PROSPECT systems can potentially avoid a crash or change the collision speeds for those crashes that cannot be avoided, for

their assessment, $f(v)$ needs to be replaced by a new crash frequency function $f_{new}(v)$; the details of how to compute this function are described below, see equation (5). Assuming, that this function is known, an estimate corresponding to $E(N)$ can be computed using the same injury risk function $r(v)$ but replacing the original crash frequency function $f(v)$ in (4) by $f_{new}(v)$.

For the assessment method described in this report, the original crash frequency function per use case can be computed based on the collisions speeds in the PCM data that was used for the simulation (see Section 2.1.3) and the injury risk functions are specified in Section 2.3.3 and 2.3.4. The way the crash frequency curve is transformed by the PROSPECT safety systems can be estimated based on the results described in Sections 2.3.1.1 and 2.3.1.2, as follows. For each crash c in the PCM data, the model developed in Section 2.3.1.1 specifies a probability $p(c)$ of the crash being avoided, and an estimate $\tilde{v}_{coll}(c)$ regarding the collision speed in case the crash is not avoided (which happens with probability $1 - p(c)$), rounded to the closest integer value. Therefore, for a given use case denoted by UC , the transformed crash frequency function can be computed by defining, for each nonnegative integer value v , the quantity

$$f_{new}(v) = \sum_{c \in UC} (1 - p(c)) 1_{\{\tilde{v}_{coll}(c)=v\}} \quad (5)$$

where $c \in UC$ means that the crash is included in the given use case and $1_{\{\tilde{v}_{coll}(c)=v\}}$ is an indicator function taking value 1 if the estimated collision speed for the crash rounded to the closest integer equals the specified value v and 0 otherwise.

Having specified all functions as above, the dose-response model quantifies the expected number of fatalities, serious injuries and slight injuries per use case and per algorithm with and without the system which can then be summarized to quantify the local benefit for all cyclist use cases, respectively all pedestrian use cases. Using the confidence intervals specified in the models in Sections 2.3.1.1 and 2.3.1.2 yields confidence intervals for the reductions as well. The model can also be used to consider a subset of crashes within the use cases, e.g. those including a cyclist aged >55 in an urban environment or crashes in daylight including a pedestrian aged ≤ 55 years, and the corresponding local percentage reduction attributable to the system can be quantified. This gives the necessary input to the method extrapolating the local benefit to EU level, described in Section 2.4.

2.4 EXTRAPOLATION

2.4.1 Recursive decision trees

The decision tree method is the best up-to-date method for extrapolation (Broughton et. al, 2010; Ferreira, et. al, 2015; Kreiss, et. al, 2015). In (Kreiss, et al., 2015) it was shown that assessment of effects of new safety systems can be carried out with this extrapolation method. First, the effects of new safety systems are reliably quantified for detailed reported accidents in GIDAS. Second, extrapolation of such a quantification of effects of new safety systems to target regions is performed. The decision tree depends on the structure of the existing accident data from the region for which the calculation is drawn from, i.e. the GIDAS data in this case.

In this report, a decision tree based on GIDAS is generated for injury distribution of cyclist involved in car-to-cyclist accidents. The decision tree is built based on the GIDAS data with variables that are present in the target region database (CARE), so that the decision tree can be applied to the target region (Europe). Therefore, it is necessary to know which accident variables are available for that target region and whether they can be harmonized with accident information within GIDAS. The accident variables should have sufficiently high quality (according to classification in CARE), have sufficiently often “known” values and same or comparable definitions in CARE and the relevant national databases (Germany, Sweden, and Hungary). According to these requirements the relevant decision variables for extrapolation, common for GIDAS and CARE, are:

- Accident type / Kind of accident
- Injury severity (slight, serious and fatal)
- Involved road users (e.g. car, cyclist)
- Location or road type
- Weather
- Surface
- Light
- Age
- Gender

The accident data from years 1999-2015 is used from GIDAS database (see section 2.1). The target variable which we want to predict is the injury severity of the cyclist involved in the crash. The categorical decision variables with more than two categories are transformed into dummy binary (0-1 value) variable. The transformation of these variables is shown in Table 17.

Table 17: Transformation of categorical variables into binary variables.

Variable name	Categories	Binary variable transformation
Light	Darkness	Light_Darkness
	Twilight	Light_Twilight
	Daylight	Light_Daylight
Surface	Snow	Surface_Snow
	Dry	Surface_Dry
	Slippery	Surface_Slippery
	Wet	Surface_Wet
Weather	Dry	Weather_Dry
	Fog	Weather_Fog
	Other	Weather_Other
	Rain	Weather_Rain
	Sleet	Weather_Sleet
Age	Snow	Weather_Snow
	Age <= 25	Age1
	Age > 25 & Age <= 55	Age2
	Age > 55	Age3

The rest of the variables with two categories are shown in Table 18.

Table 18: Variables name and their categories.

Variable name	Categories
Gender	Male
	Female
Location	Urban
	Not urban

The decision trees are implemented in the computer environment R (Team, R Core, 2016) with the package *rpart* (Therneau & Atkinson, 2017).

In the implementation of the method, the R routine *rpart* builds the structure of the tree by first selecting the variable which 'best' divides the data into two groups. This is determined by the distribution of the individual injury severity in the newly emerging nodes. The algorithm selects the decision variables so that these inner nodes' distributions differ as far as possible from each other. Subsequently, the process continues for the subgroups correspondingly until a termination criterion is reached, for example, the minimum bucket size or no improvement can be achieved. The *minimum bucket size* refers to minimum number of observations in any leaf (terminal node). In this report, the tree is built with minimum bucket size of 10 (Corliss, 2018).

Finally, this grouping is trimmed by cross-validation. The quality of the separation is determined based on Gini information index. (Detailed information on the used routines are provided in (Therneau, Atkinson, & Ripley, 2017).

After the decision tree for GIDAS is built, a decision tree with the same rules is calculated for CARE. The frequency of the injuries in the terminal nodes for both trees are used to calculate the extrapolation factors according to equation 6:

$$Factor_{in} = \frac{(Frequency\ in\ CARE)_{in}}{(Frequency\ in\ GIDAS)_{in}} \quad (6)$$

In eq. 6, *i*-is injury level (fatal, serious, slight) and *n*-is terminal node number.

2.4.2 Fleet penetration rate

Naturally, the overall socio-economic benefit of a safety system depends on the proportion of vehicles on the roads that are equipped with the system. In the status report of IIHS (IIHS, 2012), it has been found that it takes about 30 years from introduction of a promising safety feature to a 95% penetration rate. A recent study from Highway Loss Data Institute shows that in 2016 only one percent of the registered vehicles in the US were equipped with rear-end AEB (HLDI, 2017). Another study from Germany (Schneider, 2016) has been performed which is based on survey with 1,632 car owners. Prediction of future penetration rates has been done via logistic regression, by using data from 1995 -2011, for different systems including:

- Airbags: driver's, passenger and side
- ESC, ABS, ASC
- Cruise control, ACC
- Parking aid, parking assist
- Xenon headlights, swivelling headlights
- Lane keeping assist, lane change assist

- AEB, night vision, head-up display, traffic-sign recognition.

For example, the driver frontal airbag had a 94% penetration rate in the vehicle fleet already in 2009 (see Figure 75), while in U.S. the prediction was 95% in 2016. The possible reason for this difference between Germany and U.S. could be the difference in the average vehicle age of 8.5 and 10.8 years, respectively for Germany and U.S. The penetration rates for the most current systems for the new cars compared to the vehicle population for 2011 for Germany are shown in Figure 76.

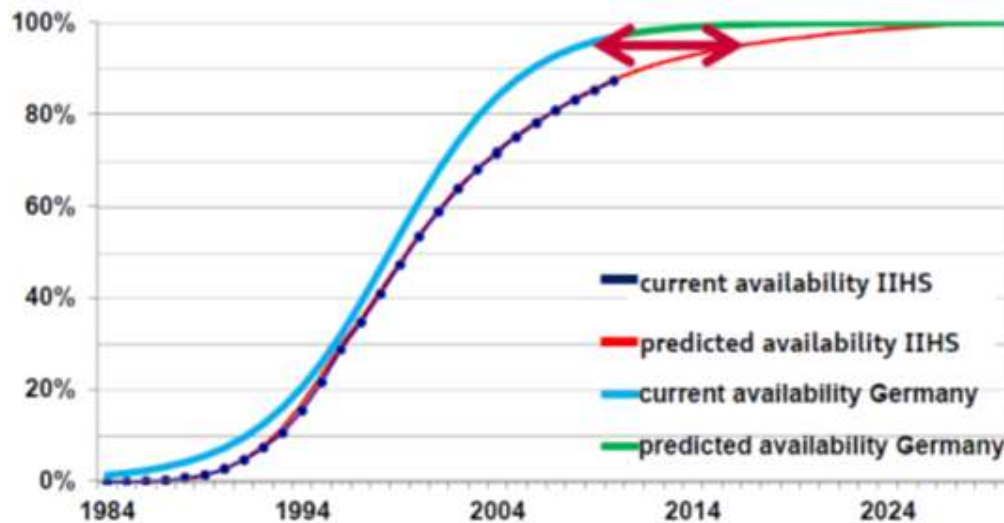


Figure 75: Fleet penetration curve for frontal airbag in Germany.

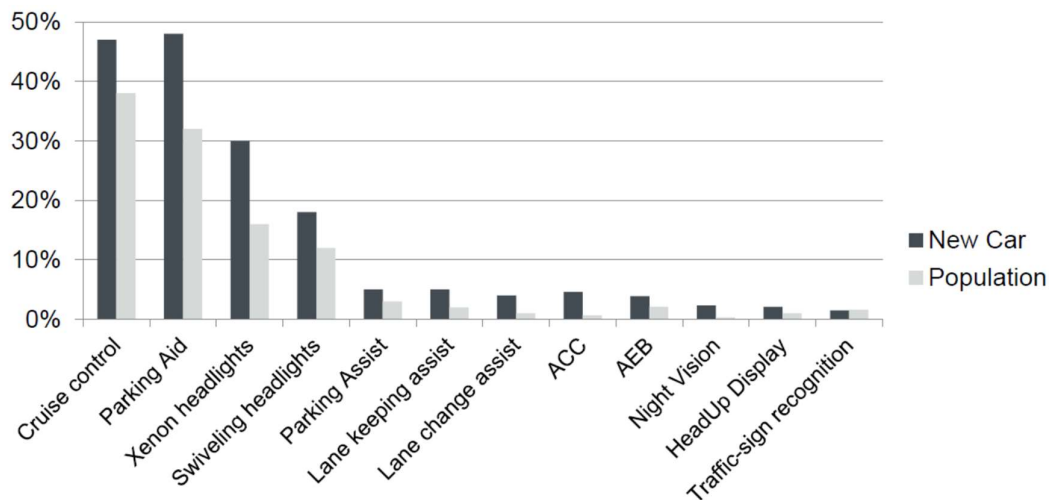


Figure 76: German penetration rates 2011 of the newest systems: new cars vs vehicle population.

2.5 SOCIETAL BENEFIT

2.5.1 User acceptance

Three partners (IFSTTAR, TME and University of Nottingham) have explored driver acceptance of the PROSPECT functions using the methodology defined in the Deliverable 7.2 (Report on methodology for balancing user acceptance, robustness and performance, (IFSTTAR, 2018)).

Acceptance of the system is assessed using three different questionnaires, described in the Deliverable 7.2 (IFSTTAR, 2018). Two of the questionnaires' measuring different dimensions of the acceptance (usefulness, ease of use, satisfaction and trust) are administered before and after having experienced the system. The third questionnaire is very short and must be completed after each event that occur during the experiments. This questionnaire aims to define the criticality of the situation (criticality, frequency, foreseeability, controllability, and the participant's feeling of it) and to provide the drivers' opinion on the support provided by the system (does it behave efficiently or not).

2.5.1.1 IFSTTAR study

IFSTTAR ran a video-based experiment to investigate acceptance of the PROSPECT functions. Drivers were faced with a series of 20 videos from a driver point of view covering various use cases derived from accident scenarios. These videos are selected from the naturalistic observations conducted within WP2 in Barcelona. Each video shows a conflict between the car and a cyclist or a pedestrian and stops when the situation becomes critical. A message informs then the driver about the action the PROSPECT system would have done (warns the driver or brakes). The order of the videos is randomized for each session.

63 participants took part in the experiment: 15 young drivers (18 to 25 years old), 33 middle-aged drivers (30 to 50 years) and 15 elderly drivers (70 to 85 years old). Middle-aged drivers were divided into 2 groups according to their car equipment in ADAS and their habit of using them.

Results and details of the experiment are reported in D7.3 (Report on simulator test results and driver acceptance of PROSPECT functions). Here is a summary of the main results investigating the willingness to buy a PROSPECT-like system and the intention to activate such a system according to the driving context.

Results

Willingness to buy a PROSPECT-like system

At the end of the experiment, participants were asked how willing they would be to buy the PROSPECT system, based on their experience of the 20 videos. The expected answer is a score ranging from 0 (not at all) to 100 (totally).

The average of the willingness to buy a PROSPECT-like system value is 74. This means that, on average, participants agree to 74% of the idea of buying a PROSPECT-like system, which represents a quite high degree of willingness to buy. No significant difference is found neither in terms of age of the drivers, nor in terms of car equipment. However, when investigating the number of kilometres driven per year (Table 19), drivers who drive more appear to be much more likely to buy the system than drivers who drive little ($H(2) = 5.511$, $p = 0.019$). It can also be seen that acceptability of the system functions in general is slightly higher at 81%, whereas trust in the system is slightly lower at 70%.

Table 19: Willingness to buy according to the drivers' mileage

	n	Willingness Mean value
< 10 000km/year	31	64,7
> 10 000km/year	32	83,0
All drivers	63	74,2

The willingness to buy the system also depends on the drivers' opinion of its functioning. After viewing each video, participants gave their opinion on the support provided by the system (did it behave correctly or not). According to their answers, they were split into 2 groups; those who consider that the system behaves effectively in more than 75% of the cases and those who consider it behaves effectively less often. The willingness to buy differs significantly between the 2 groups (Table 20): drivers who rated more often that the system works correctly are more likely to buy it than the other drivers ($t(61)=-3.682$, $p < .001$).

Table 20: Willingness to buy according to the system functioning.

	n	Willingness Mean value
$\leq 75\%$ correct	26	60,2
$> 75\%$ correct	37	85,1
All drivers	63	74,2

Intention to use the PROSPECT functions

The warning function is clearly the PROSPECT functionality for which the drivers reported the highest intention to use (Figure 77). Drivers agree to 79% of the idea of using or activating it in all driving conditions. Conversely, the steering function would only be used at 65%. The braking function is at an intermediate level.

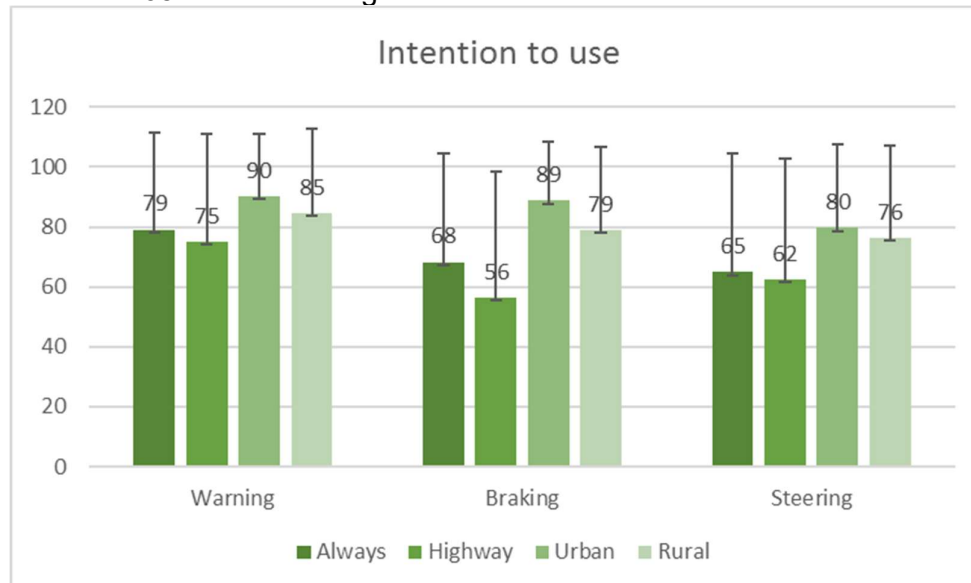


Figure 77: Drivers' intention to use the PROSPECT functions.

The participants rated very high the urban areas (90% warning, 89% braking and 80% steering), indicating they would be ready to use or activate the PROSPECT functions in this context. The intention to use the system in rural areas is somewhat lower, but

still rather high. The intention to use the system on the highway is lower than in the other two areas, especially for the braking function (56%); the warning seems to be the only acceptable option to activate on the highway (75%).

2.5.1.2 TME simulator study

Systems that can warn the driver of a possible collision with a VRU have significant safety benefits. However, incorrect warning times can have adverse effects on the driver. If the warning is too late, drivers might not be able to react; if the warning is too early, drivers can become annoyed and might turn off the system. Currently, there are no methods to determine the right timing for a warning to achieve high effectiveness and acceptance by the driver. The aim of the TME simulator study was to validate a driver model as the basis for selecting appropriate warning times. The timing of the Forward Collision Warnings (FCWs) selected for the current study were based on the comfort boundary (CB) model developed during a previous project. The comfort boundary model analysed the brake onset of drivers when encountering a cyclist crossing the road in an intersection.

Two warnings were selected: one inside the CB and one outside the CB. The scenario tested was a cyclist crossing scenario with a TTA=4 seconds. The timing of the warning inside the CB was at the time to collision (TTC) 2.6 seconds (asymptotic value of the model at TTA=4 seconds) and TTC=1.7 seconds for the warning outside the CB (value below the lower 95% value of the model at TTA=4 seconds). Thirty-one participants took part in the test track study (between subject design where warning time was the independent variable). Participants were informed that they could brake any moment they felt the scenario became critical after the warning was issued. At the end of the study, participants completed an acceptance survey.

Participants reacted faster to the warning outside the CB compared to the warning inside the CB. This confirms that the CB model represents the criticality felt by the driver. Participants also rated more disturbing the warning inside the CB and they had a higher acceptance of the system with the warning outside the CB. The above results confirm the possibility to develop well-accepted warnings based on driver models.

2.5.1.3 University of Nottingham study

The University of Nottingham conducted a longitudinal simulator study, in which forty-eight experienced drivers took part. Participants attended at the same time on each of five consecutive days (Monday to Friday), and completed the same journey, which was framed as their daily commute. The simulator was modified to replicate the PROSPECT functionality (enabling an audible warning and emergency braking intervention, as specified by deliverable 5.2 (Kunert, Krebs, Stoll, & Arbitmann, 2018), in response to potential hazards).

Towards the end of the drive, which lasted approximately 10-15 minutes, participants were asked to make a left turn. On days one to four (i.e. Monday to Thursday), the experience was 'uneventful' in that drivers completed the journey without incident. However, on day five (Friday), a cyclist was detected crossing the road into which drivers were turning. This prompted activation of the PROSPECT system in line with Use-Case 2 'crossing scenario', involving an auditory warning following by emergency

braking. Because testing was occurring in the UK, the use-case was effectively mirrored.

Half of the participants (n=24) experienced a 'true-positive' activation, i.e. the cyclist continued to cross the road, whereas the remainder of the participants (n=24) experienced a 'false-positive' intervention, i.e. the cyclist was detected as they approached the roadside and a warning was provided, followed by emergency braking. However, the cyclist actually stopped before entering the roadway. As such, it was expected that the latter intervention would be perceived as a 'false-alarm' as the cyclists did not cross the roadway.

The approach builds on previous work and aims to present a more ecologically-valid experience to participants, i.e. drivers are not inundated with warnings and interventions in rapid succession during a single-visit simulator study, which can provide a false representation of the system, and is therefore likely to generate a poor assessment of acceptance.

Driver acceptability/acceptance was subsequently assessed at the end of the week based on the testing protocol developed as part of the PROSPECT project in deliverable 7.2 (IFSTTAR, 2018). Results of the study indicate high acceptance of the PROSPECT system, even in situations where drivers' only experience was a false alarm (82.6% combined), as well as high likelihood to use or purchase the system (73.3% combined). Nevertheless, factors such as price and reliability were also highlighted by several participants as important considerations when making this decision. For full details of the study and analysis, please refer to deliverable 7.3 "Report on simulator test results and driver acceptance of PROSPECT functions" (VTI, 2018).

2.5.2 VTI simulator study and VCC test track study

VCC and VTI have developed test procedures for evaluation of warnings in combination with automatic intervention by steering with the driver in the loop in UC_DEM_9 and UC_DEM_12 from WP3. The test procedures include scenarios when the driver is distracted. Tests have been performed on test track in T7.1 and in simulator in T7.2. These studies' main objective was to assess drivers' reactions to warnings and active steering interventions in critical longitudinal VRU scenarios when drivers are distracted. The motivation for the studies is to build new knowledge of the performance of today's ADAS and for improvement of performance of future ADAS with the driver in the loop. The new knowledge will also be used in development of future ADAS test methods. The studies are reported in detail in deliverable 7.3 (VTI, 2018).

The results from these studies give a good indication of the real-life performance of forward collision warning (FCW) and active steering interventions in longitudinal small offset VRU scenarios in higher velocities (tests were done in 70 km/h). The results also make it possible to give a preliminary prognosis for future ADAS systems potential performance.

- There were no collisions in cyclist scenarios in the simulator with FCW at TTC 1.7s.
- Approximately 2/3 of collisions with the pedestrian were avoided at test track and in the simulator, with FCW at TTC 1.7s. Some more collisions can be

- expected with 25% offset. A conservative prognosis is approximately 50% avoided collisions with 25% offset.
- There was a significant reduction in collisions and distances to pedestrian with FCW at TTC of 2.2s vs 1.7 s. The distances at TTC=0 indicates a prognosis of approximately 10% collisions at TTC 2.2s with an offset of 25%. The earlier warning also gives the driver the possibility to brake to avoid a collision. An earlier warning needs to be connected to driver state estimation to reduce false positives.
 - The earlier automatic steering intervention in the cyclist scenario changed the direction (heading) and lateral position of the vehicle until the driver's own steering intervention, which causes the driver to only need to make a smaller lateral movement to avoid a collision in the cyclist scenario. This indicates that an earlier lateral intervention in a pedestrian scenario in combination with an earlier warning have a potential to reduce the accidents to 0% in scenarios with 25% offset if there is no oncoming traffic. This needs to be verified in future research at test track.

In conclusion, more research is needed for robust evaluation of different warnings and lateral interventions towards real life scenarios such as tests of different lateral interventions, test of FCW including pre-braking, tests in different vehicle speeds and offsets.

2.5.3 Societal costs

The occurrence of traffic injuries often involves human suffering and tragedies. The outcomes of crashes are however not limited to human suffering, but also result in societal costs that do not only comprise of health care costs and damage repairs but mainly result from loss of productivity. The ethical aspect of assigning monetary values to injuries can be debated at length but will not be discussed in this report. At the same time, it is clear that road traffic injuries incur high costs for the society and that there is a natural need to quantify these costs in some way. Furthermore, new safety systems that are able to prevent or mitigate crashes cost money and can be considered as an investment. From an economical point of view, there could be a driving factor to establish new systems if their benefit-cost ratio is larger or equal to 1 (meaning that the monetary benefit of the system is bigger than its costs). Moreover, the assigned monetary values also give a certain weight to the different injury outcomes, as a slight injury should not be treated equally to a fatality. It is therefore important to consider societal costs as well.

In this report, the injury costs derived in the ASSESS project will be used, updated for inflation and to reflect the developments since that report. The costs specified in Table 4-2 in (Buhne, et al. 2012) are these recalculated for the prices of 2018 based on the inflation rates in the EU (Statista, 2016) are provided in Table 21 below.

Table 21: Injury unit costs [ASSESS D2.2, updated].

Euro, 2018 prices	2005	2020	2025	2030
Fatality	1,145,098	1,227,580	1,496,413	1,824,119
Serious injury	130,524	139,926	170,568	207,922
Slight injury	13,162	14,110	17,201	20,967

The assessment of the newly developed safety systems will focus on prevented and mitigated injuries in EU28 and will quantify the impact by using the assigned costs from Table 21. These costs do however not include direct effects from the system like harmonizing traffic flow and the reduced environmental impact as these effects have shown rather marginal impacts in previous EU studies such as CORDIA (Kulmala et al. 2008) and eIMPACT (Wilmink et al. 2008). All monetary values are expressed in prices of 2018.

The system performance and expected results are computed as described in Section 2.4. These results however assume 100% fleet penetration rate and 100% acceptance and use of the system. In general, especially the fleet penetration of 100%, is not reached instantly but over a rather long period. As shown in Figure 75 for driver airbags, a market penetration of 20% needs around 10 years and a penetration of 50% around 15 years. This means that the societal benefit of the system is not reached instantly but increases over time as the penetration rate increases.

User acceptance can have a similar impact on the results. Even if new cars are equipped 100% with the new system, if users do not accept the system and therefore not use it, it will have a similar effect as a 0% penetration rate.

The societal benefit (saving in costs due to the system) can be calculated based on the avoided and mitigated crashes (system performance) in consideration of a market penetration for the respective year, using the following formula:

$$SB_{year} = [(n_{fatal} * c_{fatal, year}) + (n_{severe} * c_{severe, year}) + (n_{sligh} * c_{slight, year})] * mp_{year} * ua_{year}$$

SB – Societal Benefit

n – number of avoided casualties (either fatal, severe or slight)

c – cost of casualty in respective year (see Table 21)

mp – market penetration in % in respective year

ua – user acceptance in % in respective year

In this assessment, for reasons of simplicity it shall be assumed that a market penetration and user acceptance of a given percentage (x%) also results in the corresponding number of reduced casualties compared to the maximum benefit (e.g. only x% percent of casualties are “really” prevented by the system).

The introduction of frontal airbags in Germany (see Figure 75) has shown that it takes roughly ten years to reach 20% market penetration and another 5 years to reach a 50% market penetration. These time spans will also be assumed for the introduction of the PROSPECT systems. More detailed information on this topic can be found in the article from (Sander & Lubbe, 2018).

Furthermore, the user acceptance will be applied in a similar way as the fleet penetration rate. Results from Section 2.5.1.1 show that a user acceptance of 82% can be assumed at market introduction. For the calculation it is assumed that the acceptance will increase by 0.5% per year (as the system performance is continuously improved and users get more acquainted with the system).

3 RESULTS

3.1 SIMULATION RESULTS FROM OPENPASS

In openPASS, Algorithm 1 with different TTC trigger values for AEB has been implemented and simulated according to description in section 2.2.3. Figure 78 illustrates the simulated use case (UC_DEM_2) which is expanded by varying the lateral distance between the vehicle and cyclist to analyse the performance of the algorithm in a wide range of different conflict situations. The variation is taken from a normal distribution that covers lateral distance in a range of 2 - 10 m.

Throughout the analysis of the use case, simulations have been performed with different TTC trigger values for the AEB algorithm. The trigger values are varied in a range from 0.6 s up to 1 s. For each TTC trigger 1000 runs with different lateral distances have been simulated. Furthermore, baseline simulation with 6000 runs have been simulated and evaluated.

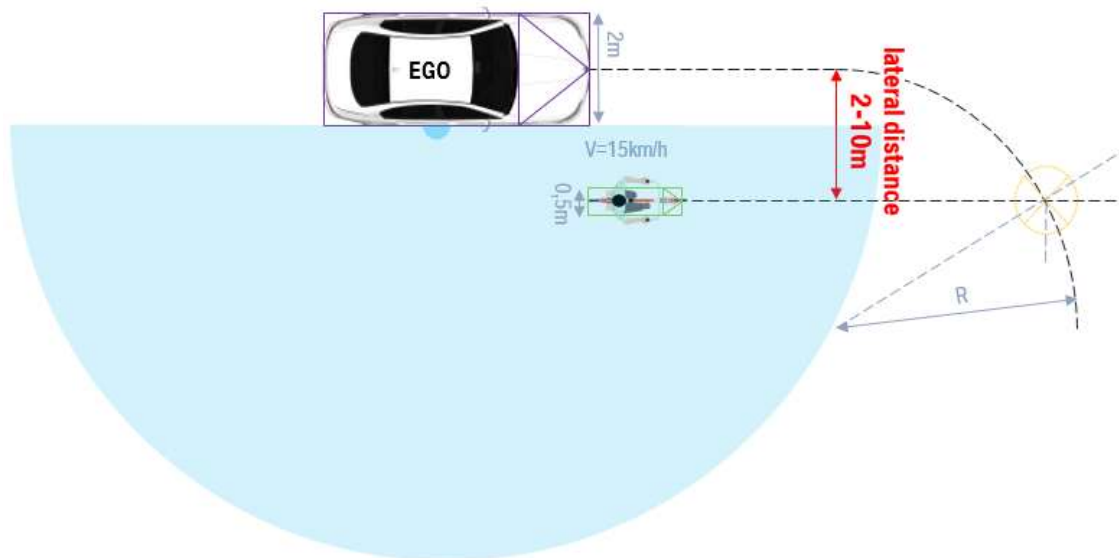


Figure 78: Layout of the simulated scenario.

The results in terms of absolute amount of detected accidents per TTC trigger values are given in Figure 79. For the baseline simulation without the AEB system, every run

led to an accident. Considering the fact that the cyclist does not react to the present situation, accidents occur also for the high TTC trigger values (the vehicle stops in the driving path and the cyclist drives into the stationary vehicle). In reality, the cyclist might avoid these accidents by his / her reaction to the situation. However, the analysis of this aspect is not in the scope of the simulated scenario, which should be in line and comparable with the demonstrator use cases.

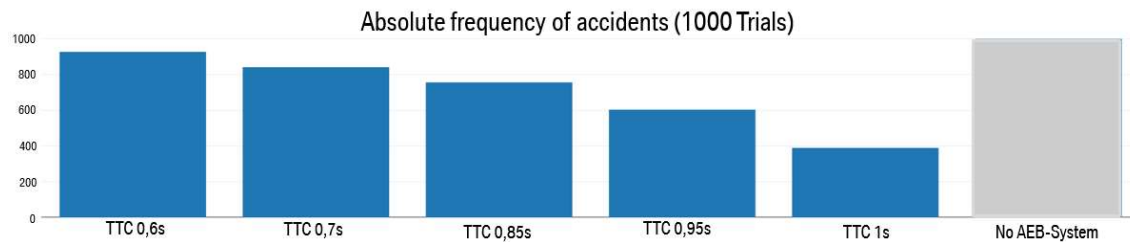


Figure 79: Absolute frequency of simulated accidents per TTC value.

3.2 LOCAL BENEFIT

3.2.1 Analysis of simulation results from rateEFFECT tool

The summary of the simulation results from rateEFFECT tool per use case and implemented algorithm are shown in Table 22 and Table 23.

Table 22: Frequency of total, avoided and mitigated crashes for algorithm 1 and 2 and use case.

Use Case	Total	Algorithm 1				Algorithm 2			
		Avoided	Mitigated	% Avoided	% Mitigated	Avoided	Mitigated	% Avoided	% Mitigated
1	131	112	19	85.5	14.5	111	20	84.7	15.3
2	143	53	90	37.1	62.9	51	92	35.7	64.3
3	244	124	120	50.8	49.2	101	143	41.4	58.6
4	216	142	74	65.7	34.3	125	91	57.9	42.1
5	496	409	87	82.5	17.5	391	105	78.8	21.2
6	105	83	22	79.0	21.0	81	24	77.1	22.9
9	21	16	5	76.2	23.8	15	6	71.4	28.6
10	342	156	186	45.6	54.4	117	225	34.2	65.8
11	216	48	168	22.2	77.8	34	182	15.7	84.3
12	20	5	15	25.0	75.0	5	15	25.0	75.0

Table 23: Frequency of total, avoided and mitigated crashes for algorithm 3 and use case.

Use Case	Total	Algorithm 3			
		Avoided	Mitigated	% Avoided	% Mitigated
1	131	112	19	85.5	14.5
2	143	51	92	35.7	64.3
3	244	104	140	42.6	57.4
4	216	126	90	58.3	41.7
5	496	395	101	79.6	20.4

6	105	82	23	78.1	21.9
9	21	15	6	71.4	28.6
10	342	122	220	35.7	64.3
11	216	36	180	16.7	83.3
12	20	5	15	25.0	75.0

The percentage of avoided crashes is greater than mitigated crashes in the use cases 1, 4, 5, 6, 9 for all 3 algorithms.

For use cases 2, 10, 11 and 12, the percentage of mitigated crashes is larger than the avoided crashes.

For use case 3, the percentage of avoided crashes is 50.9% with algorithm 1 and drops to 41.4% and 42.6% with algorithm 2 and 3, respectively.

For all use cases, except UC12, the algorithm 1 has the best performance in avoiding the crashes, compared to the other two algorithms. For use case 12, all 3 algorithms are performing the same with regards to the number of avoided and mitigated crashes.

Table 24: Frequency of avoided, mitigated and total number of crashes for steering and braking algorithm.

Use Case	Total	Avoided	Mitigated	% Avoided	% Mitigated
9	21	19	2	90.5	9.5
12	20	16	4	80.0	20.0

A fourth algorithm with both steering and braking has been implemented for use cases 9 and 12. The summary of these results are shown in Table 24.

In the following paragraphs the vehicle collision speed and several metrics that could be considered as predictors are investigated.

Pearson correlation of collision speed and vehicle initial speed, longitudinal and lateral distance of the VRU, and TTC when the VRU was first detected by the algorithm, for algorithm 1 per use case for mitigated and all crashes are shown in Table 25 and Table 26, respectively. There is positive correlation between collision speed and initial speed for all use cases.

There are 8 cases in use case 2, 4, 10 where the initial speed is zero, the car is standing still before the collision, but the collision speed is greater than zero. In four of the cases a bicycle is approaching from behind the vehicle and is not detected on time. The rest of the cases are with (not) permanent obstruction.

Table 25: Pearson correlation for collision speed and the metrics (initial speed, longitudinal distance, lateral distance, TTC at first detection) for algorithm 1 per use case for the mitigated crashes.

UC	Pearson correlation of collision speed and			
	initial speed	longitudinal distance	lateral distance	TTC at first detection
1	0.10	-0.12	0.59	-0.50
2	0.50	0.29	0.17	0.01
3	0.64	0.59	0.09	-0.01

4	0.70	0.65	-0.11	0.18
5	0.64	0.54	0.02	-0.07
6	0.48	0.29	-0.10	-0.04
9	0.97	0.93	-0.13	0.11
10	0.76	0.78	-0.05	-0.12
11	0.69	0.70	-0.03	0.01
12	0.97	0.94	0.37	0.27

Table 26: Pearson correlation for collision speed and the metrics (initial speed, longitudinal distance, lateral distance, TTC at first detection) for algorithm 1 per use case for all crashes.

UC	Pearson correlation for collision speed and			
	initial speed	longitudinal distance	lateral distance	TTC at first detection
1	0.14	0.10	0.04	-0.03
2	-0.20	-0.39	-0.06	0.04
3	0.66	0.63	0.24	-0.13
4	0.67	0.65	-0.13	-0.04
5	0.30	0.31	0.04	-0.04
6	0.16	0.06	0.06	-0.22
9	0.82	0.89	-0.13	0.39
10	0.73	0.75	0.03	-0.11
11	0.56	0.56	-0.08	-0.01
12	0.96	0.95	0.44	0.15

The prior distributions for the models described in Sections 2.3.1.1 and 2.3.1.2 were based on the simulation results. For example, for the initial speed 15 km/h specified for UC6 in Table 13, the simulated cases with initial speeds between 12.5 km/h and 17.5 km/h were considered for the prior distribution which included 20 cases in which the collision was avoided and 11 cases with a collision, for all of Algorithms 1-3. The corresponding prior distribution is illustrated in Figure 80 below.

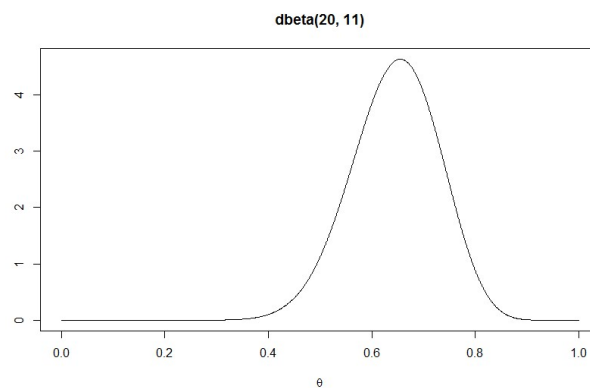


Figure 80: Prior distribution for the probability of crash avoidance in UC 6 for initial speed 15 km/h

As for the modelling collision speed in case of a crash, linear regression models based on variables as specified by Table 27 were used.

Table 27: Variables used in the linear regression models for the collision speed in case of a crash

	Car initial speed	VRU initial speed	Longitudinal distance	Lateral distance	Sight obstruction
UC1	x			x	x
UC2		x	x		
UC3	x				x
UC4	x				x
UC5	x				
UC6	x				
UC9	x	x			
UC10	x		x		x
UC11	x	x			
UC12	x	x			

The linear models using the variables specified in Table 27 gave the lowest AIC values for each of Algorithms 1-3, only the coefficients of the models were different. For the steering and braking algorithm in UC9, there were only two simulated cases with a collision. Therefore, the resulting linear model has a very large uncertainty and had so large variance that it did not make sense to consider upper and lower confidence limits. The model in this case was based on VRU initial speed only.

3.2.2 Update with test results

The simulation results were updated based on the following test results:

Table 28: Test results used for updating simulation results

Test scenario	Car initial speed (km/h)	Collision avoided (Y/N)	Collision speed
CBSF/CBIP03/CBIN01	30	Y	N/A
CBSF/CBIP03/CBIN01	30	Y	N/A
CBSF/CBIP03/CBIN01	30	Y	N/A
CBSF/CBIP03/CBIN01	40	Y	N/A
CBSF/CBIP03/CBIN01	40	Y	N/A
CBSF/CBIP03/CBIN01	40	Y	N/A
CBSF/CBIP03/CBIN01	50	Y	N/A
CBSF/CBIP03/CBIN01	50	Y	N/A
CBSF/CBIP03/CBIN01	50	Y	N/A
CBSF/CBIP03/CBIN01	50	Y	N/A
CBSF/CBIP03/CBIN01	50	Y	N/A
CBSF/CBIP03/CBIN01	50	Y	N/A
CBSF/CBIP03/CBIN01	50	Y	N/A
CBIG	10	Y	N/A
CBIG	10	Y	N/A
CBIG	10	Y	N/A

CBIG	15	Y	N/A
CBIG	15	Y	N/A
CBIG	15	Y	N/A
Longitudinal Pedestrian	30	Y	N/A
Longitudinal Pedestrian	40	Y	N/A
Longitudinal Pedestrian	50	Y	N/A
Longitudinal Pedestrian	60	Y	N/A
Longitudinal Cyclist	30	Y	N/A
Longitudinal Cyclist	40	Y	N/A
Longitudinal Cyclist	50	Y	N/A
Longitudinal Cyclist	60	Y	N/A
Crossing Static Pedestrian	20	Y	N/A
Crossing Static Pedestrian	30	Y	N/A
Crossing Static Pedestrian	40	Y	N/A
Crossing Static Pedestrian	50	Y	N/A
Crossing Static Cyclist	20	Y	N/A
Crossing Static Cyclist	30	Y	N/A
Crossing Static Cyclist	40	Y	N/A
Crossing Static Cyclist	50	Y	N/A
CBIP 01	10	Y	N/A
CBIP 01	15	Y	N/A
CBIP 01	20	Y	N/A
CBIN 05	10	Y	N/A
CBIN 05	15	Y	N/A
CBIN 05	20	Y	N/A
CBIN 06	10	Y	N/A
CBIN 06	15	Y	N/A
CBIN 06	20	Y	N/A

In particular, the simulation results for a certain use case were updated using the test results for the matched test scenario, as specified in Table 14. As noted already in Section 2.3.1.2, there are no test results that include a collision and therefore, only the crash avoidance probability model is updated.

The effect of the update by test results on the probability of crash avoidance is illustrated for the initial speed of 15 km/h in UC6. There is one test (CBIN 06) corresponding to this use case and initial speed, resulting in the avoidance of the collision. As test results are considered with weight $w = 2$, the posterior distribution is Beta (22,11), see Figure 81 below. Compared to the prior displayed as a dotted curve, this distribution is shifted to the right and is slightly more concentrated around the mean value, indicating a greater posterior probability of crash avoidance (due to having additional cases of collision avoidance) and smaller uncertainty (due to the increased sample size). As the sample size changed only slightly, the overall difference between the prior and the posterior distributions is not very large in this case.

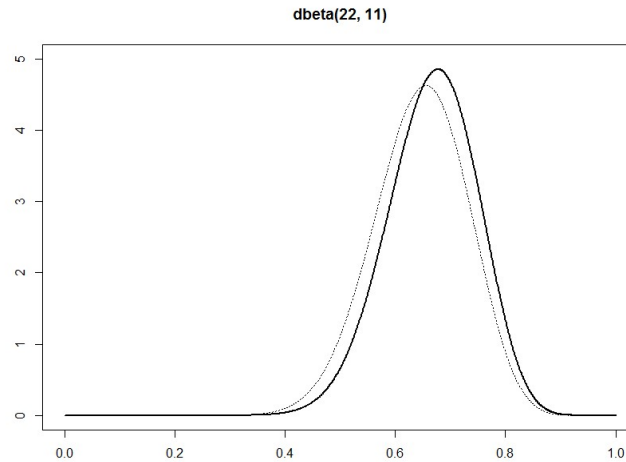


Figure 81: Posterior distribution for the probability of crash avoidance in UC 6 for initial speed 15 km/h.
The solid curve is the posterior distribution and the dotted curve is the prior.

The curve fitting procedure on the points determined by the posterior distribution as described in Section 2.3.1.1 yielded the logistic models for the probability of crash avoidance as specified in Table 29 below.

Table 29: Posterior models for the probability of crash avoidance

	Algorithm 1		Algorithm 2		Algorithm 3	
	Coefficient of car initial speed	Intercept	Coefficient of car initial speed	Intercept	Coefficient of car initial speed	Intercept
UC1	-0.214	6.084	-0.214	6.060	-0.214	6.084
UC2	0.046	-1.115	0.047	-1.192	0.047	-1.192
UC3	-0.069	1.965	-0.076	1.804	-0.076	1.865
UC4	-0.052	2.553	-0.048	2.112	-0.053	2.286
UC5	0.013	1.425	-0.038	1.813	-0.040	1.884
UC6	0.063	0.962	0.067	0.845	0.063	0.962
UC9	-0.930	52.204	-0.930	52.010	-0.930	52.010
UC10	-0.087	2.480	-0.085	1.979	-0.087	2.085
UC11	-0.033	-0.292	-0.046	-0.440	-0.051	-0.214
UC12	-0.353	16.546	-0.353	16.546	-0.353	16.546

Based on the models of crash avoidance probability and collision speed in case of a crash, the local benefits regarding fatalities, serious and slight injuries have been computed using the dose-response analysis described in Section 2.3.5. The summary of the local benefit in terms of percentage of injury reduction for algorithm 1 for all use cases is for cyclist and pedestrians are shown in Figure 82 and Figure 83, respectively, for the details for all algorithms per use case see Table 30-Table 32 below. These tables contain the estimates only for an easier overview; the corresponding tables

containing upper and lower bounds based on the confidence intervals in the above models are provided in the Appendix (Table 41).

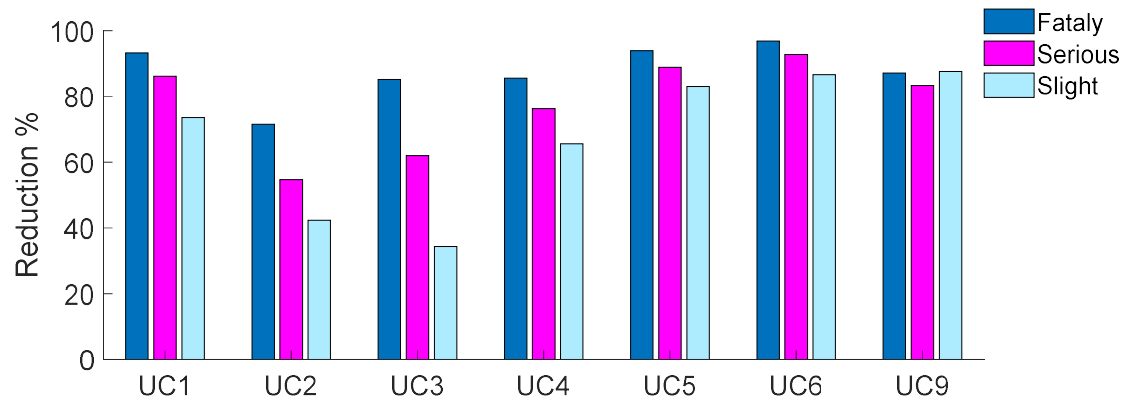


Figure 82: Local benefit for algorithm 1 per use case: percent of injury (fatal, serious, slight) reduction for cyclists.

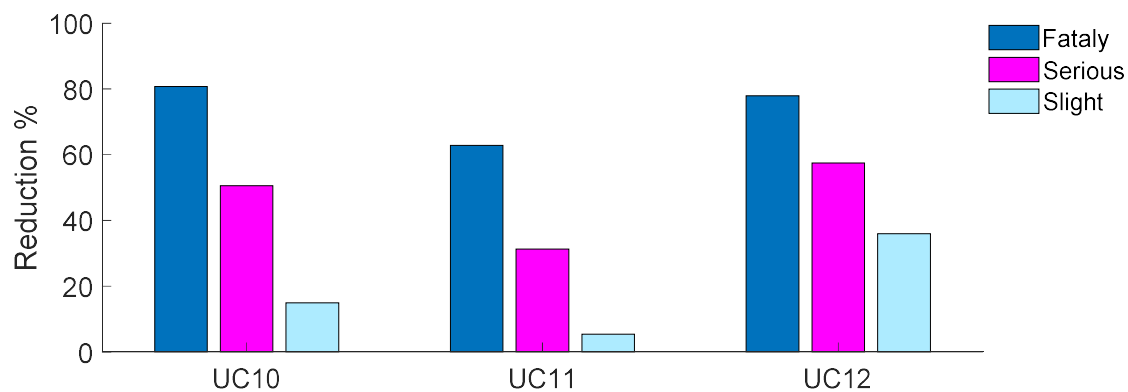


Figure 83: Local benefit for algorithm 1 per use case: percent of injury (fatal, serious, slight) reduction for pedestrians.

Table 30: Fatality reduction estimates for the PROSPECT systems

Fatalities avoided	Algo 1	Algo 2	Algo 3	Steering and braking
UC1	93%	92%	92%	N/A
UC2	72%	69%	70%	N/A
UC3	85%	81%	82%	N/A
UC4	86%	80%	81%	N/A
UC5	94%	91%	92%	N/A
UC6	97%	96%	96%	N/A
UC9	87%	80%	80%	98%
UC10	81%	74%	75%	N/A
UC11	63%	55%	56%	N/A
UC12	78%	70%	71%	98%
Overall VRUs	78%	72%	73%	N/A
Overall cyclists	86%	82%	83%	N/A

Overall pedestrians	76%	69%	69%	N/A
----------------------------	-----	-----	-----	-----

The results show a 55%-98% estimated benefit of the algorithms for the specific use cases, depending on the use case. The reduction of fatalities is greatest for UC6 and the steering and braking algorithm in UC9 and UC12, and smallest for UC11. The systems give a somewhat greater overall fatality reduction (82-86%) for cyclists than for pedestrians (69-76%, depending on the algorithm) within the considered use cases. Based on the values in Table 2, this means an estimated fatality reduction of 70-74% for car-to-cyclist crashes and 27-30% for car-to-pedestrian crashes in GIDAS.

Table 31: Estimates of the reduction of non-fatal serious injuries for the PROSPECT systems

Serious injuries avoided	Algo 1	Algo 2	Algo 3	Steering and braking
UC1	86%	85%	86%	N/A
UC2	55%	53%	53%	N/A
UC3	62%	55%	57%	N/A
UC4	76%	70%	72%	N/A
UC5	89%	85%	86%	N/A
UC6	93%	91%	91%	N/A
UC9	83%	81%	81%	93%
UC10	51%	43%	44%	N/A
UC11	31%	23%	24%	N/A
UC12	58%	53%	54%	95%
Overall VRUs	60%	54%	55%	N/A
Overall cyclists	76%	71%	72%	N/A
Overall pedestrians	44%	36%	37%	N/A

The reduction for serious injuries is somewhat lower than for fatalities, especially for pedestrians. The results for algorithms 1-3 are in the range of 53-93% for the cyclist use cases and 23-58% for the pedestrian use cases, yielding an overall reduction of 71-76% for cyclists and 36-44% for pedestrians for the different algorithms. Based on Table 2, this corresponds to a reduction of seriously injured between 53-56% for car-to-cyclist crashes and 19-23% for car-to-pedestrian crashes in GIDAS. The structure of the reduction by use case for serious injuries is similar to fatalities, i.e. the systems are most/least effective in the same sets of use cases. This again includes reductions over 90% for the steering and braking algorithm in the relevant use cases.

Table 32: Estimates of the reduction of slight injuries for the PROSPECT systems

Slight injuries avoided	Algo 1	Algo 2	Algo 3	Steering and braking
UC1	74%	73%	74%	N/A
UC2	42%	42%	42%	N/A

UC3	34%	28%	29%	N/A
UC4	66%	59%	60%	N/A
UC5	83%	78%	79%	N/A
UC6	87%	84%	85%	N/A
UC9	88%	90%	90%	90%
UC10	15%	10%	11%	N/A
UC11	5%	0%	1%	N/A
UC12	36%	46%	45%	90%
Overall VRUs	57%	53%	53%	N/A
Overall cyclists	68%	64%	65%	N/A
Overall pedestrians	12%	7%	8%	N/A

With the exception of UC9, the reduction of slight injuries is generally smaller than the reduction for serious or fatal injuries, especially for pedestrians. This is most obvious for UC11 in which the systems are predicted to provide only 0-5% reduction of slight injuries. The results for this injury severity can potentially be affected by fatal or serious injuries becoming slight injuries as a result of the system intervention.

The next section describes the results concerned with extrapolating the local benefits to EU level. This process will require the computation of the above benefits for various subsets of cases (e.g. cycle-to-car crashes in urban areas with a cyclist aged >55 years). The corresponding local benefits are given in the Appendix.

3.3 EXTRAPOLATION

The relative frequency of cyclist injuries in GIDAS and CARE are shown in [Figure 84](#). It can be seen that the relative frequency of fatal (0.4%) and slight (76.3%) injuries is lower in GIDAS than in CARE (1.2% and 82.4%, respectively), but the frequency of the severe injuries is higher (23.3% in GIDAS compared to 16.4% in CARE).

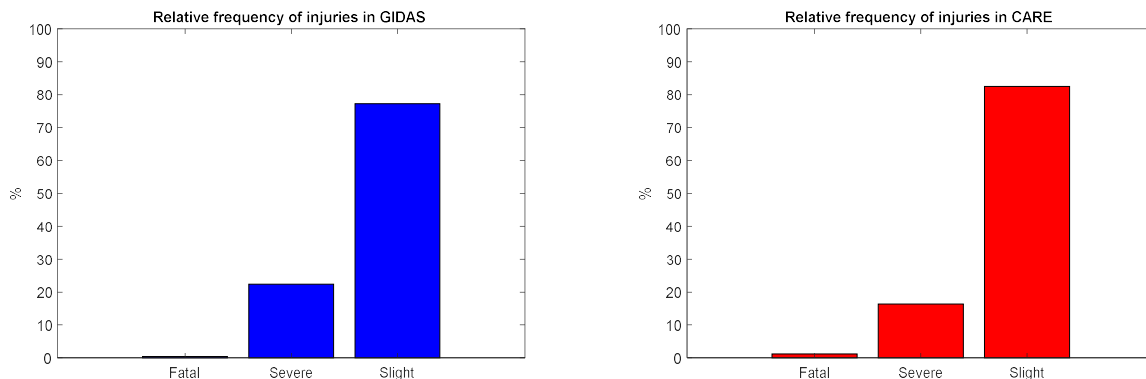


Figure 84: Relative frequencies of injuries from GIDAS and CARE.

The number of injured cyclist is 1356 including use cases 1, 2, 3, 4, 5, 6 and 9. However, 11 cases had unknown values for the variables (5 for gender, 3 for location, 1 for weather and 2 for age, see Table 17) and were filtered out, thus 1345 cases were used for the generation of the decision tree. The result of the decision tree method is

a structure that represents the GIDAS database in a tree format, see Figure 86. Each node has a node number, and the class of that node (i.e. fatal, serious or slight). The three values under the class show the number of cases to each class for that node.

The top node in the tree graphic is the so-called root, which contains all the persons involved in the analysed GIDAS crashes. Subsequently, the persons involved in the crashes are successively split according to the expression of the decision variables. In each step the existing node is divided into two subgroups using a binary query. For example, the decision variable 'Age3' is queried in the first split. In this case all persons involved in crashes that are older than 55 are divided into the subgroup 'Age >55', and the rest of the persons are divided into the subgroup 'Age ≤55'. These subgroups can be seen in the tree graphic as additional nodes (2 and 3).

In the next step, the subgroups created in this way are transformed into other decision variables, which leads to the tree structure illustrated in Figure 86. The successive division of the nodes is terminated when further divisions result into number of persons in each leaf (the end nodes that cannot be further split) to be less than the threshold of minimum size of the nodes (minimum bucket size-the minimum number of observations in any terminal node i.e. leaf). Within each leaf that describes a certain crash characteristic, the relative frequencies of the injuries are calculated. For node 3, for example the numbers show, that 3 persons are fatally injured, 208 are seriously injured and 835 slightly injured.

Data from CARE is extracted for car-to-cyclist accidents in EU-28 in years 2009-2013 (see "Deliverable 2.1 Accident data analysis, naturalistic driving studies and project implications" for data selection criteria (Wisch, et al., 2016). The proportion of data that corresponds to the cyclist use cases (77% of all car to cyclist accidents which is a projection from GIDAS, see section 2.1.3) is used for calculating the classification tree. The classification tree for CARE, build on bases of GIDAS tree is shown in Figure 86. From these two trees the factors (Table 33) were calculated according to equation 6. For example, the factor in the first row and column in Table 33 can be interpreted as one person that is fatally injured and younger than 55 years from GIDAS is corresponding to 522 persons in CARE.

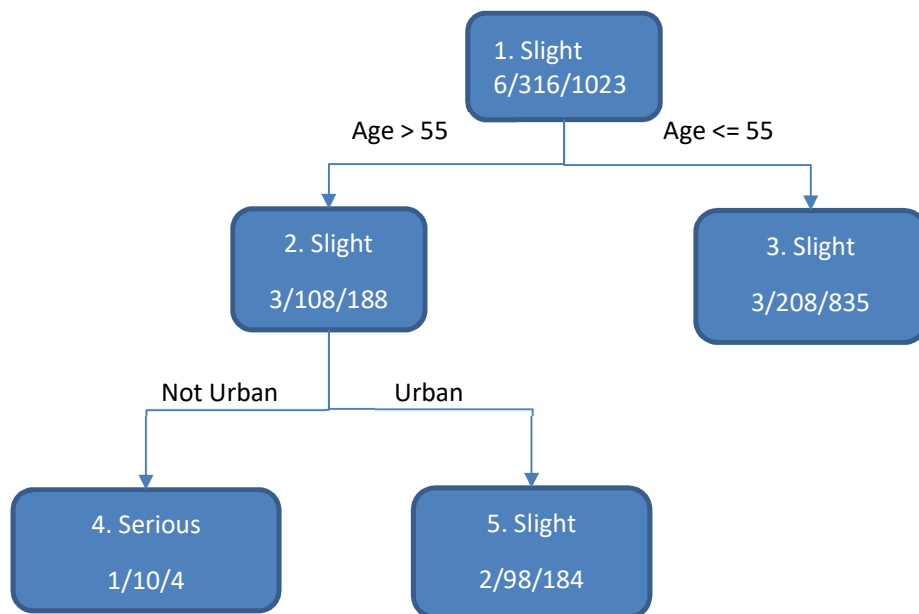


Figure 85: Classification tree for cyclist injuries from GIDAS. In each box the first row shows the node number and the predicted injury class for that node; the second row shows the number of cases that are classified as fatal/serious/slight.

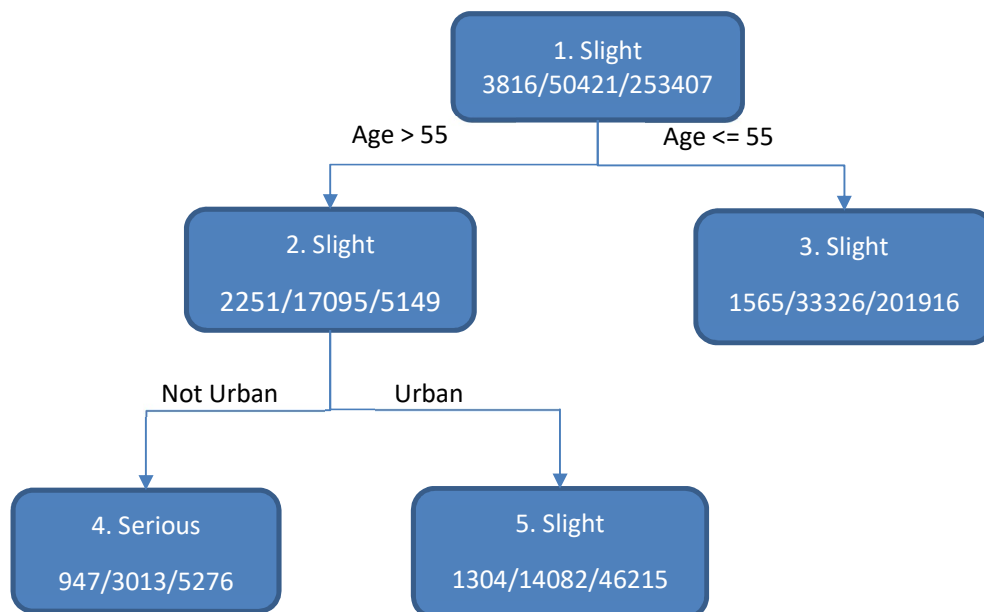


Figure 86: Classification tree for cyclist injuries from CARE. In each box the first row shows the node number and the predicted injury class for that node; the second row shows the number of cases that are classified as fatal/serious/slight.

Table 33: Factors for extrapolation of cyclist injuries from GIDAS to CARE.

	Fatal	Serious	Slight
Leaf 3 (Age <=55)	522	160	242
Leaf 4 (Age > 55 and Not Urban)	948	301	1319
Leaf 5 (Age > 55 and Urban)	652	144	251

The results for classification tree for pedestrian injuries are shown in Figure 87. The same classification tree is generated for pedestrian injuries from CARE by using the proportion of data that corresponds to the pedestrian use cases (44 % of all car-to-pedestrian accidents which is a projection from GIDAS, see section 2.1.3). From these two trees the extrapolation factors for pedestrian injuries (Table 34) were calculated according to equation 6.

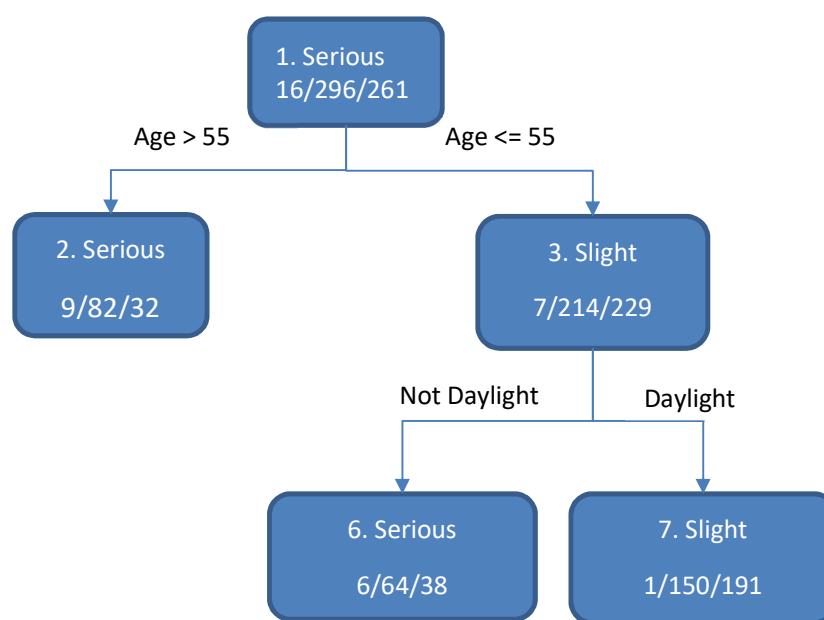


Figure 87: Classification tree for pedestrian injuries from GIDAS. In each box the first row shows the node number and the predicted injury class for that node; the second row shows the number of cases that are classified as fatal/serious/slight.

Table 34: Factors for extrapolation of pedestrian injuries from GIDAS to CARE.

	Fatal	Serious	Slight
Leaf 2 (Age > 55)	425	228	1135
Leaf 6 (Age <= 55 and Not Daylight)	408	199	927
Leaf 7 (Age <= 55 and Daylight)	767	120	375

The reduction of cyclist injuries from GIDAS (section 3.2.2) is extrapolated to CARE by using the extrapolation factors, leading to average reduction of cyclist injuries per year, shown in Table 35 and Table 36.

Table 35: Number of reduced cyclist injuries for one year by different algorithms for use cases 1-9.

	Algo 1	Algo 1 Lower bound	Algo 1 Higher bound	Algo 2	Algo 2 Lower bound	Algo 2 Higher bound	Algo 3	Algo 3 Lower bound	Algo 3 Higher bound
Fatal	693	650	719	666	617	698	673	625	702
Serious	7762	6353	8613	7322	6045	8225	7435	6020	8323
Slight	31835	19355	38935	29499	20505	36550	29809	17368	37100

Table 36: Number of reduced cyclist injuries for one year by steering and braking algorithm for use case 9.

	Steering and braking
Fatal	102
Serious	294
Slight	627

The reduction of pedestrian injuries from GIDAS (section 3.2.2) is extrapolated to CARE by using the extrapolation factors, leading to average reduction of pedestrian injuries per year, shown in Table 37 and Table 38.

Table 37: Number of reduced pedestrian injuries for one year by different algorithms for use cases 10-12.

UC 10,11, 12	Algo 1	Algo 1 Lower bound	Algo 1 Higher bound	Algo 2	Algo 2 Lower bound	Algo 2 Higher bound	Algo 3	Algo 3 Lower bound	Algo 3 Higher bound
Fatal	1147	1070	1214	1067	991	1139	1074	995	1145
Serious	4543	3454	5605	3859	2909	4858	3939	2964	4947
Slight	-1893	-6347	2900	-3251	-6705	780	-3089	-6633	1035

Table 38: Number of reduced pedestrian injuries for one year by steering and braking algorithm for use case 12.

	Steering and braking	Steering and braking Lower bound	Steering and braking Higher bound
Fatal	78	59	82
Serious	487	364	515
Slight	871	626	975

3.4 SOCIETAL BENEFIT

The maximum societal benefit of PROSPECT systems for one year, assuming 100% market penetration and 100% user acceptance, is shown in Figure 88.

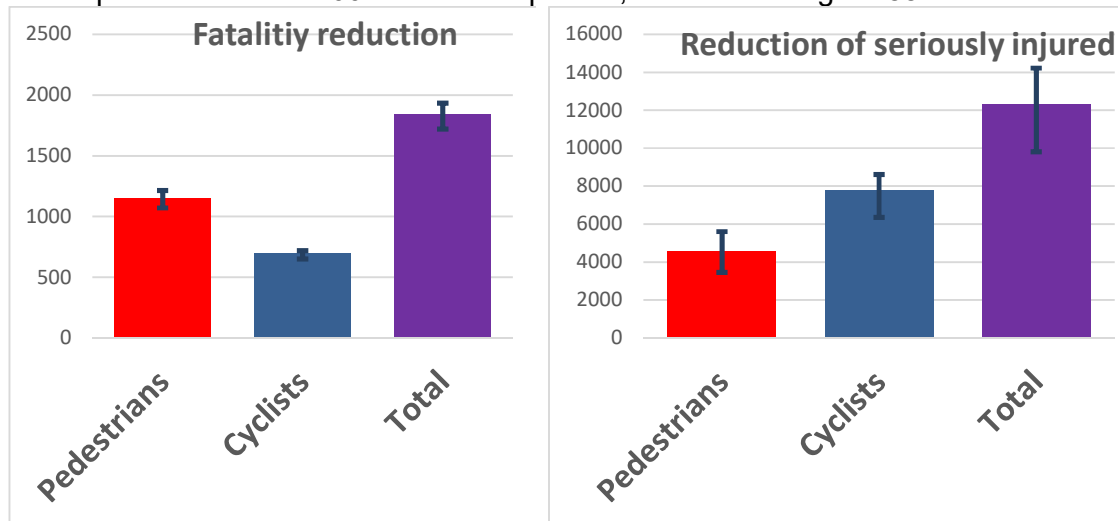


Figure 88: Reduction of casualties annually in EU-28, with lower and upper boundaries, assuming 100% market penetration and 100% user acceptance.

Taking the assumed increasing market penetration described in Section 2.4.2 (see Figure 89) and user acceptance into account described in Section 2.5.1.1 (see Figure 90), the annual number of lives saved in EU-28 increases from an estimate of 79-95 in 2025 to 280-336 in 2030, while the corresponding estimates for the reduction of seriously injured are 439-697 in 2025 and 1558-2474 in 2030. The monetary societal benefits for each algorithm, including upper and lower boundaries, in the year 2030 assuming a market penetration of 20% and a user acceptance of 87%, can be found in Table 39.

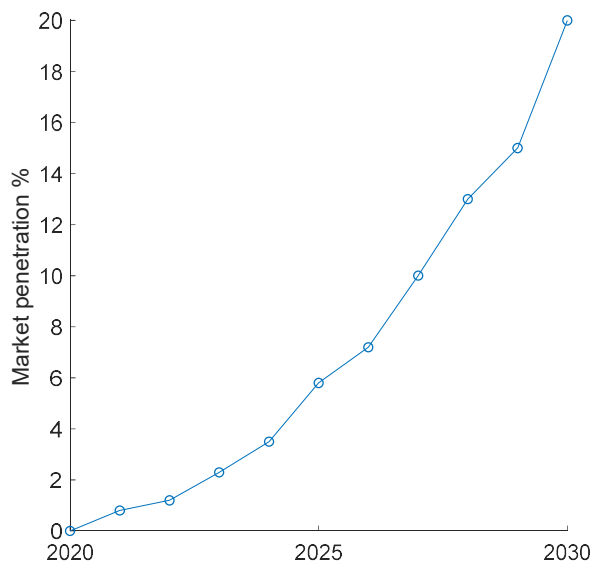


Figure 89: Yearly increasing market penetration.

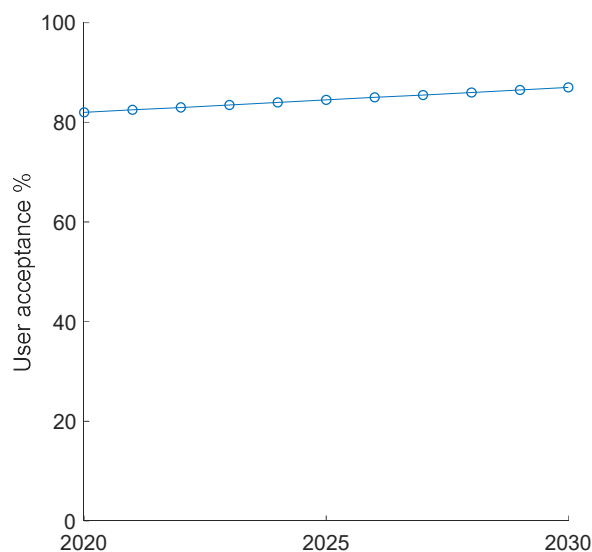


Figure 90: Yearly increasing user acceptance.

Table 39: Estimated benefits of the systems in 2030

	lower	estimate	upper
Algo 1	948 M€	1 138 M€	1 280 M€
Algo 2	885 M€	1 051 M€	1 192 M€
Algo 3	878 M€	1 063 M€	1 206 M€
Algo St&Br		91 M€	

Due to the low amount of cases, no upper and lower boundary could be calculated for the Steering and Braking Algorithm, hence only the estimate is reported.

Table 40: Estimated benefits of the systems by 2030 (sum of 10 years)

	lower	estimate	upper
Algo 1	3 387 M€	4 066 M€	4 574 M€
Algo 2	3 160 M€	3 753 M€	4 260 M€
Algo 3	3 138 M€	3 798 M€	4 306 M€
Algo St&Br		325 M€	

The yearly benefit with lower and upper boundaries for each algorithm can be seen in Figure 91 to Figure 94. Basis is the year 2020 with a market penetration of 0% and therefore no benefits of the systems. The market penetration will increase over time, reaching a 20% market share after 10 years in 2030.

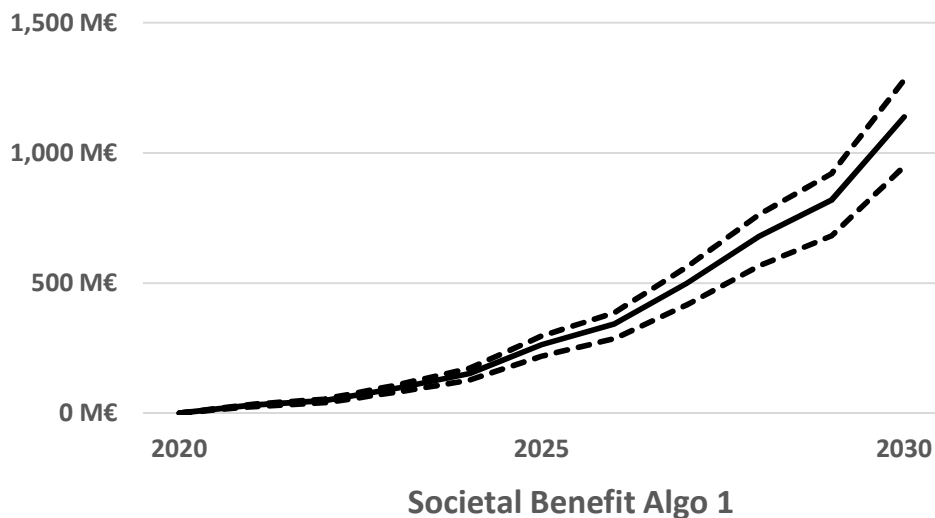
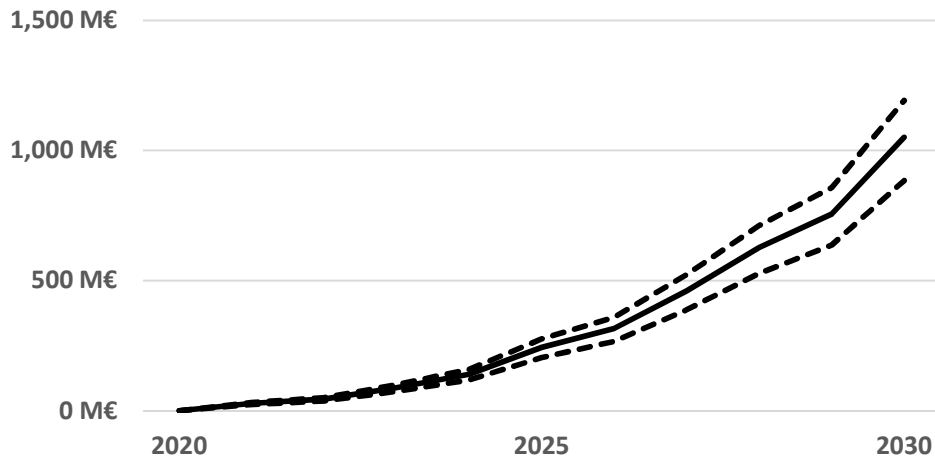
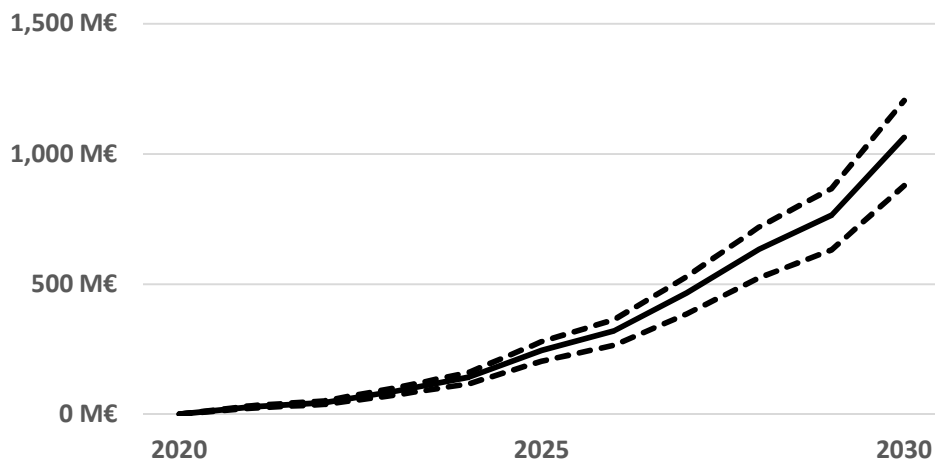


Figure 91: Yearly societal benefit of algorithm 1



Societal Benefit Algo 2

Figure 92: Yearly societal benefit of algorithm 2



Societal Benefit Algo 3

Figure 93: Yearly societal benefit of algorithm 3

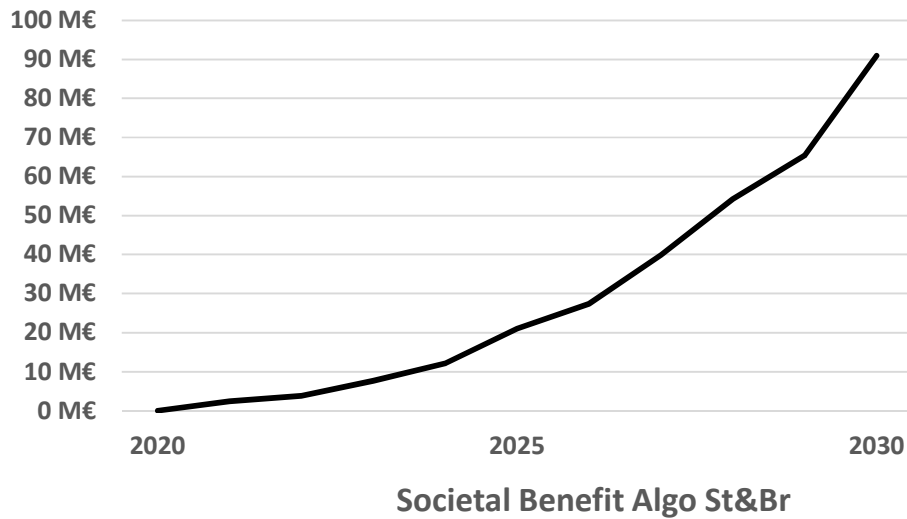


Figure 94: Yearly societal benefit of steering and braking algorithm

4 DISCUSSION

This deliverable shows the estimated real-world benefit of the developed PROSPECT systems, i.e. the improvement for traffic safety in terms of saved lives, reduced injuries as well as the resulting overall monetary benefit. This section gives a detailed discussion of the method, the results and the limitations, and the main conclusions are drawn in Section 5. A pictorial summary of the methodology is provided in Section 6.

The task 2.4 (benefit estimations) used the results from tasks 2.1 (characteristics of vehicle to VRU accidents) and 3.1 (target scenarios for PROSPECT) and work package 7 (testing and validation) to define and apply a methodology to estimate the socio-economic impact of PROSPECT safety systems. This methodology was focused on the development of framework for assessment of active safety systems (Figure 1). Benefit estimation of passive safety measures was conducted on the basis of a literature review, taking into account the benefits due to Euro NCAP, legislation and deployable systems such as pedestrian and cyclist airbags and pop-up bonnets.

Four algorithms of the PROSPECT systems have been implemented in counterfactual simulation tool rateEFFECT for all use cases, and one of the algorithms (algorithm 1) has been implemented into openPASS tool for one of the use cases (UC_DEM_2-vehicle turning right and a bicycle moving straight). The output from rateEFFECT for all use cases has been used in the benefit estimation framework. The openPASS tool is open source tool that is still in development and in this task, it was used to demonstrate the applicability and proof-of-concept for harmonization of methods and models for prospective assessment by simulation and thus the results are not incorporated in the benefit estimation framework.

Due to the relatively low number of GIDAS cases that are related to the individual 12 use cases, Injury Risk Functions (IRF) for all cyclist use cases as well as for all pedestrian use cases per severity were designed. For the injury risk functions, we used the police reported injury severity, to be able to do a projection to EU level. However, since previous studies (Wisch, et al, 2017) have used MAIS severity, we also

developed new MAIS-based IRFs (provided in the Appendix) that could be used in future studies.

The local benefit regarding fatalities, serious and slight injuries showed 55%-98% benefit of the algorithms, depending on the use case. The reduction of fatalities is greatest for UC6 (car intends to turn left and a cyclist is crossing from the left side) and smallest for UC11 (a pedestrian is crossing from the right side from an obstructed view). The system gives a somewhat greater overall fatality reduction (82-86%) for cyclists than for pedestrians (69-76%, depending on the algorithm). The reduction for serious injuries is somewhat lower than for fatalities, especially for pedestrians. The results are in the range of 53%-93% for cyclists and 23%-58% for pedestrians depending on the use case and yielding an overall reduction of 71-76% for cyclists and 36-44% for pedestrians for the different algorithms. The reduction of slight injuries was generally smaller than the reduction for serious or fatal injuries, especially for pedestrians. Considering the percentage of injuries of different severities represented by the use cases, the above results correspond to an estimated fatality reduction of 70-74% for cyclists and 27-30% for pedestrians and a reduction of seriously injured by 53-56% for cyclists and 19-23% for pedestrians in car-to-VRU crashes in GIDAS PCM. The local benefit was extrapolated to EU-28 by using decision tree method. It was assumed that market penetration and user acceptance of the PROSPECT systems gradually increase, from 5.8% and 84.5% in 2025 to 20% and 87% in 2030. Due to the assumed increasing market penetration and user acceptance, the annual number of lives saved in EU-28 increases from an estimate of 79-95 in 2025 to 280-336 in 2030, while the corresponding estimates for the reduction of seriously injured are 439-697 in 2025 and 1558-2474 in 2030. Accordingly, the socio-economic benefit of PROSPECT systems increases from 203-296 million euros in 2025 to monetary values exceeding 878-1280 million euros from 2030 on.

Limitations

This work has some limitations intrinsic to the input data, algorithms in counterfactual simulations and design of the tests, as described below. These same considerations should be taken into account in interpreting the results.

The extrapolation from micro level (simulations and tests) to macro level, EU-28 databases for accidents, provides still considerable challenges, concerning the matching of the variables, the details of information, and the availability of the data for all countries. Furthermore, underreporting of the accidents (investigated in D2.1) has not been taken into account.

Regarding the passive safety systems, it was found from the literature that every system is evaluated in its “field of action”, i.e. for those accidents where it is supposed to have an effect, which limits the comparison of different countermeasures.

Counterfactual simulations implemented the algorithms as the prototype PROSPECT systems, however to what extent these algorithms will resemble the systems in the production phase remains to be investigated in future. Driver models, and the choice of driver model have been found to have a large effect on the estimate of safety benefit of ADAS using counterfactual simulations (Bärgman, Boda, & Dozza, 2017), but are not included in the counterfactual simulations in this project. Thus, in future research and applications of counterfactual simulations for the safety benefit evaluation of ADAS, algorithms for ADAS and driver behaviour models should be studied jointly.

Furthermore, there are differences between the use cases and the test cases as well as the PCM and GIDAS cases, some of which is described in Section 2.1.4. In spite of these differences, it was assumed that the test cases matched to the use cases as specified in Table 14 give an appropriate representation of the use cases in terms of crash avoidance probability.

The results of the user acceptance have also some limitations with regards to different use cases considered in different experiments and the fact that the participants of the experiments have not used the PROSPECT systems.

The modelling of collision speed in case of a crash was done independently from the probability of a collision and was based on the simulated cases in which the collision was not avoided. A potential refinement of the current method would be a model that draws conclusions from all cases; for example, each avoided case with a braking only algorithm provides some information about the extent of speed reduction. The exploration of these dependencies and including them in the modelling process may be one possible direction for future research.

Lastly, the door opening use cases, UC_DEM_7 and UC_DEM_8, haven't been included in the simulations due to the lack of these cases in the crash database PCM from GIDAS, and the benefit of the corresponding systems could not be estimated.

5 CONCLUSION

In conclusion, the proposed framework gives an appropriate mathematical framework which allows updating prior information, based on simulation results, with new observations from test results. This framework is an improvement on the state-of-the-art benefit assessment and gives possibility of updating the results with more observations (even after the project), for example if the prototype systems have been improved in production phase.

Using this method with simulation results and test results and assuming an increasing market penetration and user acceptance, the estimate for the annual number of lives saved in EU-28 by the PROSPECT systems increases from 79-95 in 2025 to 280-336 in 2030, while the corresponding estimates for the reduction of seriously injured are 439-697 in 2025 and 1558-2474 in 2030. The estimated socio-economic benefit of PROSPECT systems increases from 203-296 million euros in 2025 to monetary values exceeding 878-1280 million euros from 2030 on. These results should be interpreted in relation to the limitations of the method, as described above.

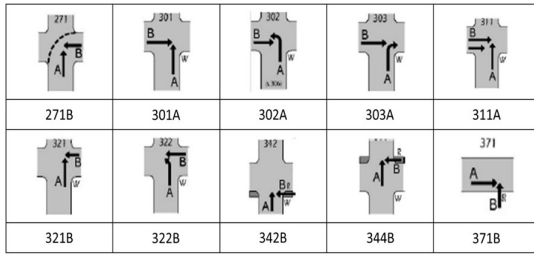
The results have potential implications for policies and regulations in understanding the real-world benefit of new ADAS. Furthermore, the importance of the proposed framework is relevant for automotive industry also in the development and evaluation of automated vehicles where the recent NHTSA (NHTSA, 2016) guidelines on automated vehicles call for the use of virtual safety evaluation.

6 SUMMARY AND HIGHLIGHTS

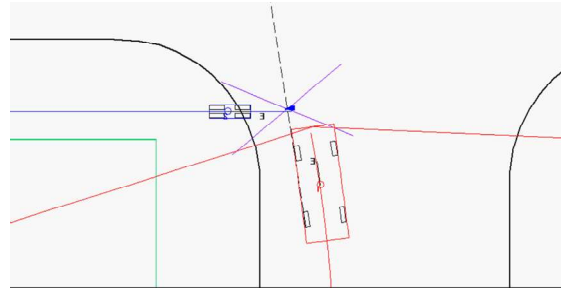
The safety assessment methodology proposed in this report, illustrated pictorially in Figure 95 below, can be summarised in the following steps:

1. Select scenarios from in-depth crash data which are relevant for use cases (identified in accident analysis).
2. Re-simulate each relevant crash assuming that the car is equipped with a PROSPECT system.
3. Calculate crash avoidance probability and collision speed reduction with the systems based on the simulation results.
4. Perform vehicle-based testing of the prototype systems for the defined test scenarios.
5. Update the crash avoidance probability and collision speed reduction model with the test results.
6. Calculate local VRU injury reduction (for the use cases) by applying the dose-response method:
 - Calculate injury risk curves per injury level (fatal, serious and slight injuries).
 - Calculate frequency of crashes without the prototype systems.
 - Calculate frequency of crashes with the prototype systems.
 - Calculate VRU injuries without the prototype systems.
 - Calculate VRU injuries with the prototype systems.
 - Calculate reduction of VRU injuries.
7. Calculate the VRU injury reduction for EU-28 by extrapolating the local VRU injury reduction, with the classification tree method, assuming that the prototype systems are fitted in all cars and accepted 100% by the users.
8. Estimate user acceptance of the prototype systems based on results from specific studies (conducted in other work packages).
9. Estimate the expected market penetration rate of the prototype systems based on historical data..
10. Calculate the socio-economic benefit: using unit costs for the prevented injuries (fatal, serious and slight), the injury reduction calculated in the step 7 and updated with the expected user acceptance and market penetration is converted into a monetary value.

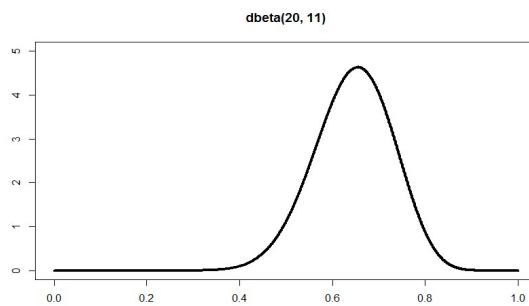
Highlights of the methodology and the resulting assessment of PROSPECT systems are provided after Figure 95.



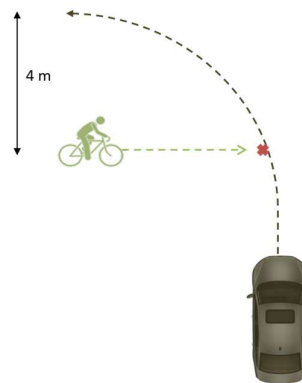
1. GIDAS scenarios relevant for a use case.



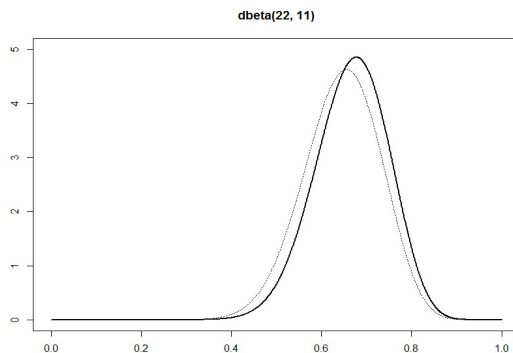
2. Counterfactual simulation.



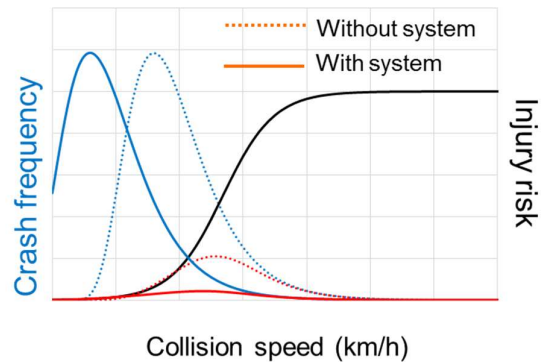
3. Crash avoidance probability based on simulation.



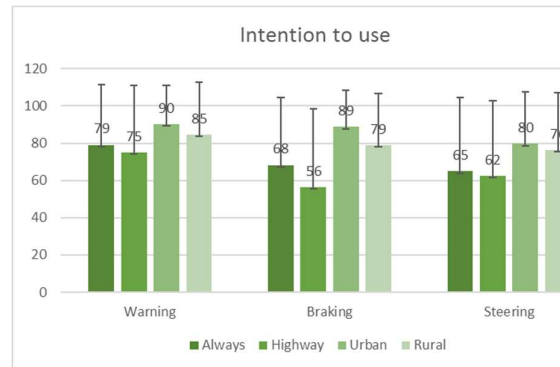
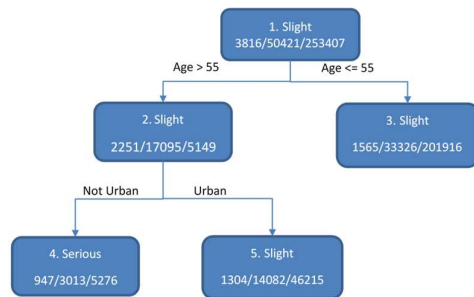
4. Vehicle-based testing.



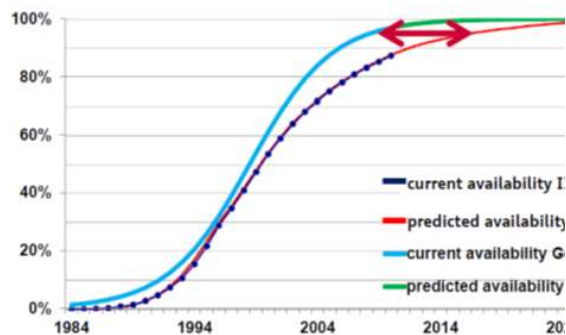
5. Crash avoidance probability updated with test results.



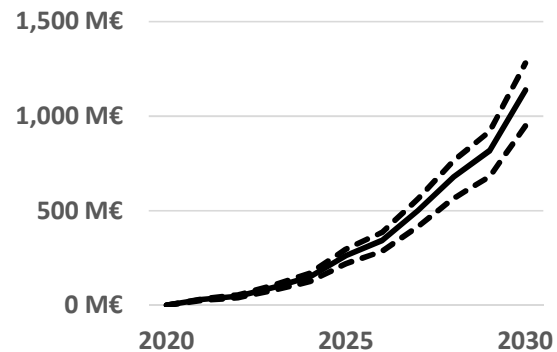
6. Illustration of dose-response method.



7. Extrapolation to EU-28 by classification tree method.



8. User-acceptance data.



9. Market penetration rates.

10. Societal benefit.

Figure 95: Illustration of the steps in the safety assessment methodology.

Highlights:

- A novel safety benefit assessment framework for active safety systems for VRU protection is proposed which combines result from computer simulations and vehicle-based tests.
- The framework is implemented for the PROSPECT prototype systems. It could also be used to update the obtained results with more observations if the prototype systems are changed in production phase.
- The estimates for the annual number of **lives saved** in EU-28 by the PROSPECT systems are **79-95** in 2025 and **280-336** in 2030.
- The estimates for the **reduction of seriously injured** are **439-697** in 2025 and **1558-2474** in 2030.
- The estimated **socio-economic benefit** of PROSPECT systems increases from **203-296 million euros** in 2025 to monetary values exceeding **878-1280 million euros** from 2030 on.
- The results have potential implications for policies and regulations in understanding the real-world benefit of new active safety systems.

7 REFERENCES

- Aitchinson, J., & Silvey, S. (1957). The generalization of probit analysis to the case of multiple responses. *Biometrika* 44, 131-140.
- Akaike, H. (1974). A new look at the statistical model identification. *IEEE Transactions on Automatic Control* 19, 716-723.
- Ames, E., & Martin, P. (2015). Pop-up hood pedestrian protection. *24th International Technical Conference on the Enhanced Safety of Vehicles*. Gothenburg, Sweden: NHTSA.
- Audi. (2016). *D3.1 The addressed VRU scenarios within PROSPECT and associated test catalogue*. PROSPECT.
- Bálint, A., Fagerlind, H., & Kullgren, A. (2013). A test-based method for the assessment of pre-crash warning and braking systems. *Accident Analysis and Prevention*, 59, 192-199.
- Barrow, A., Edwards, A., Khatry, R., Cuerden, R., Schneider, A., Labenski, V., & Veh, U. (2018). Casualty Benefits of Measures Influencing Head to Windscreen Area Protection. *IRCOBI conference*. Athens, Greece.
- BAST. (2018). *Deliverable 7.4-Test protocol as a proposal for consumer testing*.
- Bellet, T., & Banet, A. (2012). Towards a conceptual model of motorcyclists' Risk Awareness: A comparative study of riding experience effect on hazard detection and situational criticality assessment. *Accident Analysis & Prevention*, 49, 154-164.
- Boda, C. N., Dozza, M., Bohman, K., Thalya, P., Larsson, A., & Lubbe, N. (2018). Modelling how drivers respond to a bicyclist crossing their path at an intersection: How do test track and driving simulator compare? *Accident Analysis and Prevention* 111, 238-250.
- Boliang, Y. (2016). Kombiniertes Ausweichen und Bremsen zum letztmöglichen Moment. *URBAN Conference*. Garching.
- Broughton, J., & al, e. (2010). Estimation of the real number of road casualties in Europe. *Safety Science*, 48(3), 365-371.
doi:<https://doi.org/10.1016/j.ssci.2009.09.012>
- Buhne, J.-A., Ludeke, A., Schonebeck, S., Dobberstein, J. F., Balint, A., & McCarthy, M. (2012). *ASSESS D2.2 - Socio-economic impact of safety systems*. EU.
- Bärgman, J., Boda, C., & Dozza, M. (2017). Counterfactual simulations applied to SHRP2 crashes: The effect of driver behavior models on safety benefit estimations of intelligent safety systems. *Accident Analysis and Prevention* 102, 165–180. doi:10.1016/j.aap.2017.03.003
- Chauvel, C., Yves, P., Fildes, B., & Lahaussé, J. (2013). Automatic emergency braking for pedestrians effective target population and expected safety benefits. *ESV*. Seoul, Korea, South.
- Cicchino, J. (2017). Effectiveness of forward collision warning and autonomous emergency braking systems in reducing front-to-rear crash rates. *Accident Analysis and Prevention*, 99, 142-152. doi:10.1016/j.aap.2016.11.009
- CONTI. (2018). *Deliverable 4.2 - Sensor fusion*.
- Corliss, D. (August 2018). *Model Variable Selection Using Bootstrap Decision Tree*. Hämtat från SAS:
<http://support.sas.com/resources/papers/proceedings14/1300-2014.pdf>

- Cuny, S., Page, Y., & Zangmeister, T. (2008). *D4.2.2 TRACE - Evaluation of the safety benefits of existing Safety Functions*. European Commission.
- DAIMLER. (2018). *Deliverable 6.2 - Vehicle demonstrators*.
- Dirndorfer, T. (2015). *Integrale Nutzung von Pre-Crash-Sensorik zur Ansteuerung frontaler Rückhaltesysteme im Fahrzeug – Möglichkeiten und Grenzen*. Göttingen: Cuvillier Verlag, ISBN 9783736991248.
- Edwards, M., Nathanson, A., Carroll, J., Wisch, M., Zander, O., & Lubbe, N. (2015). Assessment of Integrated Pedestrian Protection Systems with Autonomous Emergency Braking (AEB) and Passive Safety Components. *Traffic Injury Prevention*, 2-11. doi:10.1080/15389588.2014.1003154
- Erbsmehl, C. (2008). Simulation realer Unfälleinlaufszzenarien der German In-Depth Accident Study (GIDAS) Erstellung und Nutzen von "pre crash scatter plots". *24 Internationale VDI/VW Gemeinschaftstagung Integrierte Sicherheit und Fahrerassistenzsysteme*. Wolfsburg.
- EU. (2009). *Official Journal of the European Union*. L 35/2.
- EUDirective, A. (2003). *Protection of pedestrians and other vulnerable road users*. Hämtat från European Union: <https://eur-lex.europa.eu/legal-content/EN/TXT/HTML/?uri=LEGISSUM:n26030&from=DE>
- EURONCAP. (2018). *EURO NCAP*. Hämtat från EU: <https://www.euroncap.com/en>
- European Commission. (2016). *Road Safety Management*. Brussels, Belgium.
- Ferreira, S. F. (2015). The quality of the injury severity classification by the police: An important step for a reliable assessment. *Safety Science*, 79, 88-93. doi:<https://doi.org/10.1016/j.ssci.2015.05.013>
- Fildes, B., Keall, M., Bos, N., Lie, A., Page, Y., Pastor, C., . . . Tingvall, C. (2015). Effectiveness of low speed autonomous emergency braking in real-world rear-end crashes. *Accident Analysis and Prevention*, 81, 24-29. doi:10.1016/j.aap.2015.03.029
- Fitch, G., Rakha, H., Arafeh, M., Blanco, M., Gupta, S., Zimmermann, R., & Hanowski, R. (2008). *Safety Benefit Evaluation of a Forward Collision Warning System: Final Report*. Blacksburg, VA: DOT HS 810 910.
- Flannagan, C., Bálint, A., Klinich, K., Sander, U., Manary, M., Cuny, S., . . . Fagerlind, H. (2015). *Comparing Motor-Vehicle Crash Risk of EU and US Vehicles*. Ann Arbor: UMTRI.
- Fredriksson, R., & Rosén, E. (2014). Head injury reduction potential of integrated pedestrian protection systems based on accident and experimental data—benefit of combining passive and active systems. *IRCOBI Conference*. Berlin, Germany.
- Hamacher, M., Kuehn, M., Hummel, T., & Eckstein, L. (2017). Effectiveness of pedestrian safety measures at the vehicle front with regards to cyclists. *25th International Technical Conference on the Enhanced Safety of Vehicles*. Detroit, Michigan, USA: NHTSA.
- HLDI. (2017). *Predicted availability of safety features on registered vehicles*. Arlington, VA.
- Hoff, P. D. (2009). *A First course in Bayesian statistical methods*. Springer.
- IDIADA. (2013). <http://www.aspecss-project.eu/>. Hämtat från <http://www.aspecss-project.eu/>
- IDIADA. (2018). *Deliverable 7.1-Report on vehicle-based functional tests*. EU.

- IFSTTAR. (2018). *Deliverable 7.2-Report on methodology for balancing user acceptance, robustness and performance*. EU.
- IIHS. (den 24 January 2012). *Estimated time of arrival*. Hämtat från Status report, Vol 47, No1 - IIHS HDLI: <https://www.iihs.org/iihs/sr/statusreport/article/47/1/1> August 2018
- ISO/NP 21934-1 ISO/TC 22 SC36 WG7. (2018). *Road vehicles-Prospective safety performance assessment of pre-crash technology by virtual simulation-Part 1: State-of-the-art and general method overview*. ISO.
- Jian, J., Bisantz, A., & Drury, C. (2000). Foundations for an empirically determined scale of trust in automated systems. *International Journal of Cognitive Ergonomics*, 4(1), 53-71.
- Korner, J. (1989). *A Method for Evaluating Occupant Protection by Correlating Accident Data with Laboratory Test Data*. SAE Technical Paper 890747, doi:10.4271/890747.
- Kreiss, J.-P., Feng, G., Krampe, J., Meyer, M., Niebuhr, T., Pastor, C., & Dobberstein, J. (2015). Extrapolation of GIDAS accident data to Europe. *ESV*. Gothenburg, Sweden: NHTSA.
- Kruschke, J. K. (2015). *Doing Bayesian Data Analysis: A Tutorial with R, JAGS and Stan*, ed. 2. Elsevier.
- Kuehn, M., Froeming, R., & Schindler, V. (2005). Assessment of vehicle related pedestrian safety. *IRCOBI Conference*. Prague, Czech Republic.
- Kuehn, M., Hummel, T., & Bende, J. (2009). Benefit Estimation Of Advanced Driver Assistance Systems For Cars Derived From Real-life Accidents. *ESV*. Stuttgart, Germany.
- Kullgren, A. (2008). Dose-response models and EDR data for assessment of injury risk and effectiveness of safety systems. *IRCOBI*. Bern.
- Kulmala, R., Rämä, P., Sihvola, N., & A., S. (2008). *Safety Impacts of Stand-alone and Cooperative IVSS, D4.3 of the eIMPACT project*. VTT Technical Research Centre of Finland.
- Kunert, M., Krebs, S., Stoll, H., & Arbitmann, M. (2018). *PROSPECT Deliverable 5.2 Advanced HMI and vehicle control concepts for VRU active safety*. IDIADA.
- Kunert, M., Stoltz, M., Flohr, F., Hartmann, B., & Koch, A. (2016). *D3.2 Specification of the PROSPECT demonstrators*. PROSPECT.
- Kusano, K. D., & Gabler, H. C. (Dec 2012). Safety benefits of forward collision warning, brake assist, and autonomous braking systems in rear-end collisions. *IEEE Transactions on Intelligent Transportation Systems*, 13(4), 1546 - 1555. doi:10.1109/TITS.2012.2191542
- Large, D., Burnett, G., Morris, A., Muthumani, A., & Matthias, R. (2017). A Longitudinal Simulator Study to Explore Drivers' Behaviour During Highly-Automated Driving. *8th International Conference on Applied Human Factors and Ergonomics*. Los Angeles, US.
- Lindman, M., Ödblom, A., Bergvall, E., Eidehall, A., Svanberg, B., & Lukaszewicz, T. (2010). Benefit Estimation Model for Pedestrian Auto Brake Functionality. *ESAR*. Hanover, Germany.
- Ljung, M., Engström, J., & Viström, M. (2013). Effects of forward collision warning and repeated event exposure on emergency braking. *Transportation Research Part F: Traffic Psychology and Behaviour*, Vol 18, 34-46.

- Matsui, Y., & Oikawa, S. (2015). Risks of Serious Injuries and Fatalities of Cyclists Associated with Impact Velocities of Cars in Car-Cyclist Accidents in Japan. *Stapp Car Crash Journal*, Vol. 59 , 385-400.
- NHTSA. (2016). *Federal Automated Vehicles Policy: Accelerating the Next Revolution in Roadway Safety (12507-091216-v9)*. Washington, DC: National Highway Traffic Safety Administration at the US Department of Transportation. Hämtat från <https://www.transportation.gov/sites/dot.gov/files/docs/AV%20policy%20guidance%20PDF.pdf>
- openPASS. (2018). *Eclipse*. Hämtat från simopenpass: <https://projects.eclipse.org/proposals/simopenpass>
- Pastor, C. (2013). Correlation between pedestrian injury severity in real-life crashes and Euro NCAP pedestrian test results. *23rd International Technical Conference on the Enhanced Safety of Vehicles*. Seoul, Korea: NHTSA.
- Rosen, E., & Sander, U. (2009). Pedestrian fatality risk as a function of car impact speed. *Accident Analysis and Prevention*, 41, 536–542.
doi:10.1016/j.aap.2009.02.002
- Sander, U., & Lubbe, N. (2018). Market penetration of intersection AEB: Characterizing avoided and residual straight crossing path accidents. *Accident Analysis & Prevention* 115. doi:10.1016/j.aap.2018.03.025.
- Schneider, A. (2015). *Feldefektivitätsanalyse integraler Sicherheitssysteme*. Göttingen: Cuvillier Verlag, ISBN 978-3954049875.
- Schneider, A. (2016). *Penetration rates in Germany and the US*. Audi.
- Seeck, A., Seiniger, P., & Zander, O. (2012). Cyclist Accidents and Euro NCAP. *Expertworkshop Deutsch Gesellschaft für Orthodödie und Unfallchirurgie (DGOU)*. Dresden.
- Seiniger, P., Bartels, O., Pastor, C., & Wisch, M. (2013). An Open Simulation Approach to Identify Chances and Limitations for Vulnerable Road User (VRU) Active Safety. *Traffic Injury Prevention*, 2-12.
doi:10.1080/15389588.2013.797574
- Seiniger, P., Bartels, O., Wisch, M., & Pastor, C. (2013). An Open Simulation Approach to Identify Chances and Limitations for Pedestrian Active Safety. *ESV*. Seoul, South Korea.
- Smith, S., Bellone, J., Bransfield, S., Ingles, A., Noel, G., Reed, E., & Yanagisawa, M. (2015). *Benefits Estimation Framework for Automated Vehicle Operations*. Washington, DC: DOT-VNTSC-FHWA.
- Statista. (2016). *Inflation rate in the European Union and Euro area from 2012 to 2022*.
- Team, R Core. (2016). *R: A language and environment for statistical computing*. Vienna, Austria: R Foundation for Statistical Computing <https://www.R-project.org/>.
- Therneau, T., & Atkinson, E. (den 12 March 2017). *An Introduction to Recursive Partitioning Using the RPART Routines*. Hämtat från CRAN R-project: <http://cran.r-project.org/web/packages/rpart/vignettes/longintro.pdf>
- Therneau, T., Atkinson, B., & Ripley, B. (den 21 April 2017). *Recursive Partitioning and Regression Trees*. Hämtat från CRAN: <https://cran.r-project.org/web/packages/rpart/rpart.pdf>

- Van Der Laan, J., Heino, A., & De Waard, D. (1997). A simple procedure for the assessment of acceptance of advanced transport telematics. *Transportation research Part C, Emerging technologies*, 5(1), 1-10.
- Wang, L., Jung, O., Helmer, T., & Kompass, K. (2015). *Prospective Effectiveness Simulation for design and assessment of ADAS*. BMW group.
- Wang, L., Vogt, T., Dobberstein, J., Bakker, J., Jung, O., Helmer, T., & Kates, R. (2015). *Multi-functional Open-Source Simulation Platform for Development and Functional Validation of ADAS and Automated Driving*.
- Wille, J. M., Jungbluth, A., Kohsiek, A., & Zatloukal, M. (2012). rateEFFECT-Entwicklung eines Werkzeugs zur Effizienzbewertung aktiver Sicherheitssysteme. *13 Braunschweiger Symposium AAET*. Braunschweig.
- Wilmink, I., Janssen, W., Jonkers, E., Malone, K., & al, e. (2008). *Impact assessment of Intelligent Vehicle Safety Systems*. eIMPACT Deliverable D4.
- Wisch, M., Lerner, M., Schneider, A. J., Attila, G., Kovaceva, J., Bálint, A., & Lindman, M. (2016). *PROSPECT Deliverable 2.1 - Accident Analysis, Naturalistic Driving Studies and Project Implications – Part A: Accident data analyses*.
- Wisch, M., Lerner, M., Vukovic, E., Hynd, D., Fiorentino, A., & Fornells, A. (2017). Injury Patterns of Older Car Occupants, Older Pedestrians or Cyclists in Road Traffic Crashes with Passenger Cars in Europe – Results from SENIORS. *IRCOBI Conference*, (ss. <http://www.ircobi.org/wordpress/downloads/irc17/pdf-files/17.pdf>). Antwerp, Belgium.
- VTI. (2018). *Deliverable 7.3-Report on simulator test results and driver acceptance of PROSPECT functions*.
- Yves, P., Fahrenkrog, F., Fiorentino, A., Gwehenberger, J., Helmer, T., Lindman, M., . . . Wimmer, P. (2015). A comprehensive and harmonized method for assessing the effectiveness of advanced driver assistance systems by virtual simulation: THE P.E.A.R.S. initiative. *ESV*. Gothenburg, Sweden.
- Zander, O., Pastor, C., & Wisch, M. (2018). Private communication.

8 APPENDIX A

8.1 BOX PLOT DESCRIPTION

- The left and right boundaries of each “box” (displayed in blue) are the 25th and 75th percentiles of the samples, respectively. The distances between the left and right boundaries of the box are the interquartile ranges.
- The red line in the middle of each box is the sample median. If the median is not centred in the box, it shows sample skewness.
- The whiskers are lines extending outside of the box to the left and right (displayed as dotted black lines). Whiskers are drawn from the ends of the interquartile ranges to the furthest observations within the whisker length. The whisker length is defined as 1.5 times the interquartile range.
- Observations beyond the whisker length are marked as outliers. By default, an outlier is a value that is more than 1.5 times the interquartile range away from the left or right boundary of the box. Outliers are displayed with a red “+” sign.
- Boxplots are non-parametric. This means that no statistic distributions are assumed for displaying the variation of the analysed accident data. As seen in the next figure, the spacing between the different parts of the box indicates the degree of dispersion (spread) and skewness in the data and shows outliers.

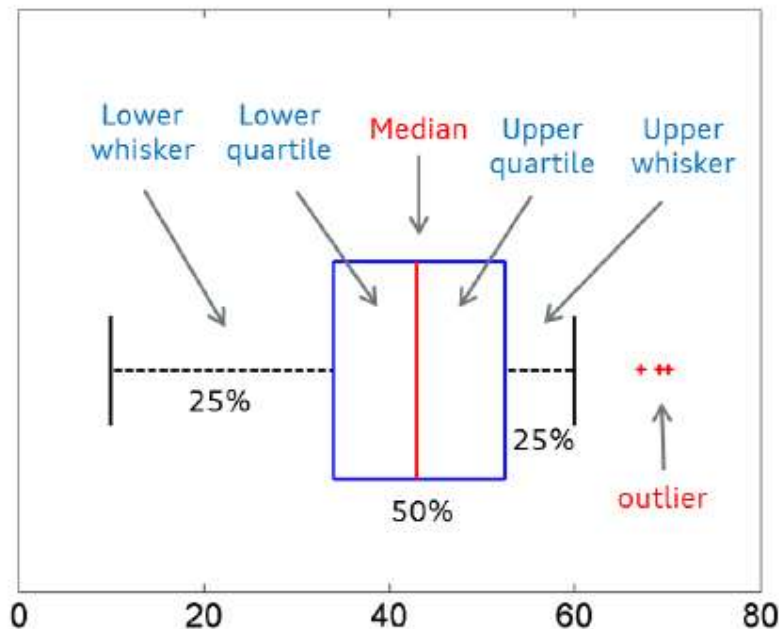


Figure 96: Exemplary boxplot.

8.2 INITIAL SPEED

The initial speed of cyclists and pedestrian in each of the use cases are shown in Figure 97, and the car initial speed is shown in Figure 98.

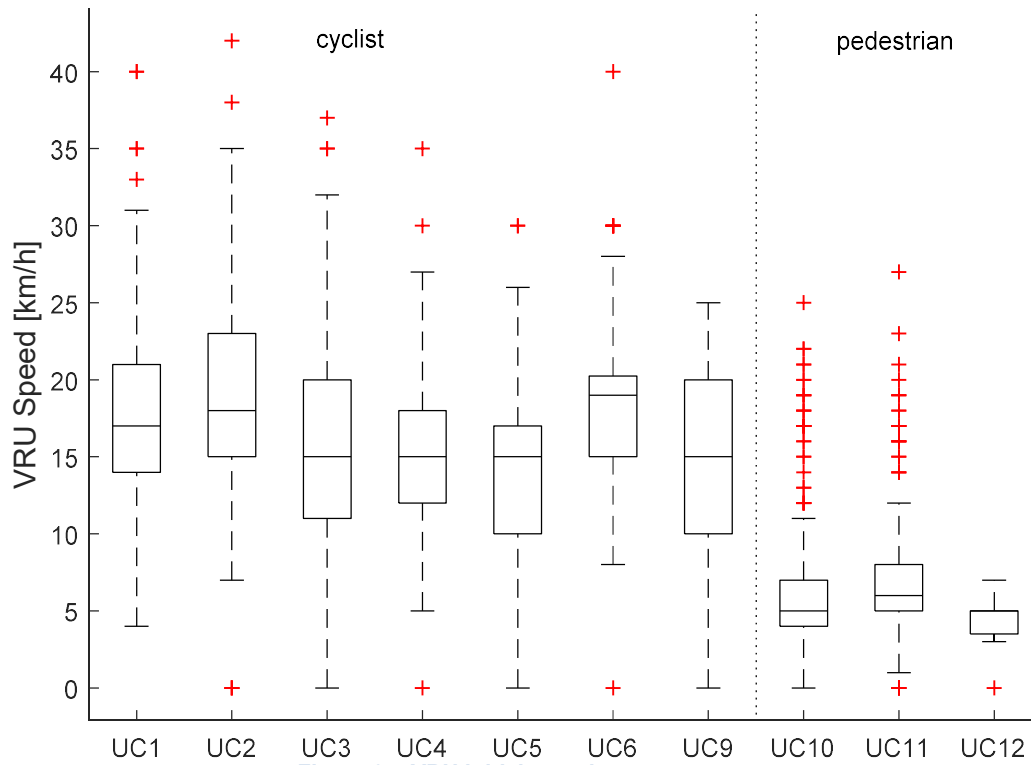


Figure 97: VRU initial speed per use case.

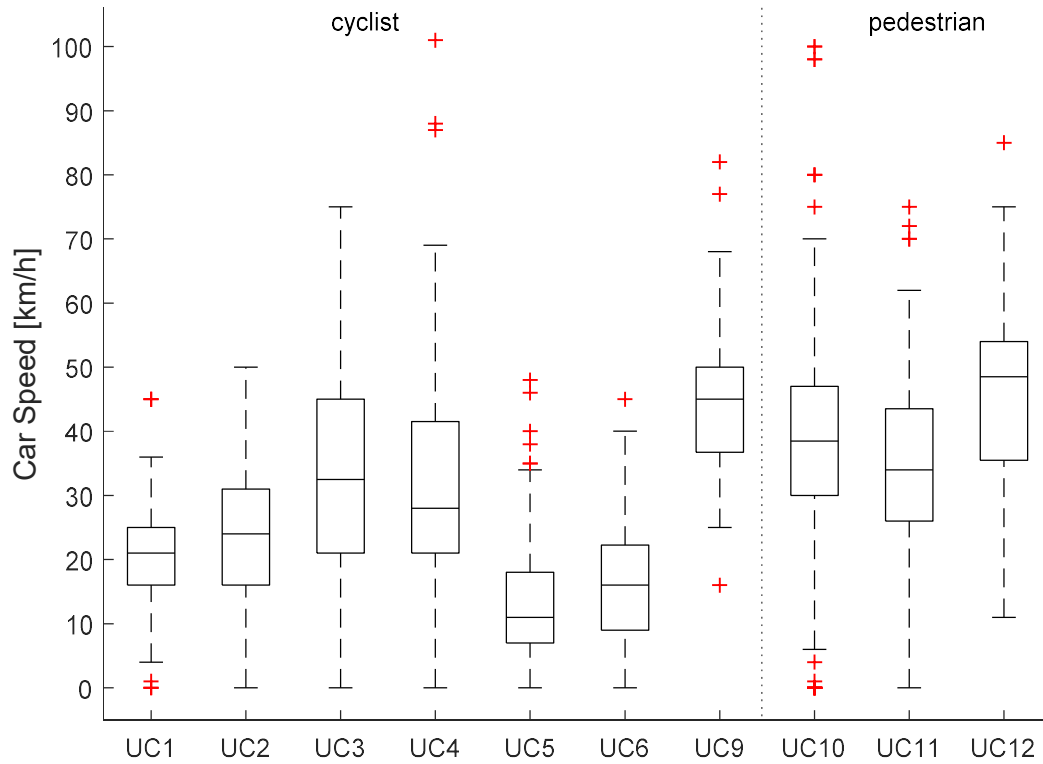
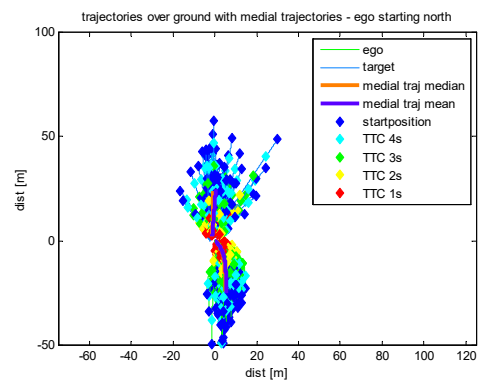
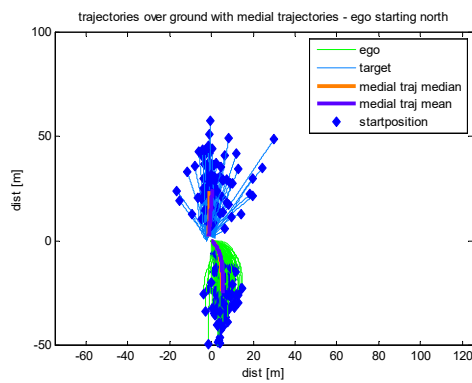
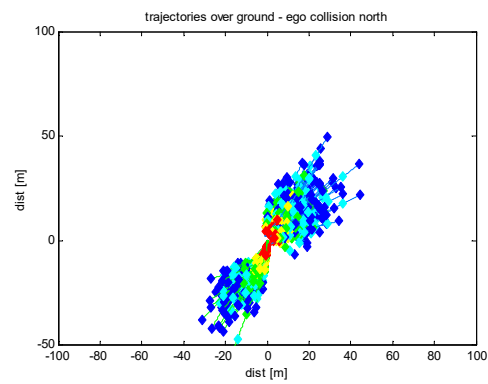
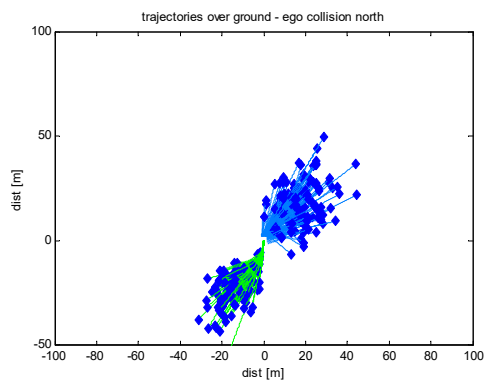
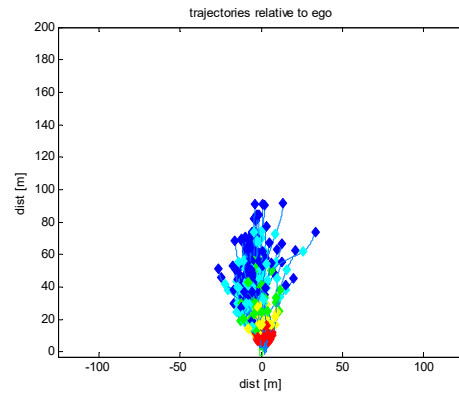
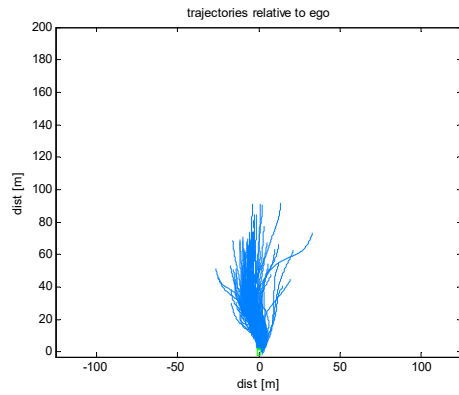


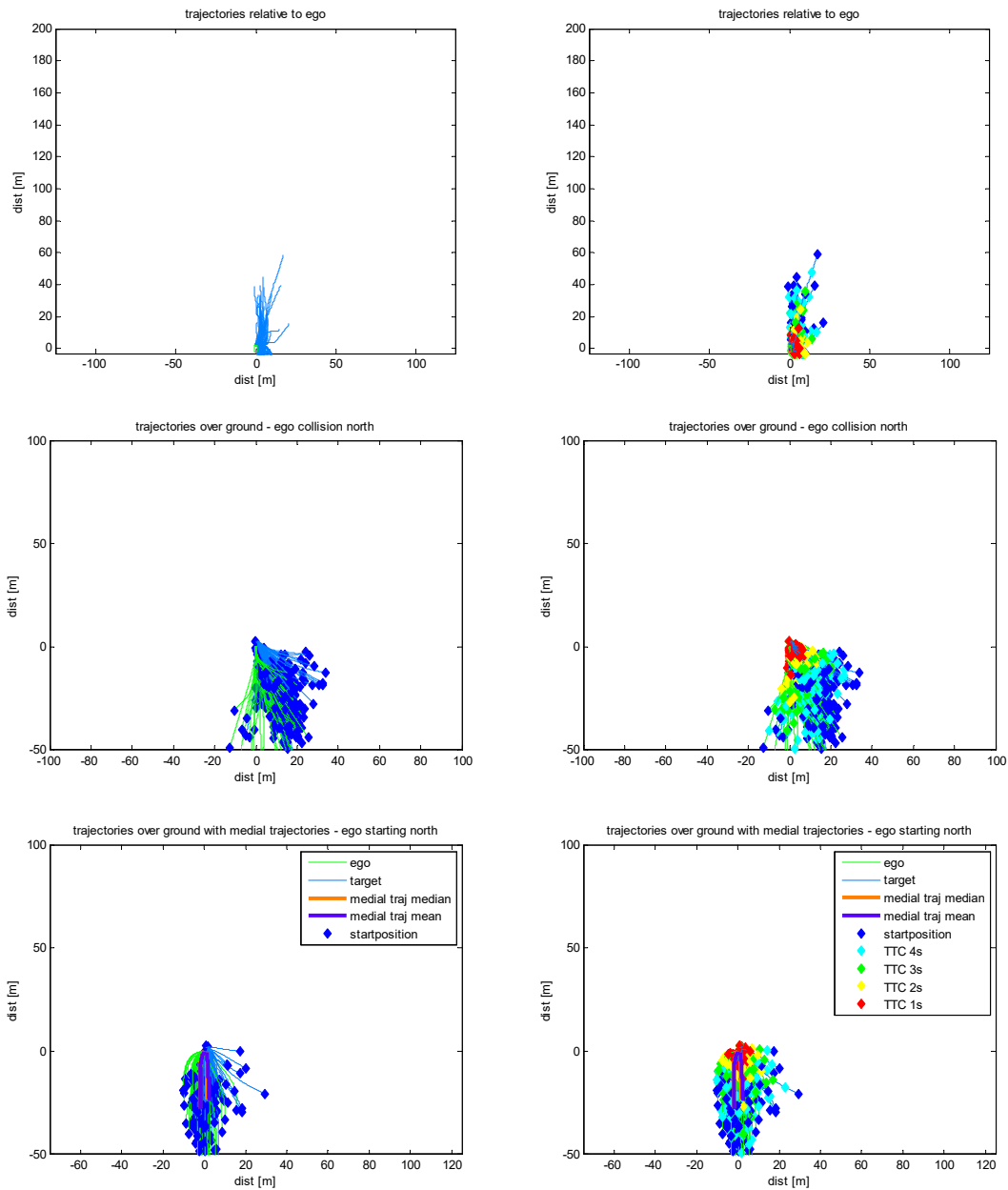
Figure 98: Car initial speed per use case.

8.3 TRAJECTORIES

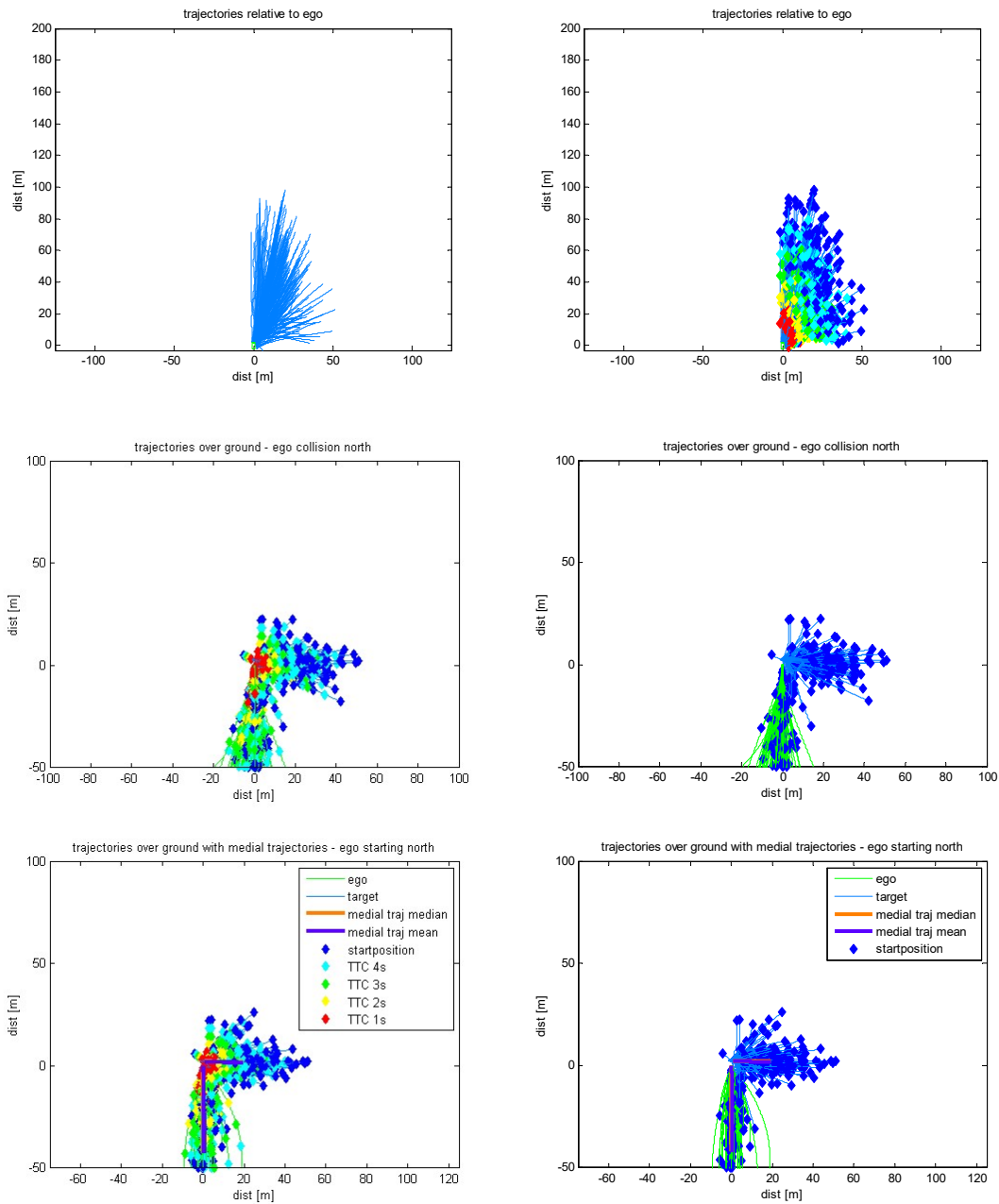
8.3.1 UC_DEM_1



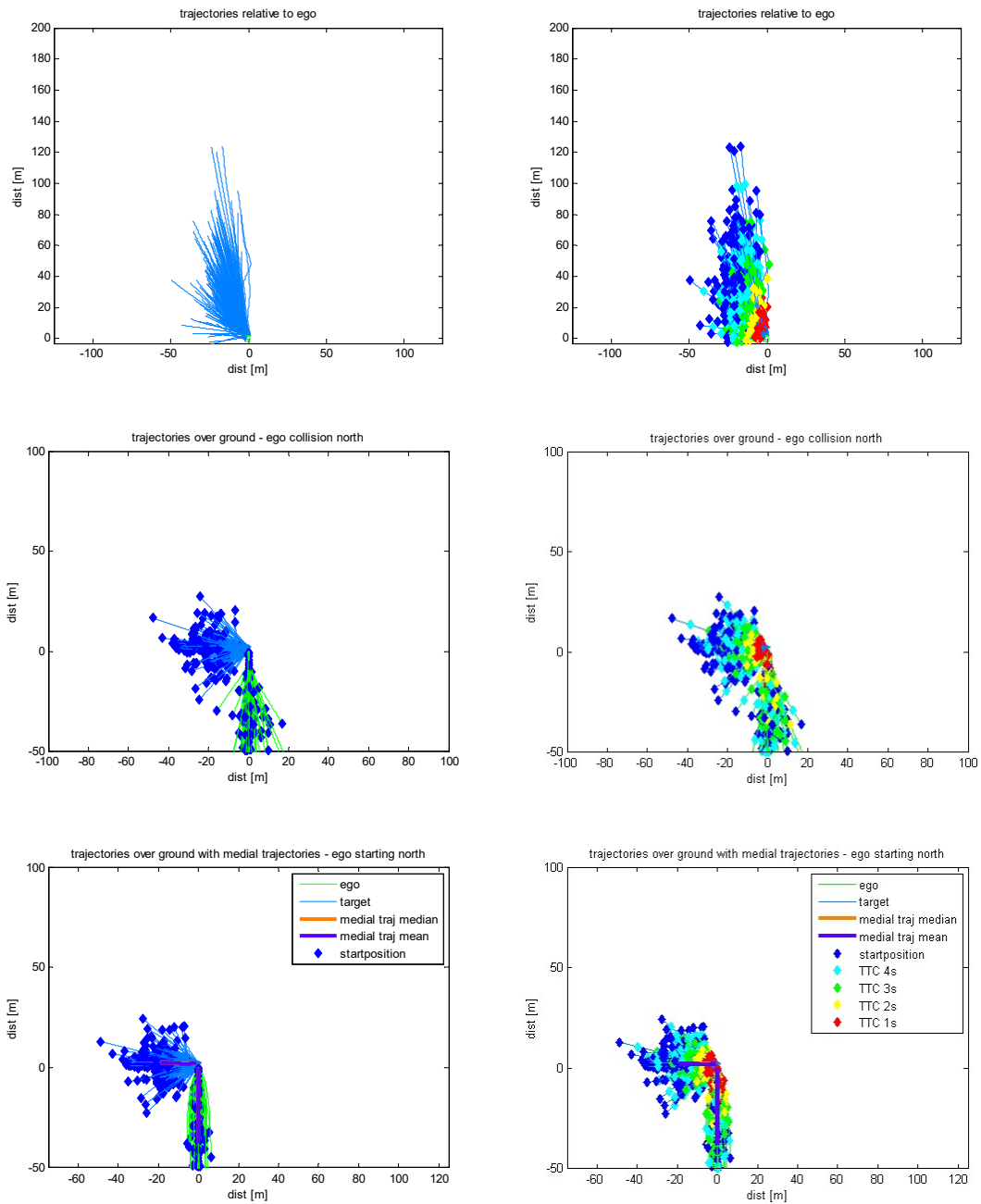
8.3.2 UC_DEM_2



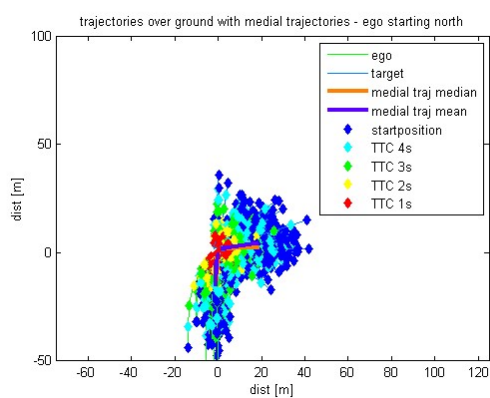
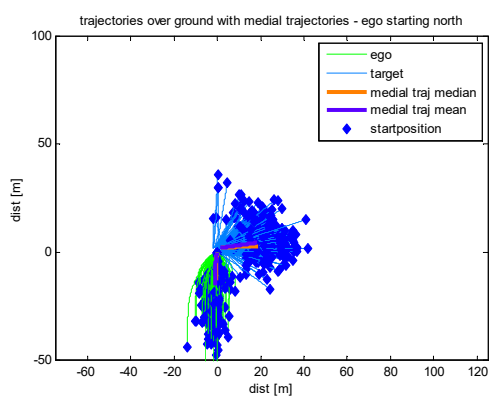
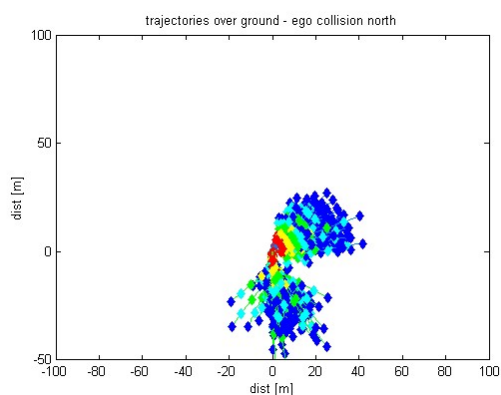
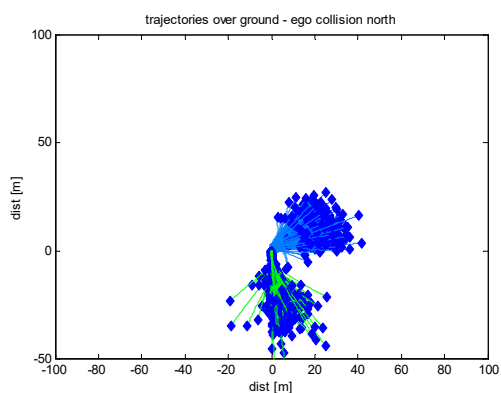
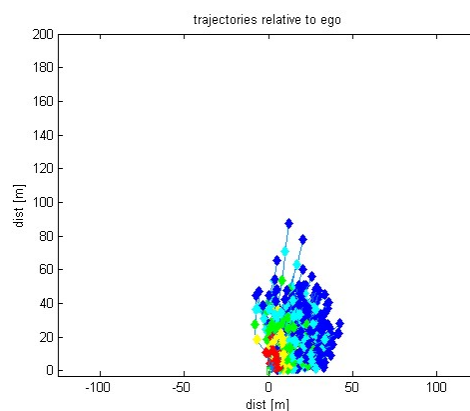
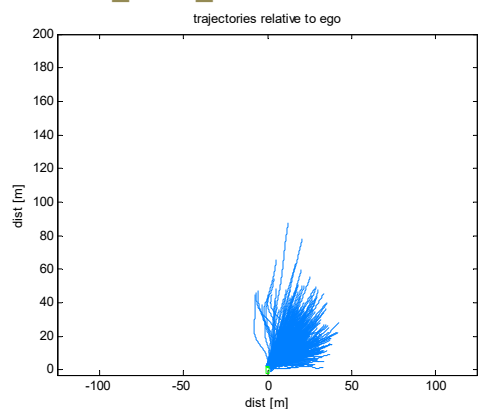
8.3.3 UC_DEM_3



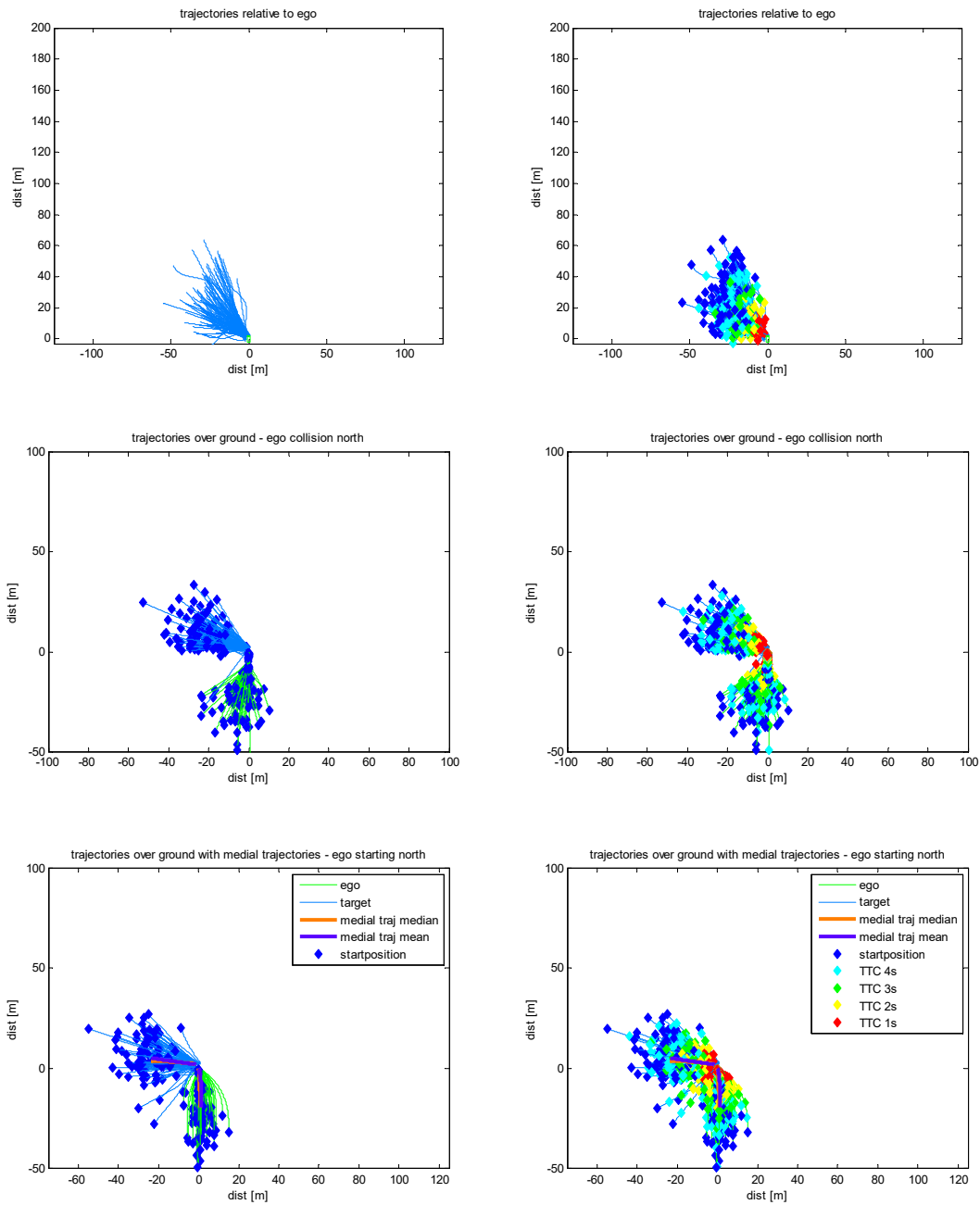
8.3.4 UC_DEM_4



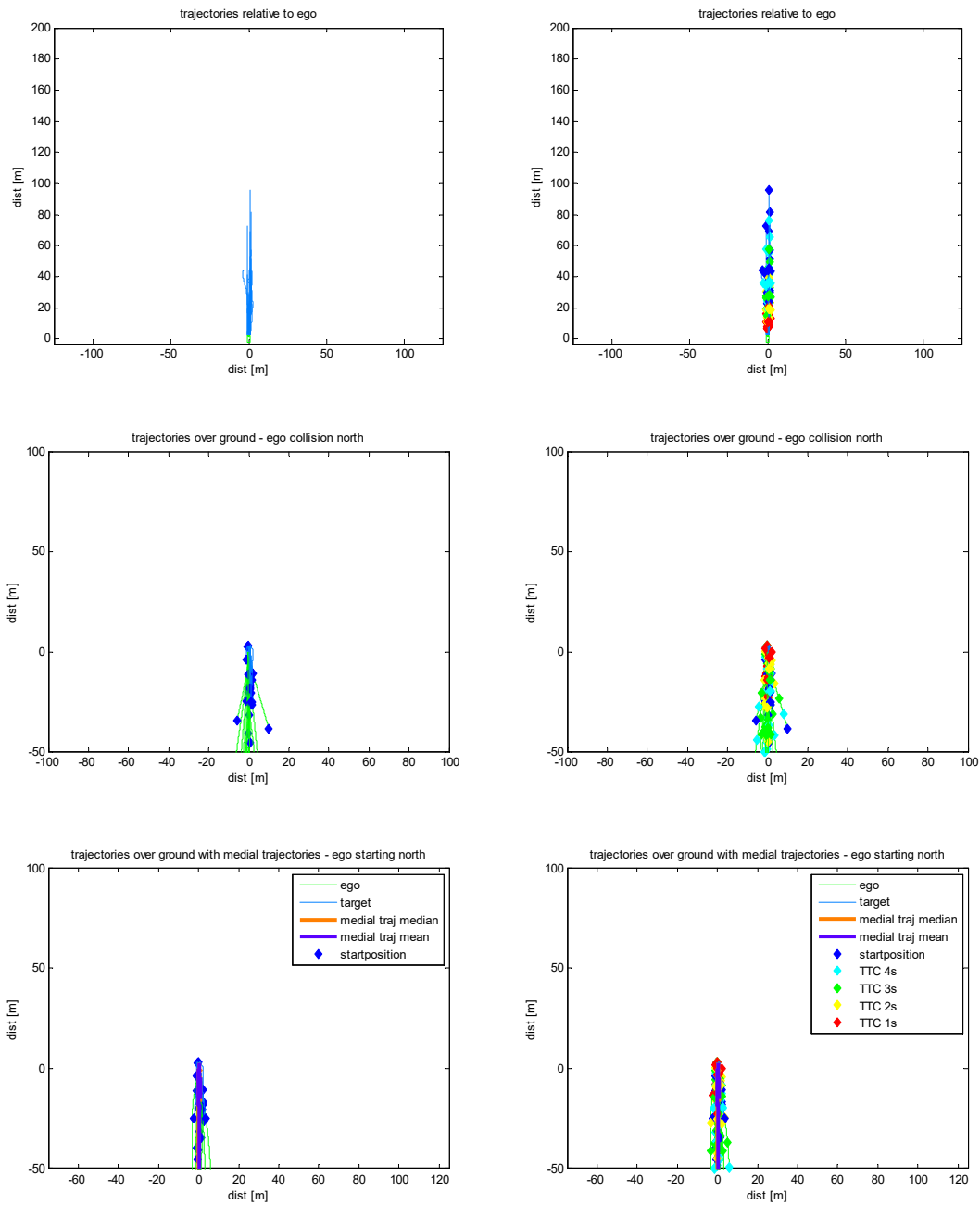
8.3.5 UC_DEM_5



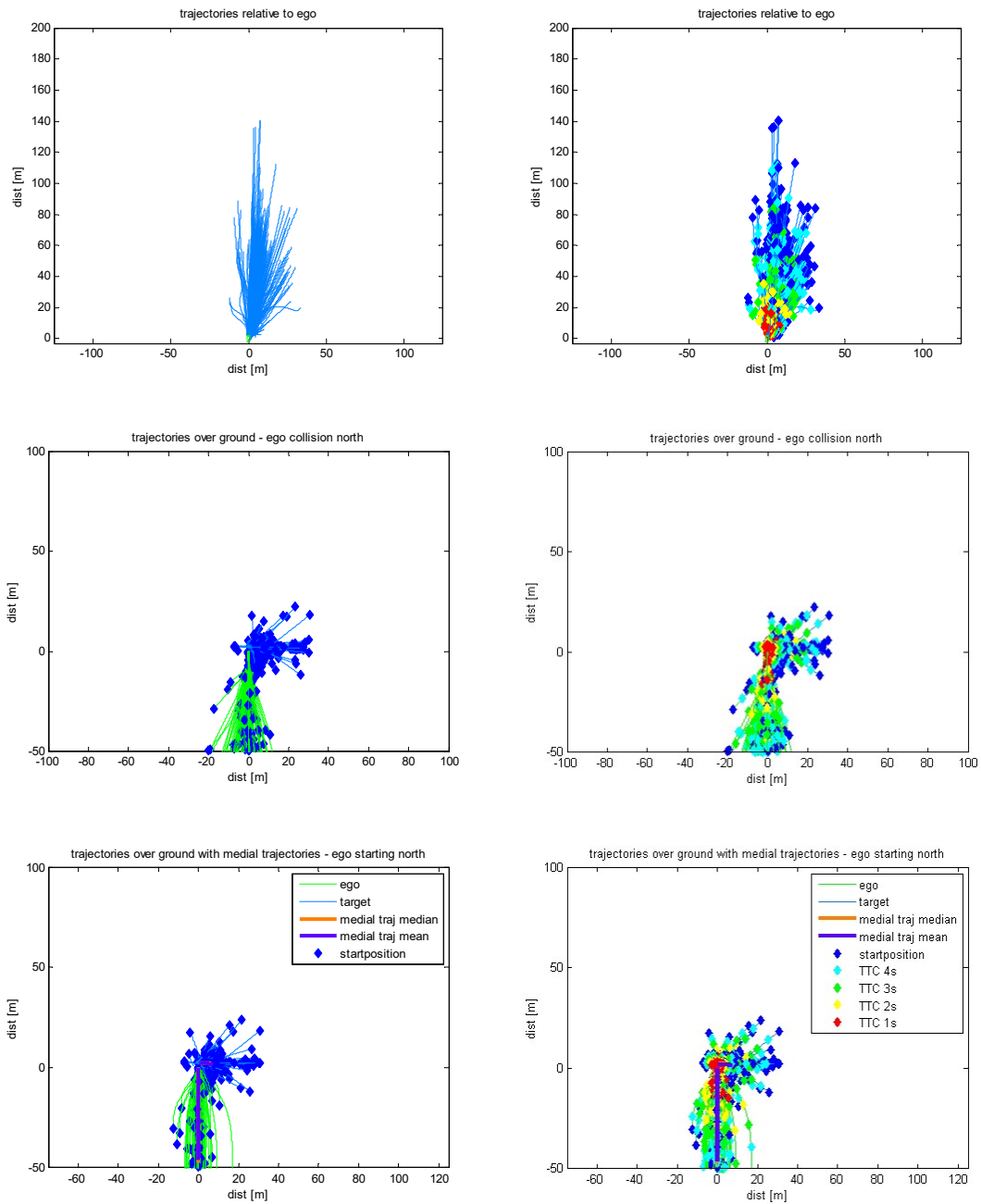
8.3.6 UC_DEM_6



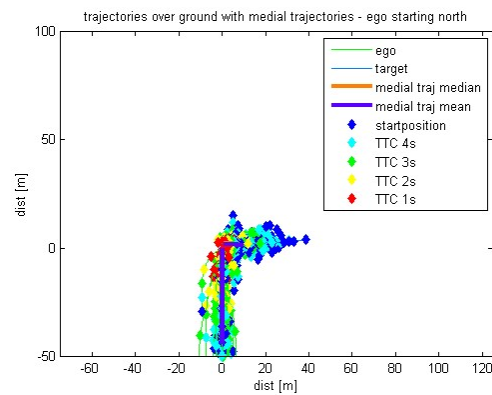
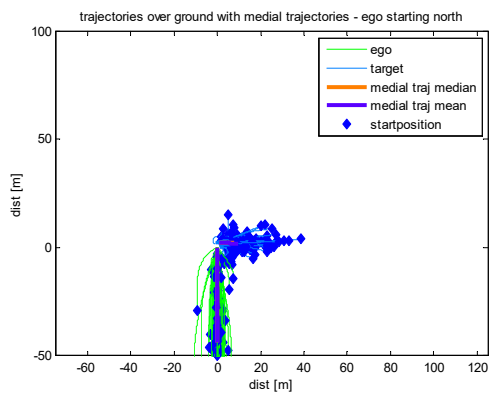
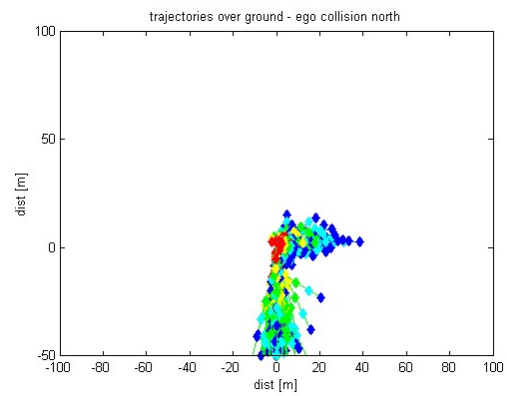
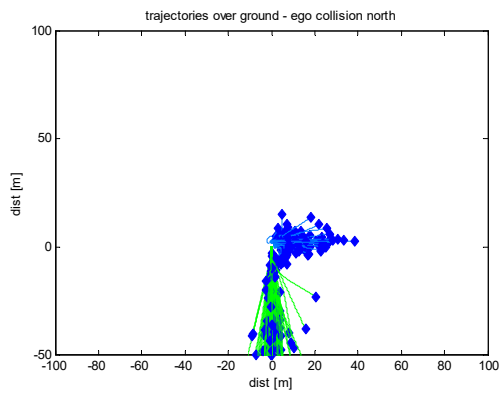
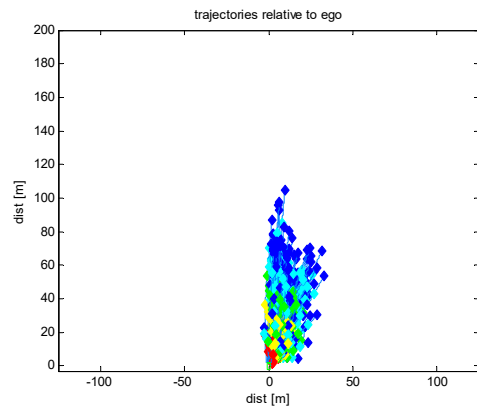
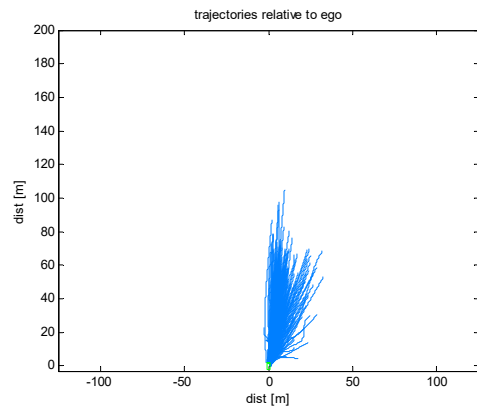
8.3.7 UC_DEM_9



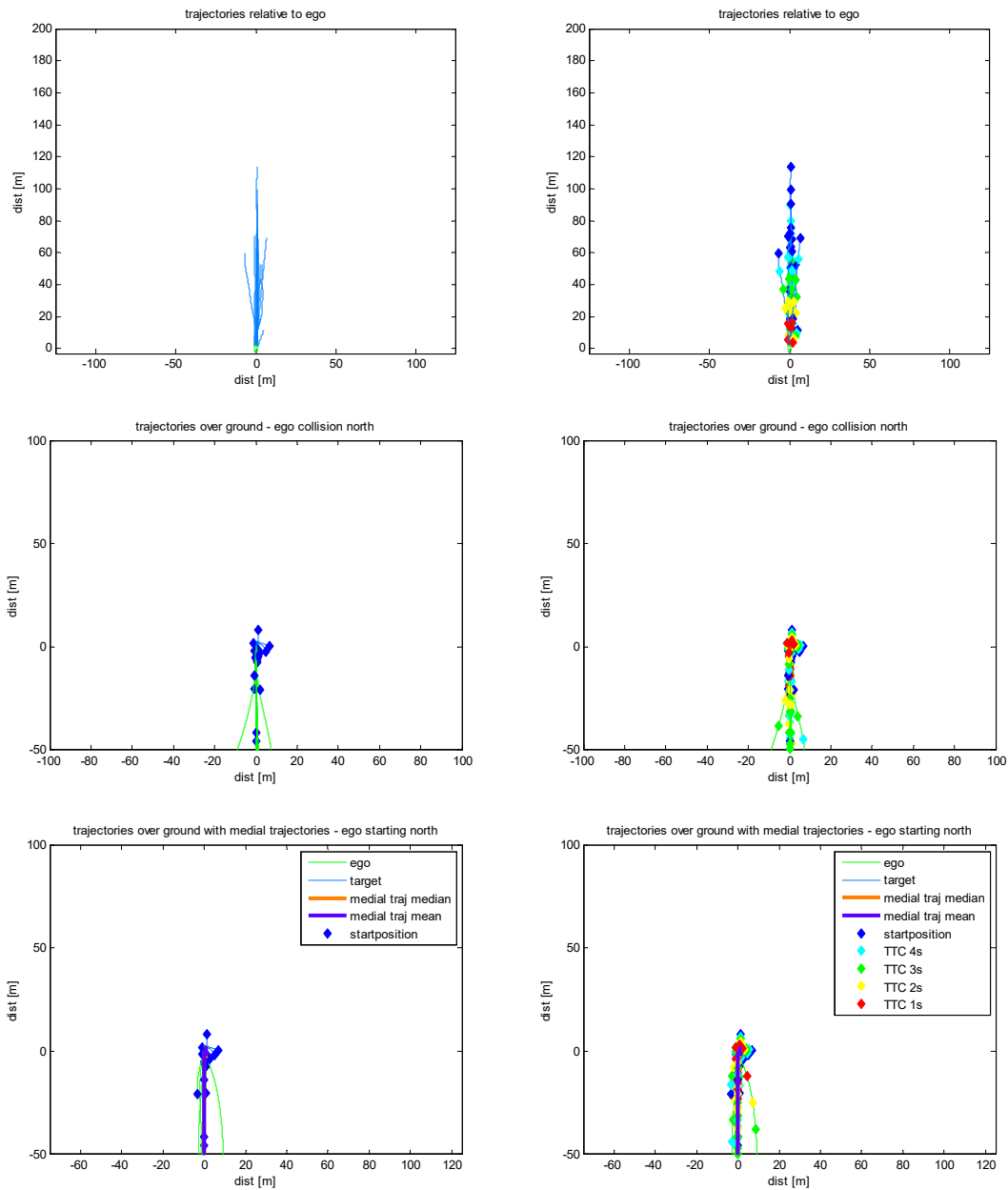
8.3.8 UC_DEM_10



8.3.9 UC_DEM_11



8.3.10 UC_DEM_12



8.4 LOCAL SAFETY BENEFITS INCLUDING CONFIDENCE INTERVALS

The first table contains the results by use case, without further restrictions, including lower and upper bounds based on the confidence intervals in the regression models.

Table 41: Reduction of casualties of different severities by use case with confidence intervals

		Algo 1 Lower bound	Algo 1 Higher bound		Algo 2 Lower bound	Algo 2 Higher bound		Algo 3 Lower bound	Algo 3 Higher bound	Steering and braking	Steering and braking Lower bound	Steering and braking Higher bound
FATALITIES	Algo 1			Algo 2			Algo 3					
UC1	93%	76%	98%	92%	74%	98%	92%	75%	98%	N/A	N/A	N/A
UC2	72%	45%	89%	72%	39%	88%	70%	41%	88%	N/A	N/A	N/A
UC3	85%	78%	90%	81%	73%	86%	82%	75%	87%	N/A	N/A	N/A
UC4	86%	76%	91%	80%	70%	87%	81%	72%	88%	N/A	N/A	N/A
UC5	94%	86%	97%	91%	84%	95%	92%	84%	96%	N/A	N/A	N/A
UC6	97%	87%	100%	96%	86%	99%	96%	86%	99%	N/A	N/A	N/A
UC9	87%	80%	91%	80%	69%	85%	80%	70%	84%	98%	N/A	N/A
UC10	81%	74%	86%	74%	68%	80%	75%	68%	80%	N/A	N/A	N/A
UC11	63%	52%	73%	55%	44%	65%	56%	45%	65%	N/A	N/A	N/A
UC12	78%	71%	86%	70%	63%	80%	71%	64%	80%	98%	79%	100%
Total	78%	70%	85%	72%	64%	79%	73%	65%	80%	N/A	N/A	N/A
Cyclists	87%	77%	92%	82%	71%	88%	83%	73%	89%	N/A	N/A	N/A
Pedestrians	76%	68%	82%	69%	61%	76%	69%	62%	77%	N/A	N/A	N/A

		Algo 1 Lower bound	Algo 1 Higher bound		Algo 2 Lower bound	Algo 2 Higher bound		Algo 3 Lower bound	Algo 3 Higher bound	Steering and braking	Steering and braking Lower bound	Steering and braking Higher bound
SERIOUS INJURIES	Algo 1			Algo 2			Algo 3					
UC1	86%	64%	96%	85%	62%	95%	86%	64%	95%	N/A	N/A	N/A
UC2	55%	24%	78%	53%	22%	79%	53%	23%	77%	N/A	N/A	N/A
UC3	62%	51%	71%	55%	45%	65%	57%	46%	66%	N/A	N/A	N/A
UC4	76%	65%	85%	70%	59%	80%	72%	61%	81%	N/A	N/A	N/A
UC5	89%	75%	95%	85%	76%	91%	86%	71%	93%	N/A	N/A	N/A
UC6	93%	74%	99%	91%	72%	98%	91%	72%	98%	N/A	N/A	N/A
UC9	83%	71%	85%	81%	67%	82%	81%	67%	82%	93%	N/A	N/A
UC10	51%	39%	61%	43%	33%	53%	44%	34%	54%	N/A	N/A	N/A
UC11	31%	20%	44%	23%	14%	35%	24%	14%	36%	N/A	N/A	N/A
UC12	58%	38%	81%	53%	30%	81%	54%	31%	81%	95%	70%	100%
Total	60%	47%	71%	54%	42%	66%	55%	42%	66%	N/A	N/A	N/A
Cyclists	76%	61%	85%	71%	58%	81%	72%	57%	82%	N/A	N/A	N/A
Pedestrians	44%	32%	55%	36%	26%	47%	37%	27%	48%	N/A	N/A	N/A

Deliverable No. 2.3
Assessment of the
PROSPECT safety systems
including socio-economic
evaluation



SLIGHT INJURIES												
	Algo 1	Algo 1 Lower bound	Algo 1 Higher bound	Algo 2	Algo 2 Lower bound	Algo 2 Higher bound	Algo 3	Algo 3 Lower bound	Algo 3 Higher bound	Steering and braking	Steering and braking Lower bound	Steering and braking Higher bound
UC1	74%	46%	90%	73%	46%	89%	74%	48%	90%	N/A	N/A	N/A
UC2	42%	16%	67%	42%	16%	66%	42%	16%	66%	N/A	N/A	N/A
UC3	34%	21%	47%	28%	16%	40%	29%	17%	41%	N/A	N/A	N/A
UC4	66%	53%	77%	59%	47%	71%	60%	48%	72%	N/A	N/A	N/A
UC5	83%	60%	91%	78%	70%	87%	79%	55%	88%	N/A	N/A	N/A
UC6	87%	56%	98%	84%	53%	97%	85%	53%	97%	N/A	N/A	N/A
UC9	88%	66%	86%	90%	70%	89%	90%	69%	89%	90%	N/A	N/A
UC10	15%	1%	28%	10%	-1%	22%	11%	-1%	23%	N/A	N/A	N/A
UC11	5%	-2%	18%	0%	-5%	10%	1%	-4%	11%	N/A	N/A	N/A
UC12	36%	-29%	87%	46%	-13%	89%	45%	-13%	89%	90%	65%	100%
Total	57%	37%	69%	53%	38%	65%	53%	34%	66%	N/A	N/A	N/A
Cyclists	68%	47%	80%	64%	49%	76%	65%	43%	77%	N/A	N/A	N/A
Pedestrians	12%	-1%	26%	7%	-3%	19%	8%	-3%	20%	N/A	N/A	N/A

The next table shows the reductions computed for the cases that are relevant for the extrapolation method. The first table shows the results that are relevant for the cyclist use cases and the second table gives the results corresponding to the pedestrian use cases.

Table 42: Local benefits for cyclists to be used for extrapolation to EU-28

	Fatal	Serious	Slight
Leaf 3 (Age <=55), Algo 1	90% (83-94%)	77% (63-86%)	63% (37-77%)
Leaf 3 (Age <=55), Algo 2	87% (79-91%)	73% (60-83%)	58% (40-72%)
Leaf 3 (Age <=55), Algo 3	87% (80-92%)	74% (60-84%)	59% (33-73%)
Leaf 3 (Age <=55), St & Br, UC9	98% (N/A)	93% (N/A)	89% (N/A)
Leaf 4 (Age > 55 and Not Urban), Algo 1	91% (88-94%)	63% (52-69%)	31% (5-43%)
Leaf 4 (Age > 55 and Not Urban), Algo 2	87% (81-90%)	57% (46-63%)	30% (5-41%)
Leaf 4 (Age > 55 and Not Urban), Algo 3	87% (83-90%)	58% (48-64%)	29% (13-42%)
Leaf 4 (Age > 55 and Not Urban), St & Br, UC9	99% (N/A)	91% (N/A)	70% (N/A)
Leaf 5 (Age > 55 and Urban), Algo 1	92% (86-95%)	79% (66-87%)	67% (46-80%)
Leaf 5 (Age > 55 and Urban), Algo 2	89% (83-93%)	75% (63-83%)	63% (46-75%)
Leaf 5 (Age > 55 and Urban), Algo 3	90% (84-93%)	76% (63-84%)	63% (42-76%)
Leaf 5 (Age > 55 and Urban), St & Br, UC9	100% (N/A)	100% (N/A)	100% (N/A)

Table 43: Local benefits for pedestrians to be used for extrapolation to EU-28

	Fatal	Serious	Slight
Leaf 2 (Age > 55), Algo 1	82% (77-86%)	47% (36-56%)	-2% (-20-12%)
Leaf 2 (Age > 55), Algo 2	76% (71-81%)	40% (31-49%)	-6% (-20-6%)
Leaf 2 (Age > 55), Algo 3	76% (71-81%)	41% (31-50%)	-5% (-19-8%)
Leaf 2 (Age > 55), St & Br, UC12	100% (89-100%)	96% (74-100%)	89% (63-100%)
Leaf 6 (Age <= 55 and Not Daylight), Algo 1	81% (75-86%)	42% (31-54%)	-29% (-45 - -7%)
Leaf 6 (Age <= 55 and Not Daylight), Algo 2	75% (70-81%)	35% (26-46%)	-30% (-42 - -14%)

Leaf 6 (Age <= 55 and Not Daylight), Algo 3	76% (70-82%)	36% (26-47%)	-30% (-43 - -14%)
Leaf 6 (Age <= 55 and Not Daylight), St & Br, UC12	96% (72-100%)	94% (69-100%)	88% (67-100%)
Leaf 7 (Age <= 55 and Daylight), Algo 1	81% (74-86%)	48% (37-60%)	2% (-12-18%)
Leaf 7 (Age <= 55 and Daylight), Algo 2	76% (69-81%)	41% (31-52%)	-5% (-16-9%)
Leaf 7 (Age <= 55 and Daylight), Algo 3	76% (69-82%)	42% (32-53%)	-4% (-16-10%)
Leaf 7 (Age <= 55 and Daylight), St & Br, UC12	95% (69-100%)	95% (65-100%)	93% (62-100%)

8.5 IRF FOR CYCLISTS USING MAIS LEVELS

The (ordered) probit regression was applied to specify the probability of sustaining a certain injury, i.e. MAIS1, MAIS2+ (excluding fatalities), and fatalities (using the police coding for identifying the fatalities).

The estimator was the collision speed of the car. This model uses the inverse standard normal distribution of the probability as a linear combination of the predictors. Model corresponding coefficients, intercepts and the Akaike Information Criterion are provided Table 44. The implementation of the model is done in R and the MASS package (function *polr*, Hess matrix = TRUE).

The resulting curves in Figure 74 show the three IRF for the 3 injury levels MAIS1, MAIS2+ (excluding fatalities) and fatalities. At each point of the x-axis the values of all 3 curves sum up to the total probability of 1.

This means, as the probability of being only MAIS1 injured goes down, the probability of being MAIS2+ injured (and being fatally injured) increases with increasing collision speed.

Table 44: Parameter estimates of the probit model for cyclists.

	Estimate	Standard Error	t-value
Vehicle collision speed	0.02809	0.003119	9.007
Intercept MAIS1 → MAIS2+	1.4249	0.0771	18.4692
Intercept MAIS2+ → fatal	3.4700	0.2028	17.1102
Residual Deviance: 1265.255			
AIC: 1271.255			

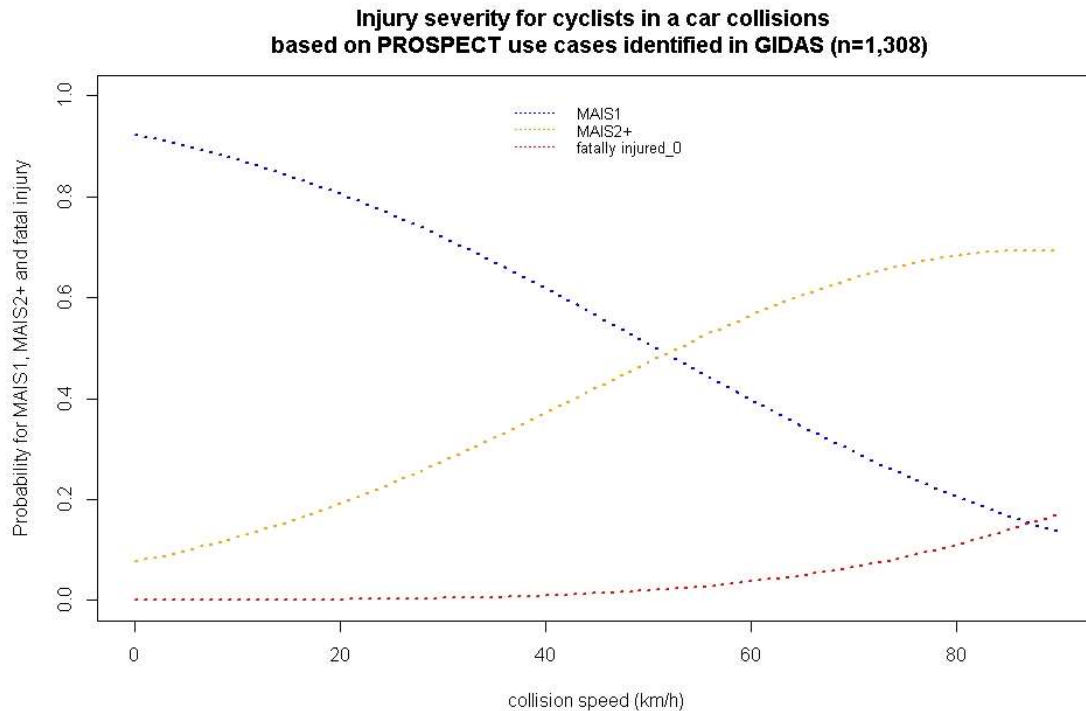


Figure 99: Probability for injury severity of MAIS1 (blue), MAIS2+ (orange), and fatality (red) for cyclists in an accident with a car based on n= 1.308 GIDAS cases identified as PROSPECT use-cases.

When using the same cases for police-coded injury severity as for the MAIS related analysis (excluding the cases where MAIS is unknown) with n= 1,308 cases, including 1011 cases of slightly injured, 292 cases of seriously injured and 5 cases of fatally injured, the results are as presented in Table 45.

Table 45: Parameter estimates of the probit model for pedestrians based on police coded injury severity.

	Estimate	Standard Error	t-value
Vehicle collision speed	0.03133	0.003085	10.16
Intercept MAIS1 → MAIS2+	1.3847	0.0754	18.3682
Intercept MAIS2+ → fatal	3.5903	0.2085	17.2198
Residual Deviance: 1,345.01			
AIC: 1,351.01			

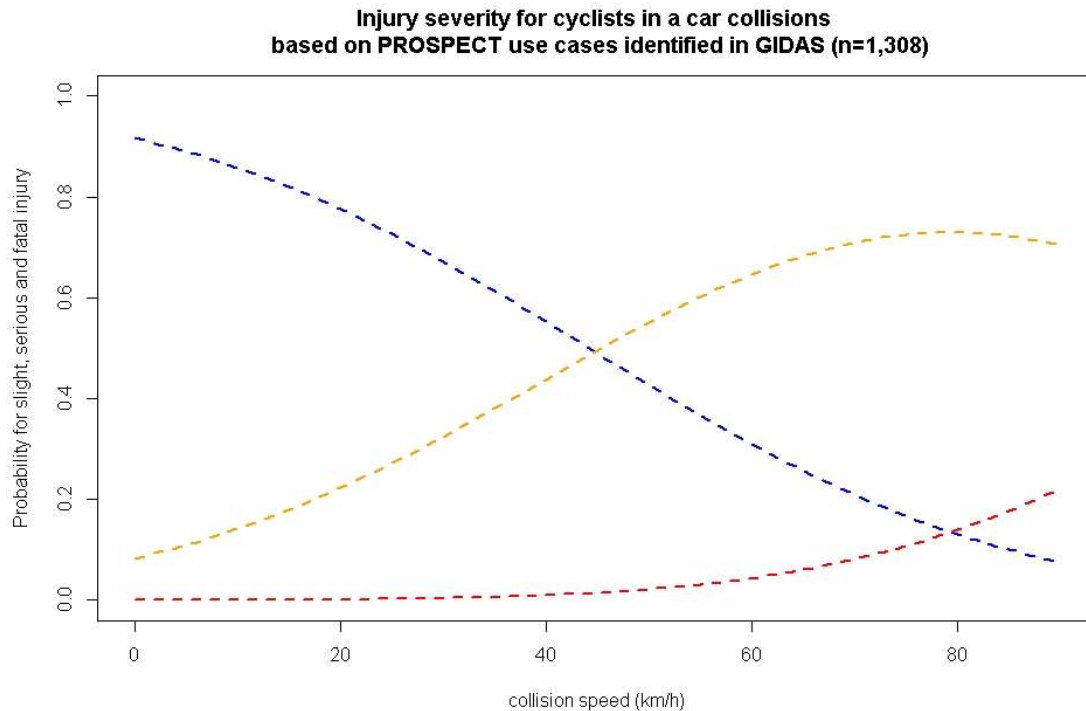


Figure 100: Probability of being slightly (blue), seriously (orange), and fatally (red) injured for cyclists in an accident with a car based on n=1,308 GIDAS cases identified as PROSPECT use-cases.

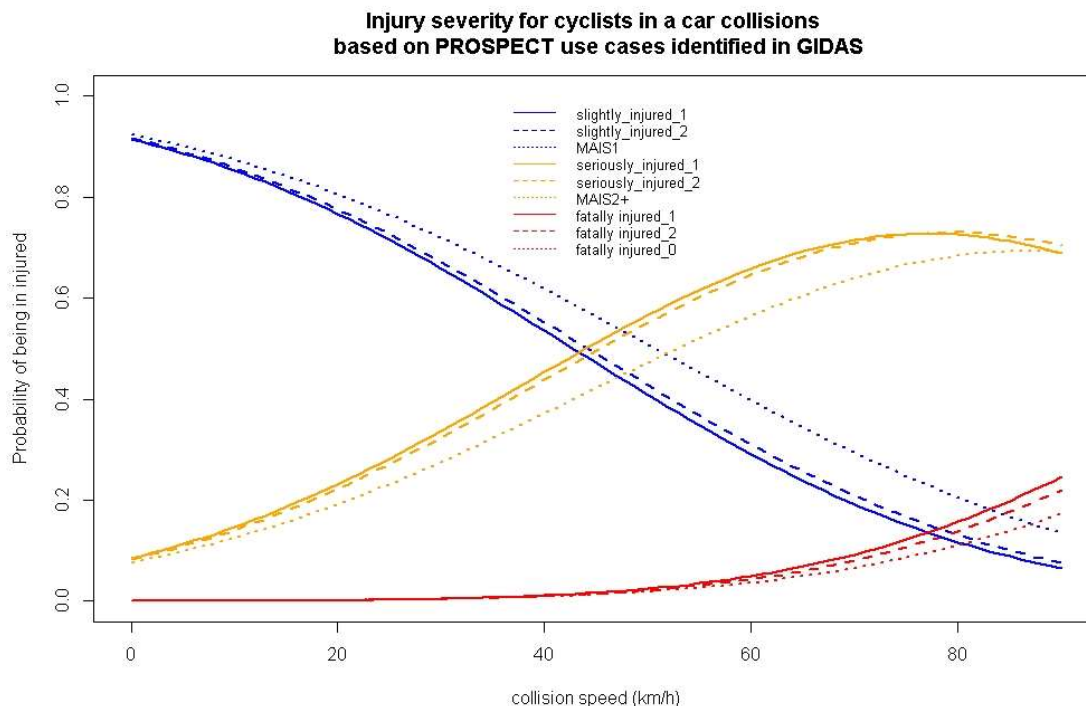


Figure 101: IRF for cyclists based both on police coding and MAIS.

8.6 IRF FOR PEDESTRIANS USING MAIS LEVELS

The data was categorized into 3 injury levels: MAIS1, MAIS2+ (excluding fatalities), fatalities (only 11 cases). Model corresponding coefficients, intercepts and the Akaike Information Criterion are provided in Table 46.

Table 46: Parameter estimates of the probit model for pedestrians based on MAIS levels.

	Estimate	Standard Error	t-value
Vehicle collision speed	0.02866	0.003784	7.575
Intercept MAIS1 → MAIS2+	1.1839	0.1313	9.0174
Intercept MAIS2+ → fatal	3.1558	0.2082	15.1594
Residual Deviance: 741.2072			
AIC: 747.2072			

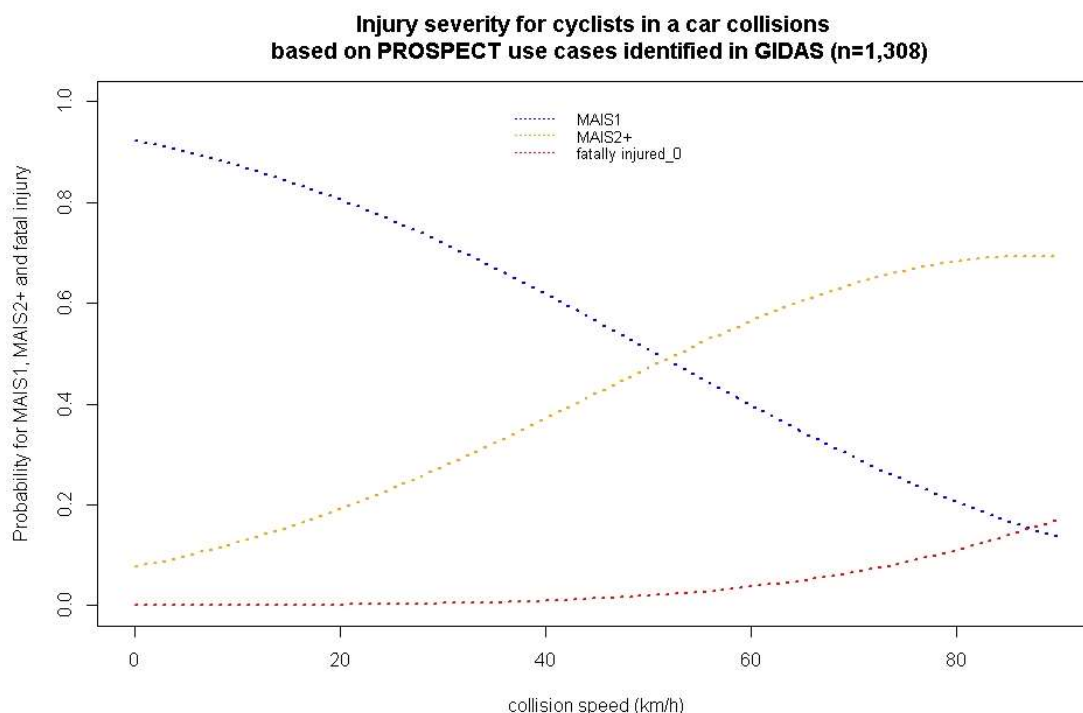


Figure 102: Probability for injury severity of MAIS1 (blue), MAIS2+ (orange), and fatality (red) for pedestrians in an accident with a car based on n=519 GIDAS cases identified as PROSPECT use-cases.

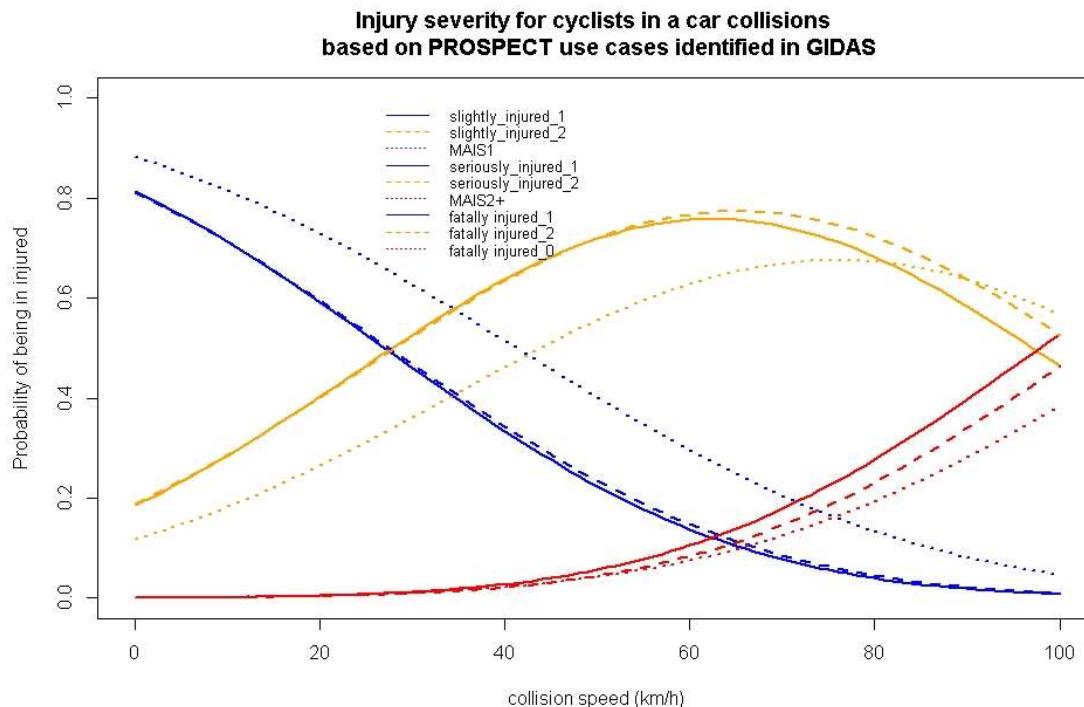


Figure 103: All IRF for pedestrians plotted together.

When using the same cases as for the MAIS related analysis (excluding 40 cases where MAIS is unknown), with $n = 537$ cases, the results are as follows:

Table 47: Parameter estimates of the probit model for pedestrians based on police coded injury severity.

	Estimate	Standard Error	t-value
Vehicle collision speed	0.03211	0.003831	8.38
Intercept MAIS1 → MAIS2+	0.8820	0.1275	6.9166
Intercept MAIS2+ → fatal	3.3021	0.2137	15.4550
Residual Deviance: 759.7613			
AIC: 765.7613			

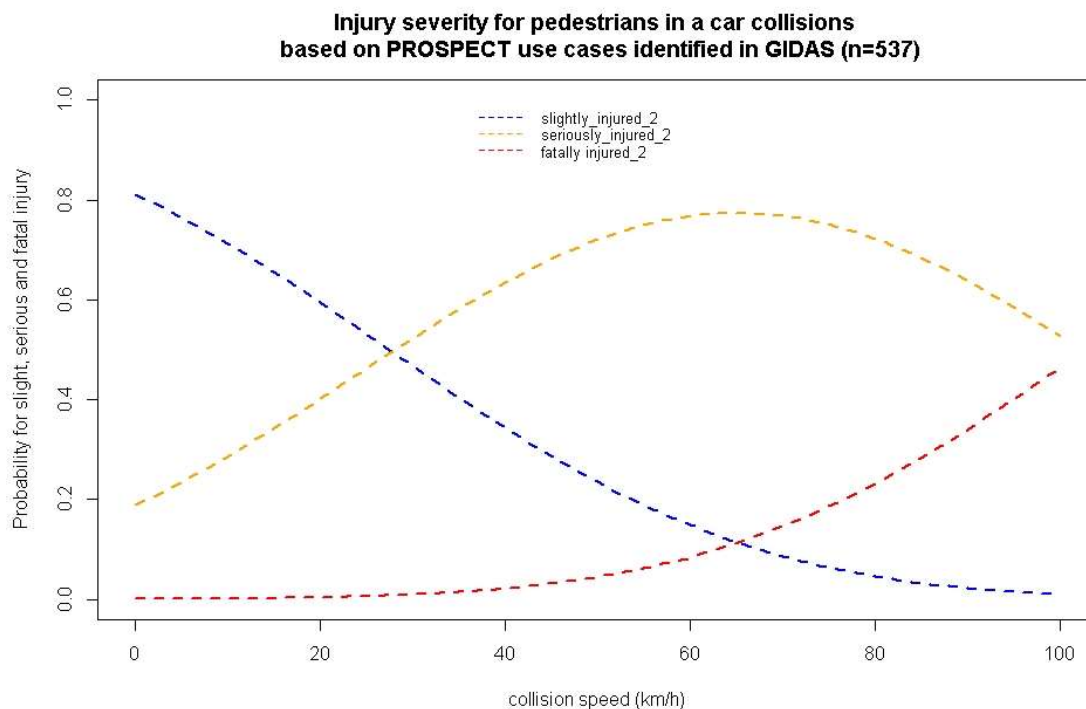


Figure 104: Probability of being slightly (blue), seriously (orange), and fatally (red) injured for pedestrians in an accident with a car based on n=537 GIDAS cases identified as PROSPECT use-cases.

Version control
Version 0.1, 2018 Aug 24 – sent to partners
Version 0.2 2018 Sep 21 – sent to internal review
Version 0.3 2018 Oct 3 – internally reviewed
Version 1.0 2018 Oct 26 – final version
Version 1.1 2019 Jan 7 – including more figures, summary and highlights

ACKNOWLEDGMENTS

We would like to thank the PROSPECT consortium and the support of Marcus Wisch (BAST) and Patrick Seiniger (BAST) in the earlier work in task 2.4, and Carol Flanagan (UMTRI) for fruitful discussions on the Bayesian methodology.



The research leading to the results of this work has received funding from the European Community's Eighth Framework Program (Horizon2020) under grant agreement n° 634149.